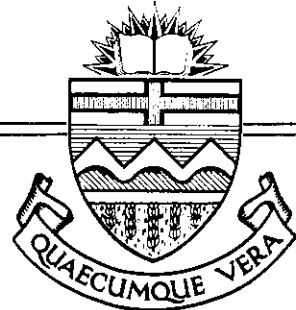


Structures Report No. 69



NUMERICAL ANALYSIS OF
GENERAL SHELLS OF
REVOLUTION SUBJECTED
TO ARBITRARY LOADING

by
AHMED M. SHAZLY
SIDNEY H. SIMMONDS
DAVID W. MURRAY

September, 1978

RECENT STRUCTURAL ENGINEERING REPORTS

Department of Civil Engineering

University of Alberta

39. Fatigue of Reinforcing Bars by I.C. Jhamb and J.G. MacGregor, February 1972.
40. Behavior of Welded Connections Under Combined Shear and Moment by J.L. Dawe and G.L. Kulak, June 1972.
41. Plastic Design of Steel Frame - Shear Wall Structures by J. Bryson and P.F. Adams, August 1972.
42. Solution Techniques for Geometrically Non-linear Structures by S. Rajasekaran and D.W. Murray, March 1973.
43. Web Slenderness Limits for Compact Beams by N.M. Holtz and G.L. Kulak, March 1973.
44. Inelastic Analysis of Multistory Multibay Frames Subjected to Dynamic Disturbances by M. Suko and P.F. Adams, June 1973.
45. Ultimate Strength of Continuous Composite Beams by S. Hamada and J. Longworth, August 1973.
46. Prestressed Concrete I-Beams Subjected to Combined Loadings by D.L.N. Rao and J. Warwaruk, November 1973.
47. Finite Element Analysis for Combined Loadings with Improved Hexahedrons by D.L.N. Rao and J. Warwaruk, November 1973.
48. Solid and Hollow Rectangular Prestressed Concrete Beams Under Combined Loading by J. Misic and J. Warwaruk, September 1974.
49. The Second-Order Analysis of Reinforced Concrete Frames by S.E. Hage and J.G. MacGregor, October 1974.
50. Web Slenderness Limits for Compact Beam-Columns by M.J. Perlynn and G.L. Kulak, September 1974.
51. Web Slenderness Limits for Non-Compact Beams by N.M. Holtz and G.L. Kulak, August 1975.
52. Decision Table Processing of the Canadian Standards Association Specification S16.1 by S.K.F. Wu and D.W. Murray, February 1976.
53. Web Slenderness Limits for Non-Compact Beam-Columns by D.S. Nash and G.L. Kulak, March 1976.

54. A Monte Carlo Study of the Strength Variability of Rectangular Tied Reinforced Concrete Columns by L.H. Grant and J.G. MacGregor, March 1976.
55. An Elastic Stress Analysis of a Gentilly Type Containment Structure - Volume 1 by D.W. Murray and M. Epstein, April 1976.
56. An Elastic Stress Analysis of a Gentilly Type Containment Structure - Volume 2 - (Appendices B to F) by D.W. Murray and M. Epstein, April 1976.
57. A System of Computer Programs for the Large Deformation In-Plane Analysis of Beams by M. Epstein and D.W. Murray, May 1976.
58. A Statistical Study of Variables Affecting the Strength of Reinforced Normal Weight Concrete Members by S.A. Mirza and J.G. MacGregor, December 1976.
59. The Destabilizing Forces Caused by Gravity Loads Acting on Initially Out-Of-Plumb Members in Structures by D. Beaulieu and P.F. Adams, February 1977.
60. The Second-Order Analysis and Design of Reinforced Concrete Frames by G.S. Mathews and J.G. MacGregor, January 1977.
61. The Effects of Joint Eccentricity in Open Web Steel Joists by R.A. Matiisen, S.H. Simmonds and D.W. Murray, June 1977.
62. Behaviour of Open Web Steel Joists by R.A. Kaliandasani, S.H. Simmonds and D.W. Murray, July 1977.
63. A Classical Flexibility Analysis for Gentilly Type Containment Structures by D.W. Murray, A.M. Rohardt, and S.H. Simmonds, June 1977.
64. Substructure Analysis of Plane Frames by A.A. Elwi and D.W. Murray, June 1977.
65. Strength and Behavior of Cold-Formed HSS Columns by Reidar Bjorhovde, December 1977.
66. Some Elementary Mechanics of Explosive and Brittle Failure Modes in Prestressed Containments by D.W. Murray, June 1978.
67. Inelastic Analysis of Prestressed Concrete Secondary Containments by D.W. Murray, L. Chitnuyanondh, C. Wong and K.Y. Rijub-Agha, July 1978.
68. Strength of Variability of Bonded Prestressed Concrete Beams by D.K. Kikuchi, S.A. Mirza and J.G. MacGregor, August 1978.
69. Numerical Analysis of General Shells of Revolution Subjected to Arbitrary Loading by A.M. Shazly, S.H. Simmonds and D.W. Murray, September 1978.

THE UNIVERSITY OF ALBERTA

NUMERICAL ANALYSIS OF GENERAL SHELLS OF
REVOLUTION SUBJECTED TO ARBITRARY LOADING

by

AHMED MOHAMED EL-SHAZLY

A THESIS

SUBMITTED TO THE FACULTY OF GRADUATE STUDIES AND RESEARCH
IN PARTIAL FULFILMENT OF THE REQUIREMENTS FOR THE DEGREE
OF MASTER OF SCIENCE

DEPARTMENT OF CIVIL ENGINEERING

EDMONTON, ALBERTA

FALL, 1978

ABSTRACT

The governing partial differential equations of a classical shell theory are reduced to a set of eight first order ordinary differential equations. A forward numerical integration process is used to obtain influence coefficients and particular solutions for shells of revolution of general geometric configuration subjected to arbitrary types of loading.

Standard stiffness methods of structural analysis are employed to obtain displacements and stress resultants everywhere within a complex shell structure. A computer program is developed to perform the analysis based on the theory presented. Example problems are selected to test the accuracy of the method. Excellent results, when compared with known solutions, are achieved.

ACKNOWLEDGEMENTS

This study was performed in the Department of Civil Engineering at the University of Alberta. Financial assistance from the National Research Council of Canada is acknowledged.

TABLE OF CONTENTS

CHAPTER	PAGE
1. INTRODUCTION	1
1.1 Introduction	1
1.2 Purpose of the Study	2
1.3 Types of Shells of Revolution	2
1.4 Loadings	4
1.5 Shell Theory	5
1.6 Methods of Analysis	7
1.7 Outline of Contents	11
2. BASIC EQUATIONS	15
2.1 Introduction	15
2.2 Fourier Series	15
2.3 Natural Boundary Conditions	22
2.4 Reduction of the Governing Equations	23
3. STIFFNESS ANALYSIS	40
3.1 Introduction	40
3.2 Influence Coefficients	40
3.3 Shell Element Influence Coefficients	42
3.4 Solution of the Governing System of Equations	44
3.5 Shell Element Stiffness Matrix	48
3.6 Stiffness Matrix Sign Convention	51

CHAPTER		PAGE
3.7	Stress Resultants and Displacements at Intermediate Points	52
3.8	Transformation from Local to Global Coordinates	53
3.9	Modification of the Stiffness Coefficients for Eccentricity	54
4.	EXAMPLE APPLICATIONS	59
4.1	Introduction	59
4.2	Logic Flow of SASHELL	60
4.3	Pinched Cylinder	64
4.4	Hyperboloid Natural Draft Cooling Tower . .	69
4.4.1	Geometry of the Tower	69
4.4.2	Load Description	71
4.4.3	Analysis Conclusions	73
4.5	Comments on Results	74
5.	LIMITATIONS	91
5.1	Introduction	91
5.2	Singularity of the Governing Equations at the Apex	91
5.3	Stability of the Numerical Integration Process	92
5.4	Convergence of Fourier Expansions	95
6.	SUMMARY AND CONCLUSIONS	105
REFERENCES	107

CHAPTER	PAGE
APPENDIX A - SHELL THEORY	110
A.1 Geometry of Shells	110
A.2 Equations of Equilibrium	112
A.3 Strain-Displacement Relations	114
A.4 Stress-Strain Relations	117
A.5 Elastic Law	119
APPENDIX B - USER'S MANUAL FOR SASHELL	131
APPENDIX C - PROGRAM LISTING.	143
APPENDIX D - DATA FILES AND SAMPLE OUTPUT OF EXAMPLE APPLICATIONS	169

LIST OF TABLES

TABLE		PAGE
2.1	Coefficient Matrices B1, B2 and load vector B3 in Eq. 2.14	34
2.2.1	Coefficient matrix A1 in Eq. 2.18	35
2.2.2	Coefficient matrix A2 and load vector A3 in Eq. 2.18	36
2.3.1	Coefficient matrix C1 and load vector C3 in Eq. 2.20	37
4.1	Stresses and radial displacement in a pinched cylinder as per Eqs. 4.6	67
5.1	Effect of length and number of integration points on the accuracy of the solution	100
5.2.1	Fourier coefficients of wind pressure load . . .	101
5.2.2	Effect of number of harmonics on representing the wind pressure load	101
5.3.1	Fourier coefficients of two diametrically opposed concentrated loads	102
	Effect of member of harmonics on representing the two concentrated loads	102

LIST OF FIGURES

Figure	Title	Page
1.1	Plate	12
1.2	Sphere	12
1.3	Cylinder	12
1.4	Cone	13
1.5	Toroid	13
1.6	Ellipsoid	13
1.7	Hyperboloid of revolution	14
1.8	Shell of revolution of arbitrary shape	14
2.1	Effective shearing forces	39
3.1	Shell theory sign convention for stress resultants and displacements	56
3.2	Stiffness matrix sign convention for stress resultants and displacements	57
3.3	Notation for transformation of stress resultants and displacements	58
3.4	Eccentricity at a node	58
4.1	"Pinched cylinder": Circumferential live load	75
4.2	"Pinched cylinder": Two concentrated loads	75
4.3	"Pinched cylinder": Circumferential live load: Stress resultants and radial displacement	76
4.4.1	"Pinched cylinder": Two concentrated loads: Radial displacement ($r = 4.0$ ft)	77

Figure	Title	Page
4.4.2	"Pinched cylinder": Two concentrated loads: Radial displacement ($r = 0.413$ ft)	78
4.5	Typical hyperboloid natural draft cooling tower	79
4.6.1	Wind pressure coefficients c_θ	80
4.6.2	Wind pressure profile ($\theta = 0$)	80
4.7.1	Hyperboloid tower dead load membrane force N_s . .	81
4.7.2	Hyperboloid tower dead load meridional moment M_s	82
4.7.3	Hyperboloid tower dead load membrane force N_θ . .	83
4.8.1	Hyperboloid tower wind load membrane force N_s ($\theta = 0$)	84
4.8.2	Hyperboloid tower wind load meridional moment M_s ($\theta = 0$)	85
4.8.3	Hyperboloid tower wind load membrane force N_θ ($\theta = 0$)	86
4.8.4	Hyperboloid tower wind load circumferential moment M_θ ($\theta = 0$)	87
4.8.5	Hyperboloid tower wind load circumferential variation of N_s	88
4.8.6	Hyperboloid tower wind load circumferential variation of N_θ	88
4.8.7	Hyperboloid tower wind load circumferential variation of S_s	89

Figure	Title	Page
4.8.8	Hyperboloid tower wind load circumferential variation of M_s	89
4.8.9	Hyperboloid tower wind load circumferential variation of W	90
4.8.10	Hyperboloid tower wind load circumferential variation of V and U	90
5.1	Fourier approximation for wind load	103
5.2	Fourier approximation for two diametrically opposed concentrated loads	104
A.1	Meridian and parallel circle of a shell of revolution	124
A.2	Shell element stress resultants and load components	125
A.3.1	Meridional rotation due to displacement V . . .	126
A.3.2	Meridional rotation due to displacement W . . .	126
A.4.1	Meridian of a shell before and after deformation	127
A.4.2	Parallel circle before and after deformation . .	127
A.4.3	Change of the right angle between live elements after deformation	128
A.5	Relation between displacement of two points on live normal to the middle surface	129
A.6	Stresses acting on a shell element	130

NOMENCLATURE

- a = constant and equal to the throat radius of the hyperboloid shell of revolution (Eq. 4.9).
- [A] = flexibility matrix in Eq. 3.2.
- [A₁], [A₂], {A₃}
- = coefficient matrices defined in Table 2.1
- [A_(s)] = coefficient matrix relating the shell fundamental variables and their derivatives at the location s (Eq. 3.5).
- b = constant
- [B₁], [B₂], {B₃}
- = coefficient matrices defined in Tables 2.2.1 and 2.2.2.
- {B_(s)} = column vector of the loading terms in the basic set of equations (Eq. 3.5)
- {c} = column vector of the eight arbitrary constant of integration defined in Eq. 3.9.
- [C₁], [C₂], {C₃}
- = coefficient matrices defined in Tables 2.3.1 and 2.3.2.
- D = extensional rigidity of the shell defined in Eq. A.18.1
- {D} = column vector of the displacements defined in Eq. 2.19.1
- {D*} = derivative of {D} with respect to s (Eq. 2.19.2)
- E = modulus of elasticity.
- [Ec] = eccentricity transformation matrix defined in Eq. 3.31.
- {F_s} = column vector of primary stress resultants defined in Eq. 2.15.1.
- {F_s*} = derivative of {F_s} with respect to s (Eq. 2.15.2)

- $\{F_\theta\}$ = column vector of secondary stress resultants defined
 in Eq. 2.15.3.
- $\{F^0\}$ = column vector of the fixed end forces in Eq. 3.3.
- G = shear modulus defined in Eq. A.13.
- $\{h_{(s)}\}$ = column vector of the homogeneous solution of the eight
 fundamental equations (Eq. 3.6).
- $[H_{(s)}]$ = transfer matrix arises from integrating the inhomogeneous
 terms in the eight fundamental equations (Eq. 3.11).
- K = flexural rigidity of the shell defined in Eq. A.18.2.
- $[K]$ = stiffness matrix
- $[L]$ = transformation matrix from local to global coordinates
 defined in Eq. 3.29.
- M_s, M_θ = meridional and circumferential moments per unit
 length, respectively.
- $M_{s\theta}, M_{\theta s}$ = circumferential and meridional twisting moments per
 unit length, respectively.
- n = harmonic number
- N_s, N_θ = normal in-plane forces per meridional and circumferential
 unit length, respectively.
- $N_{s\theta}, N_{\theta s}$ = in-plane shear forces per meridional and circumferential
 unit length, respectively.
- P_s, P_z, P_θ = intensity of load components in the direction s , z and
 θ respectively.
- Q_s, Q_θ = transverse shear forces per meridional and circumferential
 unit length, respectively.

- $\{Q_{(s)}\}$ = column vector arises from integrating the inhomogeneous terms in the eight fundamental equations (Eq. 3.14).
- r = radius of curvature of parallel circles.
- r_1 = radius of curvature of meridian.
- r_2 = length of the normal between any point on the middle surface and the axis of revolution.
- r_i^* = derivative of r_1 with respect to the coordinate s .
- R = curvature of parallel circles.
- R_1 = first principle curvature = $1/r_1$.
- R_2 = second principle curvature = $1/r_2$.
- s = coordinate measures the distance along the meridian of the shell.
- S_s = effective transverse shearing force per circumferential unit length defined in Eq. 2.6.1.
- t = thickness of the shell.
- T = change in temperature from arbitrary level.
- T_s = effective tangential shearing force per circumferential unit length defined in Eq. 2.6.2.
- T_{o1}, T_{o2} = temperature terms defined in Eq. A.19.1.
- T_{11}, T_{12} = temperature terms defined in Eq. A.19.2.
- T^o, T^i = change in temperature from arbitrary level x measured at the exterior and interior face of the shell, respectively.
- U = displacement component in the circumferential direction.
- V = displacement component in the meridional direction.

- W = displacement component in the rotation direction.
 U_z, V_z, W_z = displacement components of a point at distance z
from the middle surface.
 X = coordinate measures the distance along the axis of
revolution.
 $\{y_{(s)}\}$ = column vector of the eight fundamental variables
(Eq. 3.5).
 $\{y'_{(s)}\}$ = derivative of $\{y_{(s)}\}$ with respect to the coordinate s .
 α = coefficient of thermal expansion.
 β = rotation of the meridian due to deformation.
 γ = specific weight of the shell material.
 $\gamma_{s\theta}, \gamma_{\theta s}$ = shear strain.
 ϵ_s = meridional strain.
 ϵ_θ = hoop strain.
 θ = coordinate measures the angle in the circumferential
direction.
 ν = Poisson's ratio.
 σ_s, σ_θ = normal stresses in the meridional and circumferential
direction, respectively.
 $\tau_{s\theta}, \tau_{\theta s}$ = shearing stresses.
 ϕ = coordinate measures the angle between any point on
the middle surface and the axis of revolution.
 $()^*$ = $\frac{\partial(\)}{\partial s}$
 $()'$ = $\frac{\partial(\)}{\partial \theta}$

CHAPTER 1

INTRODUCTION

1.1 Introductory Remarks

Shells of revolution are important structural elements. Many structures such as storage tanks, pressure vessels, silos, chimneys and towers are composed of either a single shell unit or an assemblage consisting of different types of shells. Their behaviour allows the shell thickness to be reduced to a minimum and their advantageous shapes permit more modern architectural concepts.

Although the governing field equations have been known for many years, cases where analytical solutions can be obtained are relatively scarce and are restricted to simple forms of geometry, boundaries and loads. The determination of the forces and deformations in shells constitutes a difficult problem in the theory of elasticity, owing to the complexity of the mathematical equations involved. For conditions in which the analytical solution is complex, or is unknown, the application of numerical methods with the aid of a digital computer has proven to be useful and efficient. This approach allows the solution for generalized geometric configurations and loadings of shells of revolution.

1.2 Purpose of the Study

The objectives of this thesis are:

- 1) to develop a technique for evaluating the stiffness influence coefficients of any arbitrary element of a shell of revolution of general geometric configuration by means of a direct numerical integration method.
- 2) to employ the standard stiffness method of structural analysis to analyze assemblages of such elements.
- 3) to demonstrate the capability of the method to treat arbitrary surface loadings and thermal gradients, including line and concentrated loads.

1.3 Types of Shells of Revolution

The position of a point in a shell of revolution can be given by three orthogonal coordinates s , θ and z (See Appendix A, Sect. A.1, for definitions). The shape of the shell is determined by specifying the two principal radii of curvature r_1 and r_2 of the middle surface and the thickness of the shell (Fig. A.1). Instead of r_2 it is sometimes convenient to use the distance r from a point on the middle surface to the axis of revolution (Fig. A.1) where

$$r = r_2 \sin\phi$$

1.1

in which ϕ is the angular distance of the point under consideration from the axis of revolution. The generating curve of the middle

surface is defined by the equation

$$r = r(x) \quad 1.2$$

where $r(x)$ represent the radius r as a function of the distance measured along the axis of revolution, x . Therefore the principal radii of curvature can be determined by the following two equations

$$r_1 = \left[1 + \left(\frac{dr}{dx} \right)^2 \right]^{3/2} / \frac{d^2r}{dx^2} \quad 1.3.1$$

$$r_2 = r \left[1 + \left(\frac{dr}{dx} \right)^2 \right]^{1/2} \quad 1.3.2$$

The general shape of any type of shell of revolution (Fig. 1.1 to 1.8) is characterized by particular forms of Eqns. 1.3, as follows:

a) for plates (Fig. 1.1) $r_1 = \infty$ 1.4.1

$$r_2 = \infty \quad 1.4.2$$

$$\phi = 0 \quad 1.4.3$$

b) for spheres (Fig. 1.2) $r_1 = a$ 1.4.4

$$r_2 = a \quad 1.4.5$$

c) for cylinders (Fig. 1.3) $r_1 = \infty$ 1.4.6

$$r_2 = a \quad 1.4.7$$

$$\phi = \pi/2 \quad 1.4.8$$

d) for cones (Fig. 1.4) $r_1 = \infty$ 1.4.9

$$r_2 = \frac{r}{\sin\phi} \quad 1.4.10$$

$$\phi = \text{constant} \quad 1.4.11$$

e) for toroids (Fig. 1.5) $r_1 = a \quad 1.4.12$

$$r_2 = \frac{r}{\sin\phi} \quad 1.4.13$$

f) for ellipsoids (minor axis coincides with the axis of revolution) (Fig. 1.6)

$$r_1 = \frac{a^2 b^2}{(a^2 \sin^2\phi + b^2 \cos^2\phi)^{3/2}} \quad 1.4.14$$

$$r_2 = \frac{a^2}{(a^2 \sin^2\phi - b^2 \cos^2\phi)^{1/2}} \quad 1.4.15$$

g) for hyperboloids (Fig. 1.7)

$$r_1 = \frac{-a^2 b^2}{(a^2 \sin^2\phi - b^2 \cos^2\phi)^{3/2}} \quad 1.4.16$$

$$r_1 = \frac{a^2}{(a^2 \sin^2\phi - b^2 \cos^2\phi)^{1/2}} \quad 1.4.17$$

h) for arbitrary shell elements for which the form of the middle surface cannot be expressed as a closed form function (Fig. 1.8), one can describe r_1 , r_2 and r at discrete points along the meridian and interpolate numerically.

1.4 Loadings

Applied surface loads at any point of the shell can be resolved into three components in the three orthogonal directions s , θ and z . This load may vary in the direction along the meridian as well as in the circumferential direction of the shell. Therefore a load component may be written as a function of the coordinates s and θ in the following form

$$P_i = F_{1i}(s, \theta) \quad 1.5.1$$

where P_i is the magnitude of the load at the point under consideration in the direction $i(i = s, \theta, z)$ and F_{1i} is the function representing the applied load. For the special case of axisymmetric loading P_i is independent of θ , thus

$$P_i = F_{2i}(s) \quad 1.5.2$$

For non-axisymmetrical loading, the classical method of analysis is to expand this load into a Fourier series, analyze for each harmonic separately and superimpose the effects [10,27]. The number of terms considered in this series must be sufficient to give the desired degree of convergence.

Thermal loading can be considered in either case by algebraically adding the strain due to thermal expansion to the strain due to the surface loading in the stress-strain equations.

1.5 Shell Theory

Shell theories of various degrees of complexity may be derived, depending upon the degree to which the theory of linear elasticity is simplified.

In all cases one begins by reducing the three-dimensional shell problem to a two-dimensional problem expressed in terms of the deformation of the middle surface of the shell. Further simplifications establish various shell theories which may be classified into different categories [3]. Such categories are based on the terms that are retained in the strain and stress-

displacement equations with respect to the thickness coordinate.

The second order approximation theory for shells of revolution was presented in 1932 by Flugge [10] and based upon the following assumptions:

- 1) Consistent with the formulation of the classical theory of elasticity, strains and displacements under loads are small enough so that changes in geometry of the shell will not alter the equations of static equilibrium of the shell (i.e., equations of equilibrium are written in the undeformed configuration).
- 2) The components of stress normal to the middle surface are small compared to the other components of stress and may be neglected in the stress-strain relationships (i.e., the material may be considered to be in a plane stress condition).
- 3) Points on lines normal to the middle surface before deformation remain on straight lines normal to the middle surface after deformations (i.e., deformations of the shell due to the radial shears are neglected).

Contrary to other theories, Flugge's theory did not entirely neglect the ratio of the thickness to the radius of curvature (except for an occasional dropping of the fifth and higher order terms) in the stress resultant equations and in the strain-displacement relationships [10, pg. 320].

Applications of this theory have generally been restricted to circular cylindrical shapes, for which some solutions have been obtained [10,16,19] and are considered as standards against which other simplified theories may be compared [16,19].

The fundamental equations of Flugge's theory, upon which this study is based, are presented in Appendix A.

1.6 Methods of Analysis

A structure usually consists of an assemblage of many parts and tends to be complex in nature. Generally, the true structure must be replaced by an idealized approximation, or model, suitable for mathematical analysis. Structural analysis for shells may conveniently be carried out by matrix methods using influence coefficients.

In the literature, the analysis of symmetrically loaded shells of revolution is classically performed using flexibility influence coefficients [3,4,21]. These have been given, in an explicit manner, for very limited number of types of shells of revolution, such as, cylinders, spheres and cones, of uniform thickness.

For symmetrically loaded shells, the membrane solution, which represents the momentless state of stress in the shell, may approximate the particular solution which satisfies the general differential equation of the shell. Using the membrane

solution, a flexibility method of analysis can be performed by satisfying the continuity requirements at the joints at which the elements are connected. When the forces and displacements at these joints are known, the conditions within each element may be determined from the solution of the differential equation of the element.

For the case of arbitrary shells of revolutions, under arbitrary systems of loadings, the corresponding expressions for influence coefficients are unknowns. The analytical method of obtaining these expressions would involve the solution of eighth-order differential equations expressed in terms of the geometry of the shell surface and the physical constants. This method is difficult and complicated, even for a simple geometry such as a cylinder, and it is generally impossible for the case of an arbitrary shell under arbitrary loads. However, the latter case is the rule rather than the exception in modern architecture.

As a consequence of the availability of electronic computers, and the increasing familiarity of engineers with this computational tool, the application of numerical methods of analysis to shell problems has become more attractive.

Two numerical methods for the analysis of shells of revolution with arbitrary configurations have received extensive treatment in the technical literature. The first method is the finite difference method, which consists essentially of the direct replacement of the derivatives which appear in the governing

differential equations by finite difference approximations. This method transforms the differential equations into a system of algebraic equations which may be solved by an iterative procedure [26] or by means of matrix methods [6]. The method is quite general in application. Replacement of the derivatives by finite difference approximations may be undertaken at any level in the basic formulation of the shell problem. However, it is difficult to introduce boundary conditions into the problem. It also becomes cumbersome when attempting to satisfy equations involving high order derivatives [9,12].

The second method is the finite element method. In this method the displacement of each element into which a shell is subdivided are represented by an approximation [9,11,13,20,24]. The most common practice is to represent each shell by a series of short conical shell elements of uniform thickness. The variation in thickness along the generator of the shell, can be accounted for by considering the average thickness of each element [20]. Once these short segments have been defined, the problem becomes one of analyzing a shell that is an assembly of many short conical shells. Stiffness influence coefficients are evaluated using energy methods. Conditions of continuity are then applied at the boundaries of each segment to evaluate the forces and deformations.

An alternative method of numerical analysis based on direct integration of the shell equations, as proposed by

Goldberg, et al [12] for spherical domes and by Iyer and Simmonds [17] for conical shells, is presented for general shells of revolution in this thesis.

In the application of this method to the analysis of shells of revolution under arbitrary loadings, the governing partial differential equations of a consistent shell theory are expanded by means of Fourier series. Differentiation with respect to the colatitude coordinate θ may be performed to transform the governing equations to ordinary differential equations. These equations are reduced to a set of eight first-order ordinary differential equations involving eight intrinsic dependent variables and their derivatives. The intrinsic variables are the three components of displacement at the middle surface, the rotation of the tangent to the meridian, the membrane normal force in the meridian direction, the moment acting on circumferential sections and two modified shear terms in the directions perpendicular and tangent to the meridian.

This system of equations can be integrated in a stepwise fashion across a given element. By performing matrix operations, which will be described in Chapter 3, the stiffness influence coefficients can be calculated. Fixed end forces can be obtained and stiffness analysis may then be performed to determine the conditions at the element boundaries. These conditions can be used to determine the forces and deformation everywhere within the shell element.

1.7 Outline of Contents

The governing equations of the classical theory of shells of revolution are reduced to a set of eight basic equations in Chapter 2. In Chapter 3, the solution technique for the basic equations is described. Standard stiffness methods for segmented shell structures are outlined. Two example problems are handled in Chapter 4. General types of loadings are considered. In Chapter 5, limitations of the technique are discussed. Conclusions are drawn and possible future developments are outlined in Chapter 6.

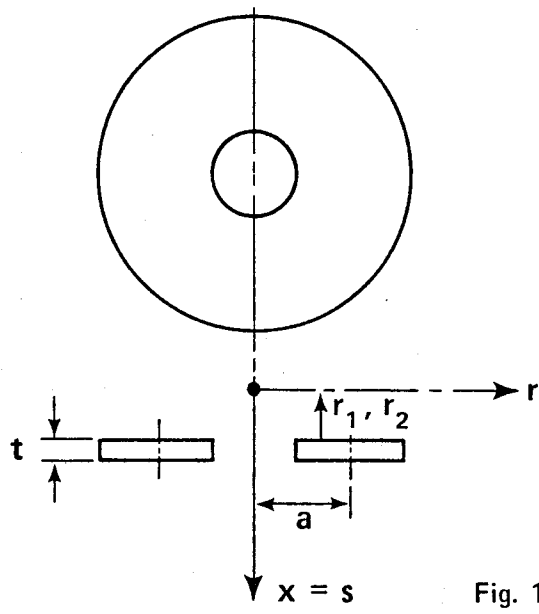


Fig. 1.1 Plate

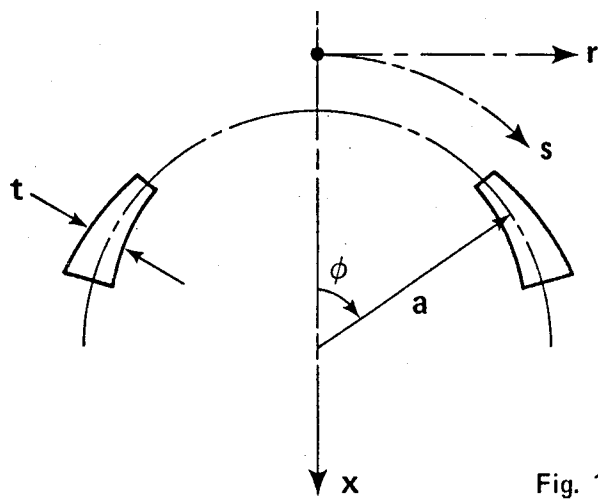


Fig. 1.2 Sphere

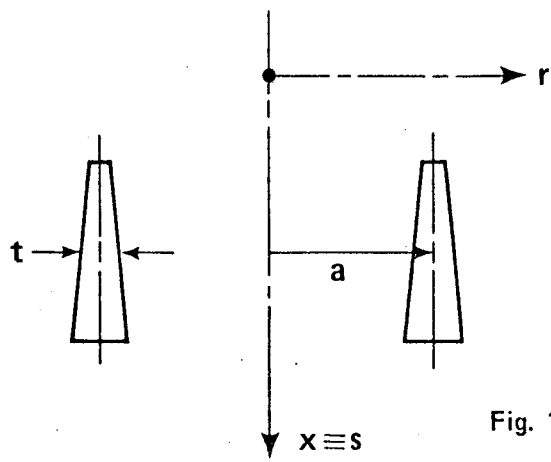


Fig. 1.3 Cylinder

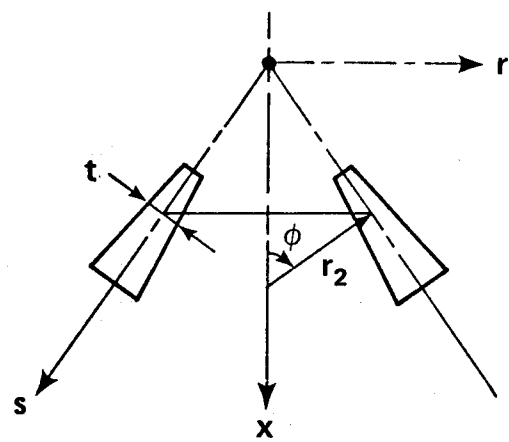


Fig. 1.4 Cone

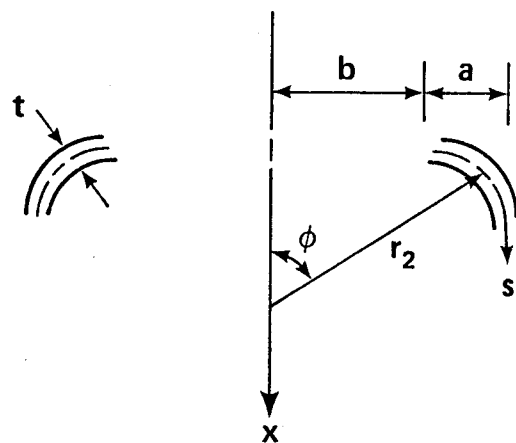


Fig. 1.5 Toroid

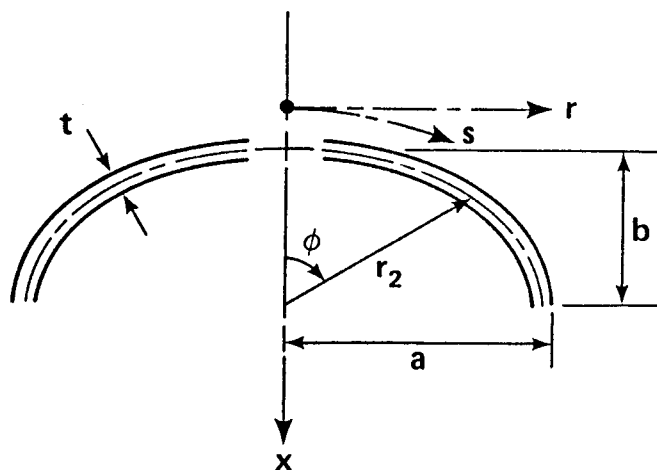


Fig. 1.6 Ellipsoid

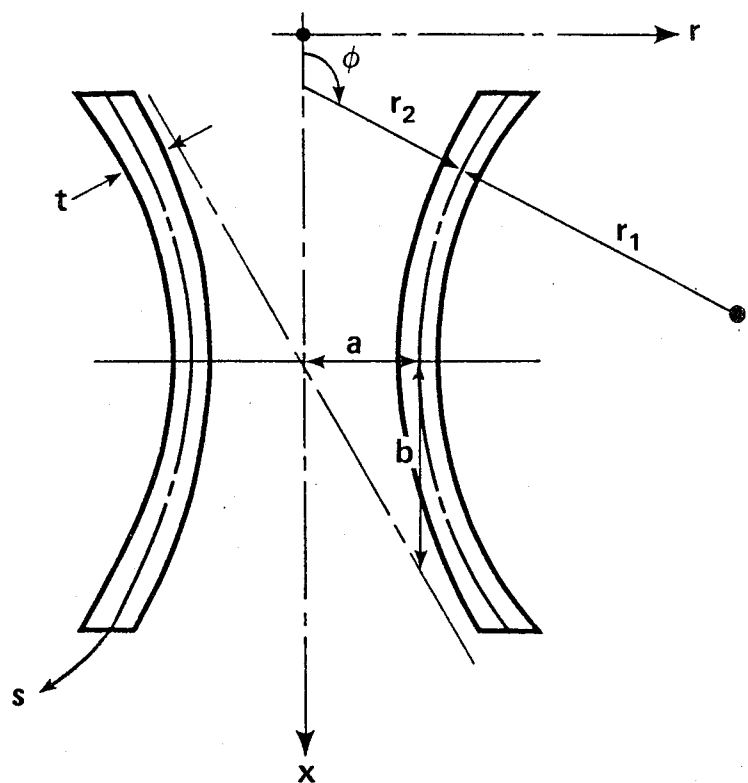


Fig. 1.7 Hyperboloid of Revolution

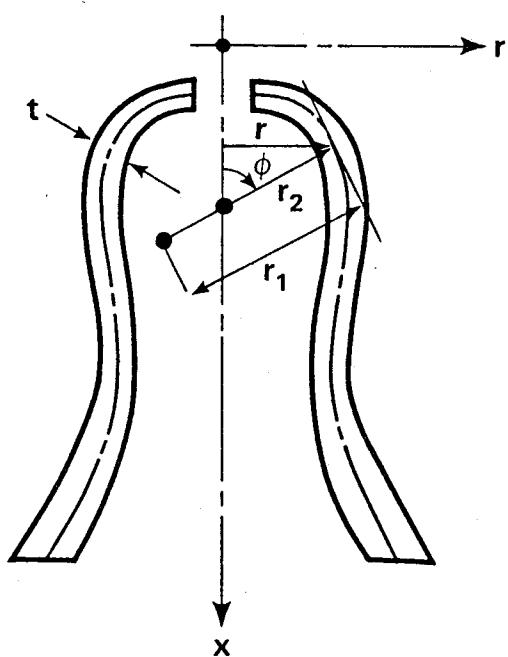


Fig. 1.8 Shell of Revolution of Arbitrary Shape

CHAPTER 2

BASIC EQUATIONS

2.1 Introduction

In this chapter the governing field equations of a shell of revolution, as derived in Appendix A, are expanded using Fourier series. Modified shear terms are introduced into the governing equations to eliminate the inplane shearing force in the circumferential direction and the meridional twisting moment, which appear at the boundaries $s = \text{constant}$. By performing matrix operations to eliminate the stress resultants in the circumferential direction (secondary stress resultants) the governing field equations are reduced to a set of eight first order equations involving four stress resultants (primary stress resultants) and four displacements and their derivatives.

2.2 Fourier Series

The load components and temperature, being arbitrary functions of s and θ , may always be represented in the form

$$P_s = \sum_{n=0}^{\infty} P_{sn}(s) \cos n\theta + \sum_{n=1}^{\infty} \bar{P}_{sn}(s) \sin n\theta \quad 2.1.1$$

$$P_\theta = \sum_{n=0}^{\infty} \bar{P}_{\theta n}(s) \cos n\theta + \sum_{n=1}^{\infty} P_{\theta n}(s) \sin n\theta \quad 2.1.2$$

$$P_z = \sum_{n=0}^{\infty} P_{zn}(s) \cos n\theta + \sum_{n=1}^{\infty} \bar{P}_{zn}(s) \sin n\theta \quad 2.1.3$$

$$T = \sum_{n=0}^{\infty} T_n(s) \cos n\theta + \sum_{n=1}^{\infty} \bar{T}_n(s) \sin n\theta \quad 2.1.4$$

where P_s , P_θ and P_z are defined in Appendix A, T represents temperature, and the functions of s on the right hand side are Fourier coefficients [10,27]. The corresponding stress resultants and displacements may be expressed as

$$N_s = \sum_{n=0}^{\infty} N_{sn}(s) \cos n\theta + \sum_{n=1}^{\infty} \bar{N}_{sn}(s) \sin n\theta \quad 2.2.1$$

$$N_\theta = \sum_{n=0}^{\infty} N_{\theta n}(s) \cos n\theta + \sum_{n=1}^{\infty} \bar{N}_{\theta n}(s) \sin n\theta \quad 2.2.2$$

$$N_{s\theta} = \sum_{n=0}^{\infty} \bar{N}_{s\theta n}(s) \cos n\theta + \sum_{n=1}^{\infty} N_{s\theta n}(s) \sin n\theta \quad 2.2.3$$

$$N_{\theta s} = \sum_{n=0}^{\infty} \bar{N}_{\theta sn}(s) \cos n\theta + \sum_{n=1}^{\infty} N_{\theta sn}(s) \sin n\theta \quad 2.2.4$$

$$Q_s = \sum_{n=0}^{\infty} Q_{sn}(s) \cos n\theta + \sum_{n=1}^{\infty} \bar{Q}_{sn}(s) \sin n\theta \quad 2.2.5$$

$$Q_\theta = \sum_{n=0}^{\infty} \bar{Q}_{\theta n}(s) \cos n\theta + \sum_{n=1}^{\infty} Q_{\theta n}(s) \sin n\theta \quad 2.2.6$$

$$M_s = \sum_{n=0}^{\infty} M_{sn}(s) \cos n\theta + \sum_{n=1}^{\infty} \bar{M}_{sn}(s) \sin n\theta \quad 2.2.7$$

$$M_\theta = \sum_{n=0}^{\infty} M_{\theta n}(s) \cos n\theta + \sum_{n=1}^{\infty} \bar{M}_{\theta n}(s) \sin n\theta \quad 2.2.8$$

$$M_{s\theta} = \sum_{n=0}^{\infty} \bar{M}_{s\theta n}(s) \cos n\theta + \sum_{n=1}^{\infty} M_{s\theta n}(s) \sin n\theta \quad 2.2.9$$

$$M_{\theta s} = \sum_{n=0}^{\infty} \bar{M}_{\theta sn}(s) \cos n\theta + \sum_{n=1}^{\infty} M_{\theta sn}(s) \sin n\theta \quad 2.2.10$$

$$U = \sum_{n=0}^{\infty} U_n(s) \cos n\theta + \sum_{n=1}^{\infty} \bar{U}_n(s) \sin n\theta \quad 2.2.11$$

$$V = \sum_{n=0}^{\infty} V_n(s) \cos n\theta + \sum_{n=1}^{\infty} \bar{V}_n(s) \sin n\theta \quad 2.2.12$$

$$W = \sum_{n=0}^{\infty} W_n(s) \cos n\theta + \sum_{n=1}^{\infty} \bar{W}_n(s) \sin n\theta \quad 2.2.13$$

where the variables on the left hand side are defined in Appendix A, Sects. A.2 and A.3, and where the term (s) indicates that the variable coefficients with subscript n are functions of the coordinate s only and n is the harmonic number. The first and the second series in each expression represent the portions of the variables which are, respectively, symmetric and anti-symmetric with respect to the meridian passing through the line $\theta = 0$.

For an arbitrary applied load expressed as a Fourier series of the order N (Eqs. 2.1.1 to 2.1.3), there are $2N+1$ terms that represent each component of load; ($n = 0, 1, 2, \dots, N$) for the symmetric series and ($n = 1, 2, \dots, N$) for the anti-symmetric series. For each value of n the (s dependent) variables with the subscript n from each series can be entered in the governing equations of shells of revolution of Appendix A, because the sequences $\cos n\theta$ and $\sin n\theta$ are linearly independent. Differentiations with respect to θ can be performed and the terms grouped according to the common factors, $\cos n\theta$ or $\sin n\theta$. Since the coefficient of each of these factors must be zero, each

factor produces a separate equation. For example, Eqn. A.5.1 is

$$rN_s^* + \cos\phi N_s + N_{\theta s} - \cos\phi N_{\theta} - \frac{r}{r_i} Q_s + rP_s = 0 \quad 2.3.1$$

for which, for any n, the cosine terms become

$$\begin{aligned} & rN_{sn}^* \cos n\theta + \cos\phi N_{sn} \cos n\theta + nN_{\theta sn} \cos n\theta \\ & - \cos\phi N_{\theta n} \cos n\theta - \frac{r}{r_i} Q_{sn} \cos n\theta + rP_{sn} \cos n\theta = 0 \end{aligned} \quad 2.3.2$$

which, upon factoring out the common term, yields

$$\begin{aligned} & rN_{sn}^* + \cos\phi N_{sn} + n N_{\theta sn} - \cos\phi N_{\theta n} - \frac{r}{r_i} Q_{sn} \\ & + rP_{sn} = 0 \end{aligned} \quad 2.3.3$$

If the Fourier expansions of Eqs. 2.1 and 2.2 are truncated such that $0 \leq n \leq N$, the governing system of equations is replaced by $(2N+1)$ ordinary differential systems of equations, each equation of the type illustrated by Eq. 2.3.3, and an analysis is carried out to obtain the solutions for the s dependent coefficients corresponding to each value of n. In the general case there are twenty-six variable coefficients associated with each $n > 0$ in Eqns. 2.2, thirteen associated with each of the factors.

Finally, since linear stress-displacement relations were assumed, the principle of superposition is valid and one can superimpose the $(2N+1)$ solutions so obtained.

The n^{th} set of equations can be written as follows.

The six equilibrium equations are obtained from Eqs. A.5 as

$$N_{sn}^* + R \cos \phi N_{sn} \pm R_n N_{\theta sn} - R \cos \phi N_{\theta n} - R_1 Q_{sn} + P_{sn} = 0 \quad 2.4.1$$

$$N_{s\theta n}^* + R \cos \phi N_{s\theta n} \mp R_n N_{\theta n} + R \cos \phi N_{\theta sn} - R_2 Q_{\theta n} + P_{\theta n} = 0 \quad 2.4.2$$

$$R_2 N_{\theta n} + R_1 N_{sn} \pm R_n Q_{\theta n} + Q_{sn}^* + R \cos \phi Q_{sn} - P_{zn} = 0 \quad 2.4.3$$

$$M_{sn}^* + R \cos \phi M_{sn} \pm R_n M_{\theta sn} - R \cos \phi M_{\theta n} - Q_{sn} = 0 \quad 2.4.4$$

$$M_{s\theta n}^* + R \cos \phi M_{s\theta n} \mp R_n M_{\theta n} + R \cos \phi M_{\theta sn} - Q_{\theta n} = 0 \quad 2.4.5$$

$$N_{\theta sn} - N_{s\theta n} - R_2 M_{\theta sn} + R_1 M_{s\theta n} = 0 \quad 2.4.6$$

where R_1 and R_2 are the principal curvatures of the shell, defined as the reciprocals of the radii of curvature r_1 and r_2 , respectively, and R is the curvature of the parallel circle.

The eight stress-displacement equations are obtained from Eqs. A17 as

$$\begin{aligned} N_{sn} &= [K R_1 (R_1 - R_2) r_1^*] \beta_n - [K(R_1 - R_2)] \beta_n^* \\ &+ [D(R_1 + vR_2) + K R^2 r_1 (R_1 - R_2)] W_n \end{aligned}$$

$$\begin{aligned}
 & + [vDR\cos\phi - KR^2_1(R_1 - R_2)r_1]V_n \\
 & + [D + KR_1(R_1 - R_2)]V_n^* \pm [vDRn]U_n \\
 & - [(1 + v)\alpha D]T_{o_2 n} \quad 2.5.1
 \end{aligned}$$

$$\begin{aligned}
 N_{\theta nn} &= [KR(R_1 - R_2) \cos\phi]\beta_n \\
 & + [D(R_2 + vR_1) + K(R_1 - R_2)(R^2 n^2 - R^2_2)]W_n \\
 & + [DR\cos\phi - KRR_2\cos\phi(R_1 - R_2)]V_n \\
 & + [vD]V_n^* \pm [DRn]U_n \\
 & - [(1 + v)\alpha D]T_{o_1 n} \quad 2.5.2
 \end{aligned}$$

$$\begin{aligned}
 N_{s\theta nn} &= \frac{1 - v}{2} \{ \pm [KR(R_1 - R_2)n]\beta_n \\
 & \pm [KR^2\cos\phi(R_1 - R_2)n]W_n \\
 & \mp [DRn + KRR_1(R_1 - R_2)n]V_n \\
 & - [DR\cos\phi - K\cos\phi(R_1 - R_2)^2]U_n \\
 & + [D + K(R_1 - R_2)^2]U_n^* \} \quad 2.5.3
 \end{aligned}$$

$$\begin{aligned}
 N_{\theta sn} &= \frac{1 - v}{2} \{ \pm [KR(R_1 - R_2)n]\beta_n \\
 & \mp [KR^2\cos\phi(R_1 - R_2)n]W_n \\
 & \mp [DRn - KRR_2(R_1 - R_2)n]V_n \\
 & - [DR\cos\phi]U_n + [D]U_n^* \} \quad 2.5.4
 \end{aligned}$$

$$M_{sn} = [KR_1r_1 - vKR\cos\phi]\beta_n - [K]\beta_n^*$$

$$\begin{aligned}
 & + [K R_1 (R_1 - R_2) - \nu K R^2 n^2] W_n \\
 & - [K R^2 r_1] V_n + [K(R_1 - R_2)] V_n^* \\
 & + [\nu K R R_2 n] U_n + [(1 + \nu) \alpha K] T_{12n} \quad 2.5.5
 \end{aligned}$$

$$\begin{aligned}
 M_{\theta n} = & [\nu K R_1 r_1^* - K R \cos \phi] \beta_n - [\nu K] \beta_n^* \\
 & - [K R^2 n^2 + K R_2 (R_1 - R_2)] W_n \\
 & - [\nu K R_1 r_1^* + K R \cos \phi (R_1 - R_2)] V_n \\
 & + [K R R_1 n] U_n + [(1 + \nu) \alpha K] T_{11n} \quad 2.5.6
 \end{aligned}$$

$$\begin{aligned}
 M_{s\theta n} = & \frac{1 - \nu}{2} \{ \pm [2 K R n] \beta_n \pm [2 K R^2 n \cos \phi] W_n \\
 & \mp [K R R_1 n] V_n - [K R \cos \phi (R_1 - 2R_2)] U_n \\
 & + [K(R_1 - 2R_2)] U_n^* \} \quad 2.5.7
 \end{aligned}$$

$$\begin{aligned}
 M_{\theta sn} = & \frac{1 - \nu}{2} \{ \pm [2 K R n] \beta_n \pm [2 K R^2 n \cos \phi] W_n \\
 & \mp [K R R_2 n] V_n + [K R R_2 \cos \phi] U_n \\
 & - [K R_2] U_n^* \} \quad 2.5.8
 \end{aligned}$$

where Eqs. A.7 have been used to eliminate the first and second derivatives of the displacement component W .

Eqs. 2.4 and 2.5 are fourteen equations in terms of the thirteen unknown functions (the variable Fourier series coefficients). As such the system of equations is overspecified. In the theory developed herein, Eq. 2.4.6 is discarded and the

remaining thirteen equations allow the solution for the thirteen functions associated with each trigonometric functions of the Fourier series expansion.

2.3 Natural Boundary Conditions

According to the classical theory of shells, the quantities which appear in the natural boundary conditions on an edge $s = \text{constant}$ of a shell of revolution are the four displacements β, W, V, U and the corresponding four forces M_s, S_s, N_s, T_s .

The forces S_s, T_s are the transverse and tangential effective shears which are commonly known as Kirchhoff's shears [27]. The Kirchhoff shears are work-equivalent forces associated with the displacements W and U , and these effective shears replace the stress resultants $Q_s, N_{s\theta}$ and $M_{s\theta}$. Such replacement is essential to describe simple boundary conditions [10,27]. Although the expressions for these forces may be derived rigorously from variational principles, the following physical interpretation, due to Kelvin and Tait [27, pg.45], is more instructive. If the twisting moment $M_{s\theta}$ acting on an infinitesimally small element of the shell is replaced by a statically equivalent force as shown in Fig. 2.1, one can write from statics the expression for the effective transverse shearing force as [27]

$$S_s = Q_s + \frac{M'_{s\theta}}{r}$$

2.6.1

and the effective tangential shearing force as

$$T_s = N_{s\theta} - \frac{M_{s\theta}}{r_2} \quad 2.6.2$$

Writing Eqs. 2.6.1 and 2.6.2 in Fourier series terms, and separating the linearly independent terms, we may define

$$S_{sn} = Q_{sn} \pm \frac{nM_{s\theta n}}{r} \quad 2.7.1$$

$$T_{sn} = N_{s\theta n} - \frac{M_{s\theta n}}{r_2} \quad 2.7.2$$

Using the geometrical relations in Eqs. A.2, the derivatives of these forces with respect to the coordinate s may be written as

$$S'_{sn} = Q'_{sn} \pm Rn M'_{s\theta n} + R^2 n \cos \phi M_{s\theta n} \quad 2.8.1$$

$$\begin{aligned} T'_{sn} &= N'_{s\theta n} - \frac{r_2 M'_{s\theta n} - M_{s\theta n} r'^2}{r'^2} \\ &= M'_{s\theta n} - R_2 M'_{s\theta n} - R_2 (R_1 - R_2) \cot \phi M_{s\theta n} \end{aligned} \quad 2.8.2$$

$$2.8.2$$

2.4 Reduction of the Governing Equations

It can be seen that the stress resultants Q_θ , N_θ , M_θ , $M_{\theta s}$ and $N_{\theta s}$ do not enter into any boundary conditions on an edge for which $s = \text{constant}$. Therefore, it is preferable to

$$M_s = F_{11}(\beta, \beta^*, w, v, v^*, u, T_{12}) \quad 2.10.5$$

$$M_\theta = F_{12}(\beta, \beta^*, w, v, u, T_{11}) \quad 2.10.6$$

$$M_{s\theta} = F_{13}(\beta, w, v, u, u^*) \quad 2.10.7$$

$$M_{\theta s} = F_{14}(\beta, w, v, u, u^*) \quad 2.10.8$$

where the form of the functions F_1 to F_{14} is obtained from Eqs.

2.4 and 2.5. In addition, Eqs. A.7.1, 2.7 and 2.8, which will be called auxiliary equations, may be written in the following symbolic form,

$$\beta = F_{15}(w^*, v) \quad 2.11.1$$

$$S_s = F_{16}(Q_s, M_{s\theta}) \quad 2.11.2$$

$$T_s = F_{17}(N_{s\theta}, M_{s\theta}) \quad 2.11.3$$

$$S_s^* = F_{18}(Q_s^*, M_{s\theta}^*, M_{s\theta}) \quad 2.11.4$$

$$T_s^* = F_{19}(N_{s\theta}^*, M_{s\theta}^*, M_{s\theta}) \quad 2.11.5$$

It should be noted that for shells with equal radii of curvature (i.e., $r_1 = r_2$), the sixth equation of equilibrium Eq. 2.4.6 will be an identity as

$$N_{s\theta} = N_{\theta s}$$

$$M_{s\theta} = M_{\theta s}$$

Therefore, this equation will be discarded, as mentioned in

eliminate them in terms of the other stress resultants and evaluate them after the solution of the governing equations.

For convenience, the subscript n in Fourier coefficients will be omitted and the governing equations (Eqs. 2.4 and 2.5) can be written, for each set of equations, in the following symbolic form. The equilibrium equations (Eqs. 2.4) may be written symbolically as:

$$F_1 (N_s^*, N_s, N_{\theta s}, N_\theta, Q_s, P_s) = 0 \quad 2.9.1$$

$$F_2 (N_{s\theta}^*, N_{s\theta}, N_\theta, N_{\theta s}, Q_\theta, P_\theta) = 0 \quad 2.9.2$$

$$F_3 (N_\theta, N_s, Q_\theta, Q_s^*, Q_s, P_z) = 0 \quad 2.9.3$$

$$F_4 (M_s^*, M_s, M_{\theta s}, M_\theta, Q_s) = 0 \quad 2.9.4$$

$$F_5 (M_{s\theta}^*, M_{s\theta}, M_\theta, M_{\theta s}, Q_\theta) = 0 \quad 2.9.5$$

$$F_6 (N_{\theta s}, N_{s\theta}, M_{\theta s}, M_{s\theta}) = 0 \quad 2.9.6$$

The stress resultant-displacement equations (Eqs. 2.5) may be written symbolically as:

$$N_s = F_7(\beta, \beta^*, W, V, V^*, U, T_{o_2}) \quad 2.10.1$$

$$N_\theta = F_8(\beta, W, V, V^*, U, T_{o_1}) \quad 2.10.2$$

$$N_{s\theta} = F_9(\beta, W, V, U, U^*) \quad 2.10.3$$

$$M_{\theta s} = F_{10}(\beta, W, V, U, U^*) \quad 2.10.4$$

Appendix A, Sect. A.5 and as noted in Sect. 2.3.

In solving the above equations, the displacements which may be physically imposed on the boundary of a shell are β , W , V and U . The external forces associated with these displacements (in a work-equivalent sense) are M_s , S_s , N_s and T_s . The first set of variables are specified in the case of displacement boundary conditions while the latter set is specified in the case of mechanical or force boundary conditions. In general a combination of four of these eight quantities must be specified to properly define a boundary condition, provided that if one of the displacements is specified the associated force should not be specified and vice-versa. Since the remaining five of the thirteen variables cannot be determined at the boundary, it is desirable to eliminate them from the governing equations. The objective in the following is, therefore, to reduce the thirteen governing equations (Eqs. 2.9.1 to 2.9.5 and Eqs. 2.10) to a set of eight governing equations in terms of the eight variables which may arise in the specification of the boundary conditions. It is also desirable to keep the order of these differential equations to a minimum in order to facilitate the numerical solution. The final set of equations will be of first order.

Combining Eq. 2.9.1 and Eq. 2.11.2 to eliminate Q_s , one can get

$$N_s^* = R_1 S_s - R \cos \phi N_s + RR_1 M_{s\theta} + R \cos \phi N\theta + R_n N_{\theta s} - P_s$$

Using Eqs. 2.9.2 and 2.9.5 to eliminate Q_θ and then substituting for $M_{s\theta}$, $N_{s\theta}$, $N'_{s\theta}$ by means of Eqs. 2.11.3 and 2.11.5, one can write

$$\begin{aligned} T_s^* &= -R \cos \phi T_s \mp RR_2 n M_\theta + RR_2 \cos \phi M_{\theta s} \\ &\quad - R \cos \phi (R_1 - R_2) M_{s\theta} \pm Rn N_\theta \\ &\quad - R \cos \phi N_{\theta s} - P_\theta \end{aligned} \quad 2.12.2$$

Eqs. 2.9.4 and 2.11.2, after eliminating Q_s are in the form

$$\begin{aligned} M_s^* &= -R \cos \phi M_s + S_s + R \cos \phi M_\theta \\ &\quad \mp Rn M_{\theta s} \mp Rn M_{s\theta} \end{aligned} \quad 2.12.3$$

Using Eq. 2.9.3, after eliminating Q_θ by means of Eq. 2.9.5, together with Eqs. 2.11.2 and 2.11.4 results in the equation

$$\begin{aligned} S_s^* &= -R \cos \phi S_s - R_1 N_s + R^2 n^2 M_\theta \mp R^2 n \cos \phi M_{\theta s} \\ &\quad \mp R^2 n \cos \phi M_{s\theta} - R_2 N_\theta + P_z \end{aligned} \quad 2.12.4$$

Eqs. 2.12, which represent the equilibrium equations, may now be written symbolically as

$$M_s^* = F_{20} (M_s, S_s, M_\theta, M_{\theta s}, M_{s\theta}) \quad 2.13.1$$

$$S^*_{\text{s}} = F_{21} (S_{\text{s}}, N_{\text{s}}, M_{\theta}, M_{\theta\text{s}}, M_{s\theta}, N_{\theta}, P_z) \quad 2.13.2$$

$$N^*_{\text{s}} = F_{22} (S_{\text{s}}, N_{\text{s}}, M_{s\theta}, N_{\theta}, N_{\theta\text{s}}, P_s) \quad 2.13.3$$

$$T^*_{\text{s}} = F_{23} (T_{\text{s}}, M_{\theta}, M_{\theta\text{s}}, M_{s\theta}, N_{\theta}, N_{\theta\text{s}}, P_{\theta}) \quad 2.13.4$$

or in matrix notation

$$\{F^*_{\text{s}}\} = [B1 \quad B2] \begin{Bmatrix} F_{\text{s}} \\ F_{\theta} \end{Bmatrix} + \{B3\} \quad 2.14$$

where the loading terms in these equations are separated in the vector $\{B3\}$, and

$$\langle F_{\text{s}} \rangle = \langle M_{\text{s}} \quad S_{\text{s}} \quad N_{\text{s}} \quad T_{\text{s}} \rangle \quad 2.15.1$$

$$\langle F^*_{\text{s}} \rangle = \langle M^*_{\text{s}} \quad S^*_{\text{s}} \quad N^*_{\text{s}} \quad T^*_{\text{s}} \rangle \quad 2.15.2$$

$$\langle F_{\theta} \rangle = \langle M_{\theta} \quad M_{\theta\text{s}} \quad M_{s\theta} \quad N_{\theta} \quad N_{\theta\text{s}} \rangle \quad 2.15.3$$

The coefficients of the matrices $[B1]$, $[B2]$ and $\{B3\}$ are defined in Table 2.1

In Eq. 2.14, the stress resultants have been separated into the vector $\langle F_{\text{s}} \rangle$, whose components are desired in the final formulation, and the vector $\langle F_{\theta} \rangle$, which remains to be eliminated from the formulation.

Let us now turn our attention to the displacement variables. Eqs. 2.10.1 and 2.10.5, which are two equations in

β^* , v^* , can be converted to the following two equations

$$\begin{aligned}\beta^* &= \frac{1}{CA_2} \left\{ -\left[\frac{CA_1}{K} \right] M_s + [R_1 - R_2] N_s \right. \\ &\quad + [R_1 r^*_1 CA_2 - v R \cos \phi CA_1] \beta \\ &\quad - [v D R_2 (R_1 - R_2) + v R^2 n^2 CA_1] W \\ &\quad - [R_1^2 r^*_1 CA_2 + v D R \cos \phi (R_1 - R_2)] V \\ &\quad \left. \mp [v R R_1 n CA_2] U + (1 + v)\alpha [D(R_1 - R_2) T_{o2} + CA_1 T_{12}] \right\} \\ &\quad 2.16.1\end{aligned}$$

in which

$$CA_1 = D + K R_1 (R_1 - R_2) \quad 2.16.2$$

$$CA_2 = D + K R_2 (R_1 - R_2) \quad 2.16.3$$

and

$$\begin{aligned}v^* &= \frac{1}{CA_2} \left\{ -[R_1 - R_2] M_s + N_s \right. \\ &\quad - [v K R \cos \phi (R_1 - R_2)] \beta \\ &\quad - [CA_2 R_1 + v D R_2 + v K R^2 n^2 (R_1 - R_2)] W \\ &\quad - [v D R \cos \phi] V \mp [v R n CA_2] U \\ &\quad \left. + (1 + v)\alpha [DT_{o2} + K(R_1 - R_2) T_{12}] \right\} \\ &\quad 2.16.4\end{aligned}$$

Eq. 2.11.1 is in the form

$$W^* = -\beta + R_1 V \quad 2.16.5$$

Finally, Eq. 2.10.3, after eliminating $N_{s\theta}$ by means of Eq. 2.11.3 can be written as

$$\begin{aligned} U^* = & \frac{1}{CA_3} \left\{ \left[\frac{2}{1-v} \right] T_s \mp [KR_n(R_1 - 3R_2)]\beta \right. \\ & \mp [KR^2 n \cos \phi (R_1 - 3R_2)]W \pm [R_n CA_1 - K RR_1 R_2 n]V \\ & \left. + [R \cos \phi CA_3]U \right\} \end{aligned} \quad 2.16.6$$

in which

$$CA_3 = D + K(R^2_1 - 3R_1 R_2 + 3R^2_2) \quad 2.16.7$$

Eqs. 2.16.1, 2.16.4, 2.16.5 and 2.16.6 can be written in a symbolic form as

$$\beta^* = F_{24}(\beta, W, V, U, M_s, N_s, T_{o2}, T_{12}) \quad 2.17.1$$

$$W^* = F_{25}(\beta, V) \quad 2.17.2$$

$$V^* = F_{26}(\beta, W, V, U, M_s, N_s, T_{o2}, T_{12}) \quad 2.17.3$$

$$U^* = F_{27}(\beta, W, V, U, T_s) \quad 2.17.4$$

or can be written in matrix notation as

$$\{D^*\} = [A1 \quad A2] \begin{Bmatrix} D \\ F_s \end{Bmatrix} + \{A3\} \quad 2.18$$

where

$$\langle D \rangle = < \beta \quad W \quad V \quad U > \quad 2.19.1$$

$$\langle D^* \rangle = < \beta^* \quad W^* \quad V^* \quad U^* > \quad 2.19.2$$

The coefficients of the matrices [A1], [A2] and the column vector {A3} are shown in Tables 2.2.

The stress resultants appearing in the vector $\langle F_\theta \rangle$ of Eq. 2.15.3 can be expressed in terms of the fundamental displacements by selecting Eqs. 2.10.2, 2.10.4, 2.10.6, 2.10.7 and 2.10.8 and writing them in matrix notation

$$\{F_\theta\} = [C1 \quad C2] \begin{Bmatrix} D^* \\ D \end{Bmatrix} + \{C3\} \quad 2.20$$

where $\{F_\theta\}$, $\{D\}$ and $\{D^*\}$ are defined in Eqs. 2.15.3, 2.19.1 and 2.19.2 respectively, and the coefficients of [C1], [C2] and {C3} are defined in Tables 2.3.

The three sets of equations (Eqs. 2.14, 2.18 and 2.20) can now be used to form a set of eight first order differential equations relating the eight fundamental variables; four displacements β , W , V , U , and four corresponding forces M_s , S_s , N_s , T_s and their derivatives. By substituting Eq. 2.20 into Eq. 2.14, to replace $\{F_\theta\}$

$$\{F^*_{s}\} = [B1]\{F_s\} + [B2] \left\{ [C1]\{D^*\} + [C1]\{D\} + \{C3\} \right\} + \{B3\} \quad 2.21.1$$

and by substituting for $\{D^*\}$, from Eq. 2.18,

$$\begin{aligned} \{F^*_{s}\} &= [B1]\{F_s\} + [E1] \left\{ [A1]\{D\} + [A2]\{F_s\} + \{A3\} \right\} \\ &\quad + [E2]\{D\} + \{E3\} \end{aligned} \quad 2.21.2$$

or

$$\{F^*_{s}\} = [G1]\{D\} + [G2]\{F_s\} + \{G3\} \quad 2.22$$

where

$$[E1] = [B2][C1] \quad 2.23.1$$

$$[E2] = [B2][C2] \quad 2.23.2$$

$$\{E3\} = [B2]\{C3\} + \{B3\} \quad 2.23.3$$

$$[G1] = [E1][A1] + [E2] \quad 2.23.4$$

$$[G2] = [E1][A2] + [B1] \quad 2.23.5$$

$$\{G3\} = [E1]\{A3\} + \{E3\} \quad 2.23.6$$

Eq. 2.18 and Eq. 2.22, can be combined into one matrix equation as

$$\begin{aligned} \begin{Bmatrix} D^* \\ F^*_{s} \end{Bmatrix} &= \begin{bmatrix} A1 & A2 \\ G1 & G2 \end{bmatrix} \begin{Bmatrix} D \\ F_s \end{Bmatrix} + \begin{Bmatrix} A3 \\ G3 \end{Bmatrix} \\ &= [GA] \begin{Bmatrix} D \\ F_s \end{Bmatrix} + \{GB\} \end{aligned} \quad 2.24$$

Therefore, for the applied loads, stresses and displacements being periodic functions of the coordinate θ , the general governing partial differential equations, Eqs. A.5 and Eqs. A.17, have been transformed into a system of eight first order ordinary differential equations for each harmonic member n . These equations relate, at any point, the eight fundamental dependent variables, that appear in the natural boundary conditions of shells of revolution, and their derivatives with respect to the independent variable s .

As was seen, the reduction of the shell equation into this form involves only straight forward algebraic manipulations. The equations have been put in this form to facilitate numerical integration. They can be integrated with the aid of an appropriate integration technique, such as the Runge-Kutta process. Since a digital computer is needed to perform this integration, the reduction of the equations to the final form, as in Eq. 2.24, is not necessary and can be performed by feeding the three sets of equations (Eqs. 2.14, 2.18 and 2.20) into the computer.

It can be seen that the elements of the matrix GA in Eq. 2.24 are dependent only on the shell thickness, the physical constants and the coordinate s . It should be noted that in the case of shell of revolution under symmetrical loading conditions (i.e., $n = 0$) the system of the eight equations reduces naturally to a system of six first order equations as the displacement component U and the corresponding force T_s vanish due to the symmetry of the applied load.

TABLE 2.1 Coefficients of Matrices B1, B2 and Load Vector B3 in Eq. 2.14

Matrix B1 Matrix B2 Vector B3

$-R \cos \phi$		$R \cos \phi$	$\mp Rn$	$\mp Rn$	
$-R \cos \phi$	$-R_1$	$R^2 n^2$	$\mp R^2 n \cos \phi$	$\mp R^2 n \cos \phi$	$-R_2$
R_1	$-R \cos \phi$			$\mp RR_1 n$	$R \cos \phi \quad \mp Rn$
		$\mp RR_2 n$	$RR_2 \cos \phi$	$-R \cos \phi$ $(R_1 - R_2)$	$\pm Rn \quad -R \cos \phi$
					$-P_\theta$

$R_1 r^* - \nu R \cos \phi$	$\frac{CA_1}{CA_2}$	$-\nu \frac{DR_2(R_1 - R_2)}{CA_2}$	$-R^2 r^* R_1$	$\mp \nu R R_1 n$
		$-\nu R^2 n^2 \frac{CA_1}{CA_2}$	$-\nu D \frac{R \cos \phi}{CA_2} (R_1 - R_2)$	
-1			R_1	
$-\nu K \frac{R \cos \phi}{CA_2} (R_1 - R_2)$	$-R_1 - \frac{\nu D R_2}{CA_2}$	$-\nu \frac{D R}{CA_2} \cos \phi$	$\mp \nu R n$	
	$-\nu K \frac{R^2 n^2}{CA_2} (R_1 - R_2)$			
$\mp K \frac{R n}{CA_3} (R_1 - 3R_2)$	$\mp K \frac{R^2 n \cos \phi}{CA_3} (R_1 - 3R_2)$	$\pm R n \frac{CA_1}{CA_3}$	$R \cos \phi$	
		$-K \frac{R R_1 R_2}{CA_3} n$		

TABLE 2.2.1 Coefficients of Matrix A1 in Eq. 2.18

$-\frac{CA_1}{K \cdot CA_2}$	$\frac{R_1 - R_2}{CA_2}$	$\frac{(1 + \nu)\alpha}{CA_2} \{ D(R_1 - R_2) T_{o2} + CA_1 T_{12} \}$
$-\frac{(R_1 - R_2)}{CA_2}$	$\frac{1}{CA_2}$	$\frac{(1 + \nu)\alpha}{CA_2} \{ K(R_1 - R_2) T_{12} + DT_{o2} \}$
	$(\frac{2}{1 - \nu}) \frac{1}{CA_3}$	

Matrix A2

Vector A3

TABLE 2.2.2 Coefficient of Matrix A2 and Load Vector A3 in Eq. 2.18

$-\nu K$		$(1 + \nu) \alpha K T_{11}$
		$-(\frac{1 - \nu}{2}) K R_2$
		$(\frac{1 - \nu}{2}) \{K(R_1 - R_2)\}$
		$-(1 + \nu) \alpha D T_{01}$
νD		$(\frac{1 - \nu}{2}) D$

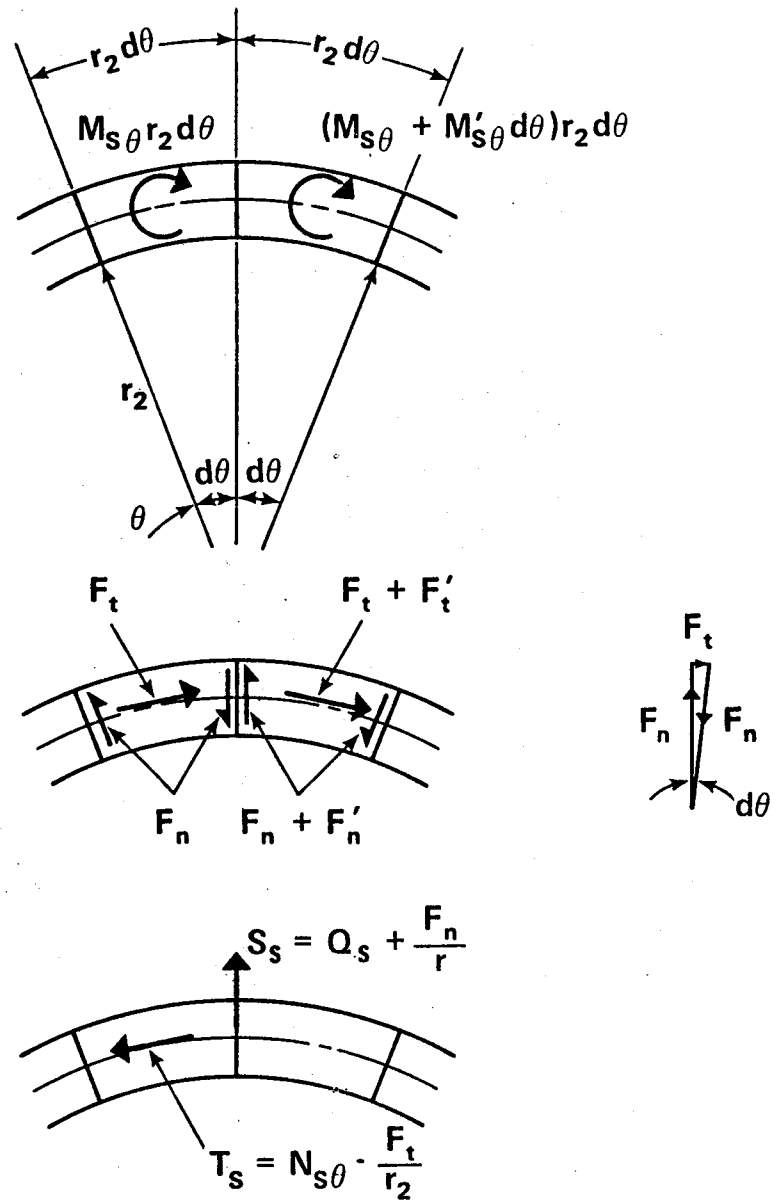
Matrix C1

Vector C3

TABLE 2.3.1 Coefficients of Matrix C1 and Load Vector C3 in
Eq. 2.20

$\nu K R_1 r_1^* - K R \cos \phi$	$- K R^2 n^2 - K R_2 (R_1 - R_2)$ $- K R \cos \phi (R_1 - R_2)$	$- \gamma K R_1^2 r_1^*$ $- K R \cos \phi (R_1 - R_2)$	$\mp K R R_1 n$
$\pm (\frac{1-\nu}{2}) (2K Rn)$	$\mp (\frac{1-\nu}{2}) (2K R^2 n \cos \phi)$	$\mp (\frac{1-\nu}{2}) (K R R_2 n)$	$(\frac{1-\nu}{2}) (K R R_2 \cos \phi)$
$\mp (\frac{1-\nu}{2}) (2K Rn)$	$(\frac{1-\nu}{2}) (2K R^2 n \cos \phi)$	$\mp (\frac{1-\nu}{2}) (K R R_1 n)$	$-(\frac{1-\nu}{2}) (K R \cos \phi (R_1 - 2R_2))$
$K R \cos \phi (R_1 - R_2)$	$D(R_2 + \nu R_1)$ $+ K(R_1 - R_2)(R^2 n^2 - R_2^2)$	$R \cos \phi \{D - K R_2 (R_1 - R_2)\}$	$\pm D R n$
$\mp (\frac{1-\nu}{2}) \{K R n (R_1 - R_2)\}$	$\mp (\frac{1-\nu}{2}) \{K R^2 n \cos \phi (R_1 - R_2)\}$	$\mp (\frac{1-\nu}{2}) \{Rn[D - K(R_1 - R_2)^2]\}$	$-(\frac{1-\nu}{2}) D R \cos \phi$

TABLE 2.3.2 Coefficients of Matrix C2 in Eq. 2.20



* F_n, F_t are the Equivalent Static Forces of $M_{S\theta}$

Fig. 2.1 Effective Shearing Forces

CHAPTER 3

STIFFNESS ANALYSIS

3.1 Introduction

This chapter describes how the standard methods of structural analysis can be employed to obtain a complete solution in terms of the stresses and the displacements at any point within a complex structure composed of many elements of any type of shell of revolution, using the eight fundamental equations derived in Chapter 2.

3.2 Influence Coefficients

If a perfectly elastic structural component, supported against rigid body motion, is acted upon by a set of forces $F_1, F_2, F_3, \dots, F_n$ at points 1, 2, 3, ..., n and if in addition to this set of forces, intermediate loads are applied simultaneously to the structural member, the induced deformation d_i at the point i due to the forces F_j ($j = 1, 2, 3, \dots, n$) can be expressed in the form

$$d_i = \sum_{j=1}^n a_{ij} F_j + d_i^0 \quad 3.1$$

where d_i^0 is the additional deformation at point i due to the intermediate applied loads and a_{ij} represents the deflection d_i due to a unit value of F_j . The elastic constants a_{ij} are

independent of the magnitude of the applied forces F_j . Eq. 3.1, which represent the linear relation of deformations and forces, can be written in matrix form as

$$\{d\} = [A]\{F\} + \{d^0\} \quad 3.2$$

where the square matrix $[A]$ is known as the flexibility matrix.

For the same problem the relation given in Eq. 3.2 can also be written in a form which represents the equilibrium conditions for the structure as

$$\begin{aligned} \{F\} &= [K]\{d - d^0\} \\ &= [K]\{d\} + \{F^0\} \end{aligned} \quad 3.3$$

where the square matrix $[K]$ is defined the element stiffness matrix. The element K_{ij} is defined as the force F_j due to unit displacement at d_j . $\{F^0\}$ is the column vector $\{F^0_1, F^0_2, \dots, F^0_n\}$ which are the equivalent forces that replace the intermediate applied loads (equivalent in the sense that the work done during any incremental deformation approximates the work done by the actual applied load). These forces are numerically equal to the so-called fixed end forces.

As stated above, while establishing the flexibility matrix the structure is assumed to be supported against rigid body motion, a condition not necessary for the stiffness matrix. For the latter case the structure can be free to move as a rigid

body when a set of nodal displacements is applied. The stiffness matrix, thus obtained, is called "the direct stiffness matrix" which is singular. The elements in any column represent a force system in equilibrium.

The well known advantage of the direct stiffness method is that for an assembly of structural elements, the total structural stiffness matrix can be easily formed by superposition of the individual stiffness matrices irrespective of the boundary conditions. The boundary conditions are considered only after assembly in the actual solution of the system of equations. This permits the consideration of different boundary conditions while the total structure stiffness matrix remains unaltered.

3.3 Shell Element Influence Coefficients

By a procedure similar to that used for a beam element, the stiffness matrix for an element of shell of revolution can be obtained. Since the shell element is a rotationally symmetric element, the nodal points are replaced with nodal circles (Fig. 3.1). The forces and displacements can be expressed as the amplitude of a harmonic number along the nodal circles.

Consider the shell element shown in Fig. 3.1. The eight fundamental stress resultants per unit length at the two edges of the element are shown acting in the positive sense according to the shell theory sign convention. Should the edge $s = a$ of the element be subjected to a unit value of displacement

in the direction of W while preventing any other displacement of the two ends of the element, the forces per unit length that would be required to maintain equilibrium of the element are the influence coefficients for a unit displacement W_a . If one writes the degrees of freedom of the element in the order $\beta_a \ W_a \ v_a \ U_a \ \beta_b \ W_b \ v_b \ U_b$, the element stiffness equation (Eq. 3.3) can be written as

$$\left\{ \begin{array}{l} M_{sa} \\ S_{sa} \\ N_{sa} \\ T_{sa} \\ M_{sb} \\ S_{sb} \\ N_{sb} \\ T_{sb} \end{array} \right\} = [K] \left\{ \begin{array}{l} \beta_a \\ W_a \\ V_a \\ U_a \\ \beta_b \\ W_b \\ V_b \\ U_b \end{array} \right\} + \left\{ \begin{array}{l} M^o_{sa} \\ S^o_{sa} \\ N^o_{sa} \\ T^o_{sa} \\ M^o_{sb} \\ S^o_{sb} \\ N^o_{sb} \\ T^o_{sb} \end{array} \right\} \quad 3.4$$

where M^o_s , S^o_s , N^o_s , T^o_s are the fixed end stress resultants, at the ends a or b as subscripted, due to the applied loads or thermal gradients.

In order to establish the stiffness matrix and the fixed end stresses, the predetermination of the relationship between the edge displacements and the edge forces is necessary. The stiffness coefficients and fixed end forces for a beam element can be evaluated by the well known method, such as consistent deformation, or solving the pertinent differential equations.

If an analytical solution of the relevant differential equations for a specific geometry of shells is known, both influence coefficients and fixed end forces due to the applied loads can be found. Such a solution is not available for an arbitrary element of shells of revolution with variable thickness and subjected to arbitrary loadings. However, the forces can be evaluated by solving the basic differential equations numerically.

3.4 Solution of the Governing System of Equations

For any given shell element with given geometry and applied load, the governing system of equations (Eq. 2.24) is in the form

$$\{y^*(s)\} = [A(s)]\{y(s)\} + \{B(s)\} \quad 3.5$$

where $\{y(s)\}$ is a vector of the eight dependent variables, four displacements and four corresponding forces, at a particular location $s = \text{constant}$; $\{y^*(s)\}$ is a vector of the derivatives of the eight variables with respect to the coordinate s , i.e., $d/ds\{y(s)\}$; $[A(s)]$ is the coefficient matrix relating the variables and their derivatives and consists only of functions of the shell thickness and the geometrical parameters of the location s ; and, $\{B(s)\}$ is a vector of the inhomogeneous terms in the equations and is a function of the applied loads and the location s .

The general solution of Eq. 3.5 consists of two parts:

- 1) The solution of the homogeneous part of the equations, i.e., the differential equations when all loading terms, $\{B_{(s)}\}$, are set equal to zero. This homogeneous solution involves the evaluation of eight constants of integration as the result of eight boundary conditions at the two discontinuous edges of the shell.
- 2) The particular solution of the equations in which all loading terms are considered. This solution does not depend upon the boundary conditions.

Therefore, the general solution that satisfies the governing system of equations together with the appropriate boundary conditions at the two edges of the shell element can be written as

$$\{y_{(s)}\} = \{h_{(s)}\} + \{P_{(s)}\} \quad 3.6$$

where $\{P_{(s)}\}$ represents the particular solution that satisfies the equation.

$$\{P^*_{(s)}\} = [A_{(s)}] \{P_{(s)}\} + \{B_{(s)}\} \quad 3.7$$

and, $\{h_{(s)}\}$ is the homogeneous solution that satisfies the equation.

$$\{h^*(s)\} = [A(s)]\{h_{(s)}\} \quad 3.8$$

Consider now the solution of Eq. 3.8 for an element which spans the region $b \geq s \geq a$. Since Eq. 3.8 represents eight first order linear differential equations, the solution should contain eight arbitrary constants of integration. Let these arbitrary constants of integration be the eight (arbitrary) boundary values which can be imposed at edge "a", and denote these values by $\{c\}$. Then at edge "a"

$$\{h_{(a)}\} = \{c\} \quad 3.9$$

Substituting into Eq. 3.8 yields, for $s = a$

$$\{h^*(s)\}_{s=a} = [A(s)]_{s=a} \{c\} \quad 3.10$$

Integrating this numerically, as an initial value problem, allows the value of $h_{(s)}$ at any point $s > a$ to be determined as

$$\{h_{(s)}\} = [H(s)]\{c\} \quad 3.11$$

where $[H(s)]$ represents the matrix arising from the integration of the $[A(s)]$ matrix along the length of the element.

Since the matrix $[H_{(s)}]$ is independent of the initial conditions ($\{c\}$), it is a property of the element and may be interpreted as follows. As $\{c\}$ is arbitrary, assign a unit value to one component, say component c_j , and set the others equal to zero. Then the j^{th} column of $[H_{(s)}]$ represents the values of $\{h_{(s)}\}$ for a unit value of the j^{th} boundary condition at "a". It is apparent that when $s = a$, Eq. 3.11 must reduce to Eq. 3.9 in order to match the arbitrary boundary conditions, and hence $[H_{(a)}]$ must be the identity matrix, i.e.

$$[H_{(a)}] = [I] \quad 3.12$$

Eq. 3.12 may be considered to be a "boundary condition" on the numerical integration of the matrix $[H]$.

Turning now to the solution of Eq. 3.7, the equation at $s = a$ may be written as

$$\{P^*(s)\}_{s=a} = [A_{(s)}]_{s=a} \{c^*\} + \{B_{(s)}\} \quad 3.13$$

where $\{c^*\}$ represents an arbitrary set of initial values of $\{P_{(a)}\}$. Numerical integration of this equation yields

$$\{P(s)\} = [H_{(s)}] \{c^*\} + \{Q_{(s)}\} \quad 3.14$$

where $[H_{(s)}]$ is the matrix that arises in Eq. 3.11 and $\{Q_{(s)}\}$ is a vector arising from the integration of the inhomogeneous terms. Since the particular solution is any solution which

satisfies the inhomogeneous equations it is adequate to select

$$\{c^*\} = 0 \quad 3.15$$

in which case Eq. 3.14 reduces to

$$\{P_{(s)}\} = \{Q_{(s)}\} \quad 3.16$$

and consequently the general solution, Eq. 3.6, becomes

$$\{y_{(s)}\} = [H_{(s)}]\{c\} + \{Q_{(s)}\} \quad 3.17$$

For $s = b$, Eq. 3.17 becomes

$$\{y_{(b)}\} = [H_{(b)}]\{y_{(a)}\} + \{Q_{(b)}\} \quad 3.18$$

in which each column vector of $[H]$ represents the variables at "b" corresponding to each unit variable applied at "a" in the absence of any applied loads. The vector $\{Q\}$ represents the variables at "b" corresponding to zero displacements and stresses resultants at "a" in the presence of the applied loads.

3.5 Shell Element Stiffness Matrix

The column vector $\{y_{(s)}\}$ represents the vector of Eq. 2.24 consisting of the four displacements as defined by Eq. 2.15.1 and the four stress resultants as defined by Eq. 2.19.1.

Let

$$\{y_{(a)}\} = \begin{Bmatrix} D_a \\ F_a \end{Bmatrix} \quad 3.19$$

and

$$\{y_{(b)}\} = \begin{Bmatrix} D_b \\ F_b \end{Bmatrix} \quad 3.20$$

Eq. 3.18 can be written in partitioned form as

$$\begin{Bmatrix} D_b \\ F_b \end{Bmatrix} = \begin{bmatrix} H_1 & H_2 \\ H_3 & H_4 \end{bmatrix} \begin{Bmatrix} D_a \\ F_a \end{Bmatrix} + \begin{Bmatrix} Q_d \\ Q_f \end{Bmatrix} \quad 3.21$$

where

D represents the four displacement variables,

F represents the four stress resultant variables, and

Q_d , Q_f are the displacement and the stress resultant parts of the particular solution respectively.

The total matrix appearing in Eq. 3.21 is usually referred to as a "transfer matrix" [23]. Eq. 3.21 can be expanded to form two equations as follow

$$\begin{Bmatrix} D_a \\ D_b \end{Bmatrix} = \begin{bmatrix} I & 0 \\ H_1 & H_2 \end{bmatrix} \begin{Bmatrix} D_a \\ F_a \end{Bmatrix} + \begin{Bmatrix} 0 \\ Q_d \end{Bmatrix}$$

$$= [Y_1] \begin{Bmatrix} D_a \\ F_a \end{Bmatrix} + \begin{Bmatrix} 0 \\ Q_d \end{Bmatrix} \quad 3.22$$

and

$$\begin{Bmatrix} F_a \\ F_b \end{Bmatrix} = \begin{bmatrix} 0 & I \\ H_3 & H_4 \end{bmatrix} \begin{Bmatrix} D_a \\ F_a \end{Bmatrix} + \begin{Bmatrix} 0 \\ Q_f \end{Bmatrix}$$

$$= [Y_2] \begin{Bmatrix} D_a \\ F_a \end{Bmatrix} + \begin{Bmatrix} 0 \\ Q_f \end{Bmatrix} \quad 3.23$$

Solving Eq. 3.22 for the vector $\langle D_a \ F_a \rangle^T$ and substituting into Eq. 3.23, yields

$$\begin{Bmatrix} F_a \\ F_b \end{Bmatrix} = [Y_2] [Y_1]^{-1} \begin{Bmatrix} D_a \\ D_b - Q_d \end{Bmatrix} + \begin{Bmatrix} 0 \\ Q_f \end{Bmatrix} \quad 3.24$$

or

$$\begin{Bmatrix} F_a \\ F_b \end{Bmatrix} = [K] \begin{Bmatrix} D_a \\ D_b \end{Bmatrix} + \begin{Bmatrix} F^o_a \\ F^o_b \end{Bmatrix} \quad 3.25$$

It can be seen that each column of $[K]$ represents the stress resultants at each end for a unit displacement applied at one end while the other displacements are restrained and $\{F^o\}$ represents the stress resultants corresponding to the totally restrained boundaries.

3.6 Stiffness Matrix Sign Convention

In the derivation of the element stiffness matrix and the fixed end stresses, the sign convention used corresponds to that generally used in shell theory as given in Fig. 3.1. As a result, the stiffness matrix will have some negative elements on the main diagonal. This can be corrected by adapting the so called "stiffness matrix sign convention". This sign convention is shown in Fig. 3.2. It can be seen that the positive direction of the top normal in plane force N_s , the top tangential shearing force T_s , the bottom moment M_s and the bottom transverse shear S_s have been changed to the opposite direction. Therefore, the stiffness matrix and fixed end stresses in Eq. 3.25 are to be premultiplied by the diagonal matrix

$$\begin{bmatrix} 1 & & & \\ & 1 & & \\ & & -1 & \\ & & & -1 \\ & & & & -1 \\ & & & & & 1 \\ & & & & & & 1 \end{bmatrix}$$

3.7 Stress Resultants and Displacements at Intermediate Points

For a shell structure composed of a number of elements, the element stiffness matrices and fixed end forces are evaluated and assembled in the master stiffness equations of the structure. Boundary conditions are imposed, and the displacements at the boundaries of each element are obtained from the solution of the master equations. By substituting the final known boundary displacements of each element into the corresponding element stiffness equation (Eq. 3.25), the primary stress resultants at the element boundaries can be obtained. Thus the correct boundary conditions, displacements and primary stress resultants, for each element are known. In order to evaluate the displacements and the stress resultants at any desired number of intermediate points within the element, the correct boundary conditions at one end of the element, say the end at $s = a$, are used as initial conditions in integrating the governing set of equations (Eq. 3.5). At each intermediate point, the secondary stress resultants (which were eliminated from the governing equations) can be evaluated, first by evaluating the derivatives of the displacements using Eq. 2.18.

$$\{D^*\} = [A1]\{D\} + [A2]\{F_s\} + \{A3\} \quad 3.26$$

and then substituting into Eq. 2.20

$$\{F_\theta\} = [C1]\{D^*\} + [C2]\{D\} + \{C3\} \quad 3.27$$

A simple check on the results of the integration is that the displacements and the primary stress resultants at the termination end of the element should agree exactly with the known boundary conditions at this end.

3.8 Transformation from Local to Global Coordinates

Displacements and stress resultants, at any point along the generator, are presented in the direction tangent to the meridian at this point and the direction perpendicular to it. Due to possible discontinuity of the meridian curve at a junction between two elements, it is necessary to transform the influence coefficients and the fixed end forces at this junction, to a new coordinates system. It is simplest to adopt the direction of the structure's axis of revolution, x , and the direction perpendicular to it, r . According to the stiffness matrix sign convention, the transformation equations may be written as follow

$$\{D_L\} = [L]\{D_G\} \quad 3.28.1$$

$$\{F_G\} = [L]^T\{F_L\} \quad 3.28.2$$

where

$$[L] = \begin{bmatrix} 1 & 0 & 0 \\ 0 & \sin \phi_i & -\cos \phi_i \\ 0 & \cos \phi_i & \sin \phi_i \\ 0 & 0 & 0 \end{bmatrix} \quad 3.29$$

$\{D\}$ and $\{F\}$ represent the displacement and forces respectively and the subscripts L, G represent local and global coordinates.

ϕ_i is the angle measured from the global axis of rotation to the meridian at the point $s = i$ (Fig. 3.3).

3.9 Modification of Stiffness Coefficients to Account for Eccentricity

In many cases the middle surfaces of two elements which meet at a node do not coincide at the same point (Fig. 3.4).

A transformation of the stiffness coefficients and fixed end stresses to a common reference point is then necessary before assembling the element stiffness matrices into the master stiffness matrix. Eqs. A.10 relate the displacement components of a point at a distance z from the middle surface to the displacement components of a point on the middle surface lying in the same plane. By expanding Eqs. A.10, by means of Fourier series, one can write the following equation

$$\begin{Bmatrix} \beta_z \\ w_z \\ v_z \\ u_z \end{Bmatrix} = \begin{bmatrix} 1 & 0 & 0 & 0 \\ 0 & 1 & 0 & 0 \\ z & 0 & 1 & 0 \\ 0 & \frac{nz}{r} & 0 & \frac{r_2+z}{r_2} \end{bmatrix} \begin{Bmatrix} \beta \\ w \\ v \\ u \end{Bmatrix} \quad 3.30$$

where Eq. A.7.1 has been used to eliminate the derivative of w with respect to s and the subscript z refers to the point at a

distance z from the middle surface. Inverting Eq. 3.30 results in

$$\begin{Bmatrix} \beta \\ W \\ V \\ U \end{Bmatrix} = \begin{bmatrix} 1 & 0 & 0 & 0 \\ 0 & 1 & 0 & 0 \\ -z & 0 & 1 & 0 \\ 0 & \frac{-nr_2z}{r(r_2+z)} & 0 & \frac{r_2}{r_2+z} \end{bmatrix} \begin{Bmatrix} \beta_z \\ W_z \\ V_z \\ U_z \end{Bmatrix} \quad 3.31$$

or

$$\{D\} = [EC]\{D_z\} \quad 3.32$$

From the work equivalence requirements, the relation between the stresses at the two points can be written as

$$\{F_z\} = [EC]^T\{F\} \quad 3.33$$

Eq. 3.32 and 3.33 are used to transform the displacements and stresses of a point on the middle surface to a point at a distance z from the middle surface.

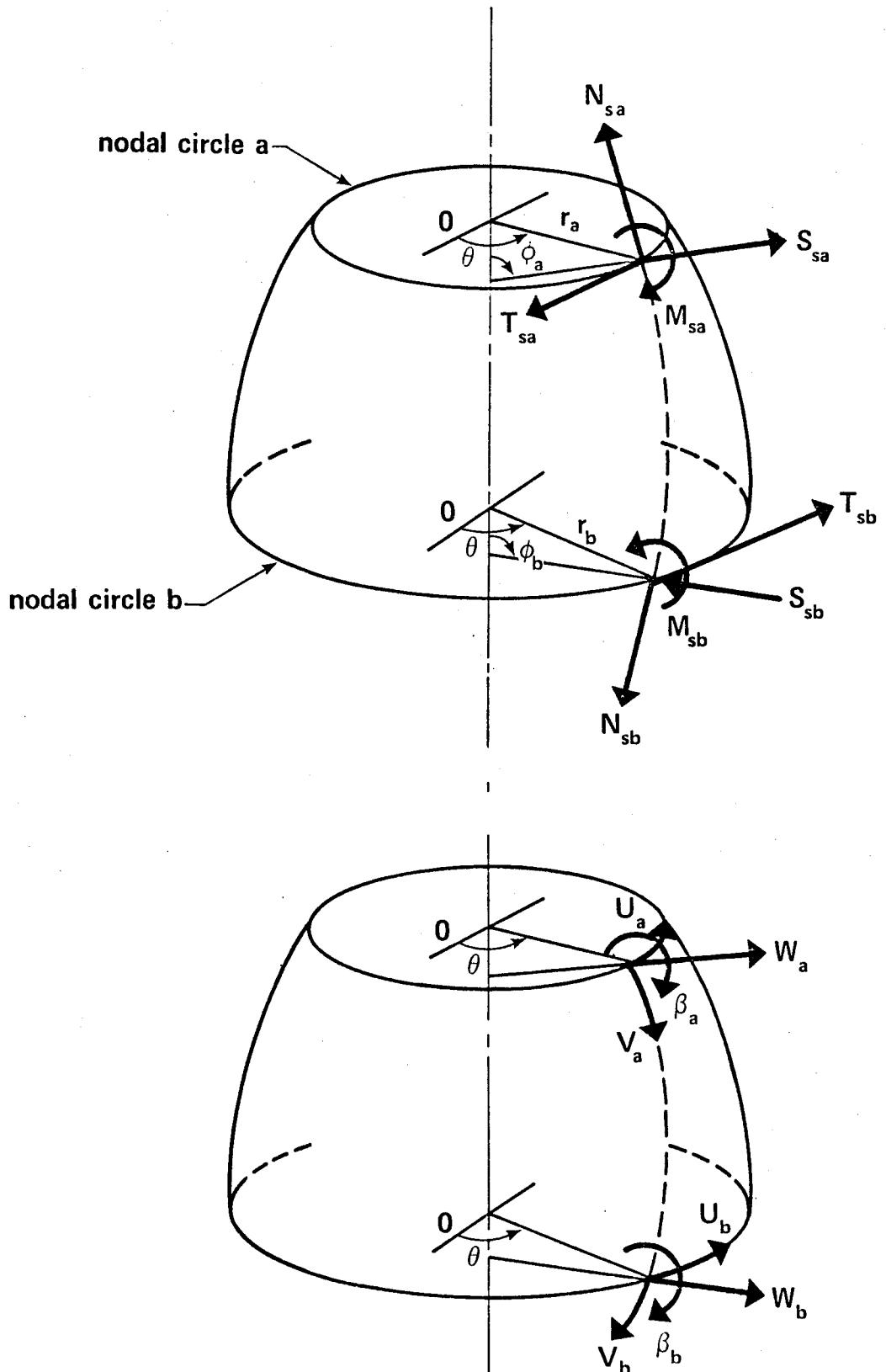


Fig. 3.1 Shell Theory Sign Convention for Stress Resultants and Displacements

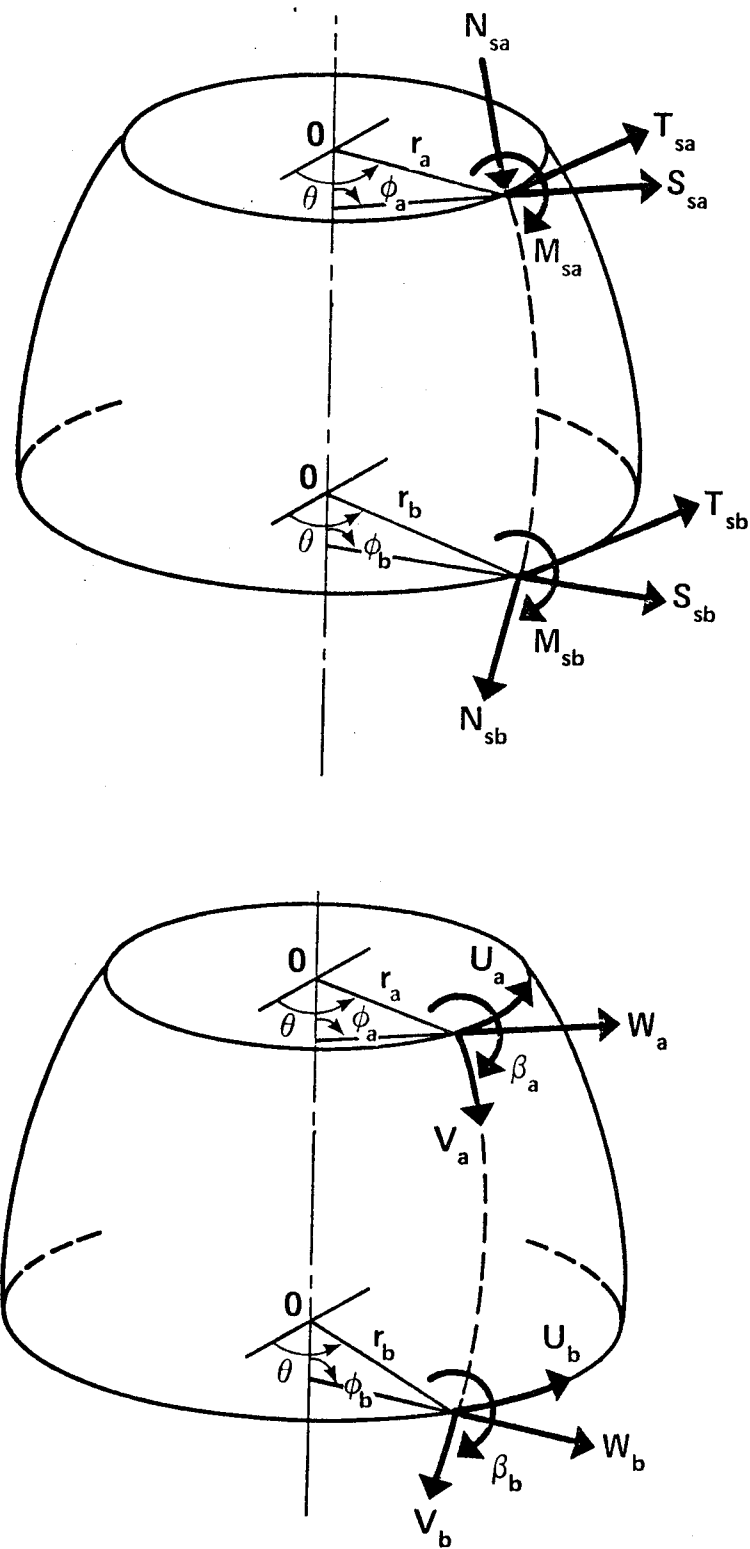


Fig. 3.2 Stiffness Matrix Sign Convention for Stress Resultants and Displacements.

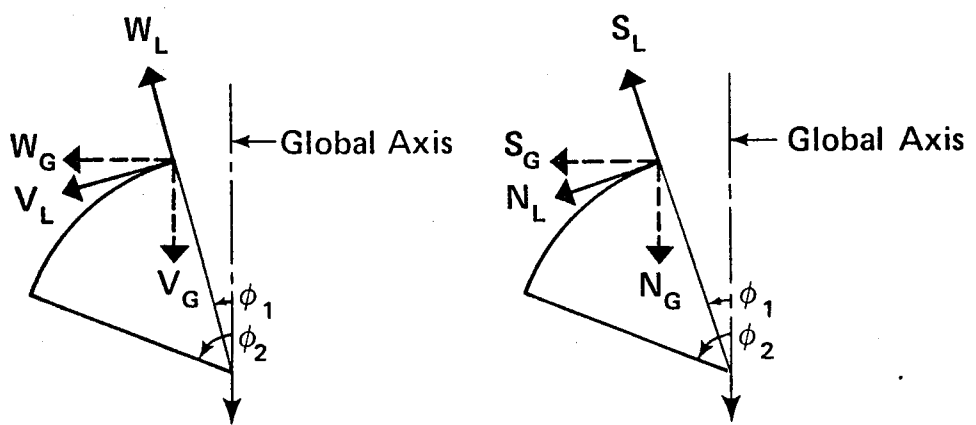


Fig. 3.3 Notation for Transformation of Stress Resultants and Displacements

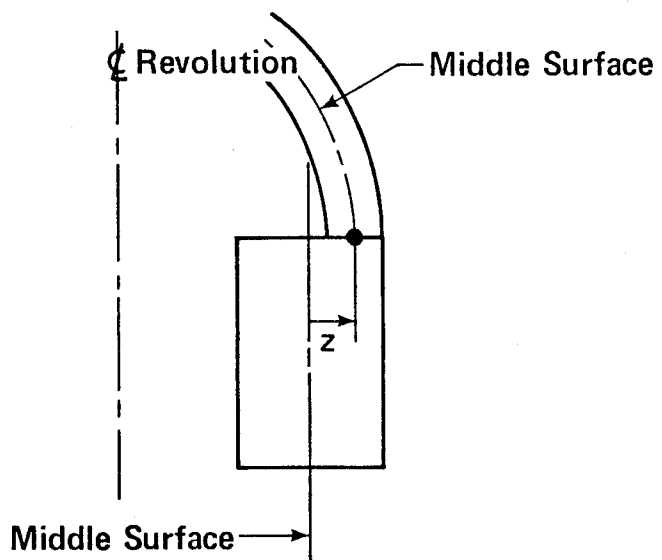


Fig. 3.4 Eccentricity at a Node

CHAPTER 4

EXAMPLE APPLICATIONS

4.1 Introduction

A computer program, named SASHELL, has been developed to perform the stiffness analysis of segmented shell structures based on the theory presented in the preceding chapters. The logic flow of SASHELL is outlined in Sect. 4.2 and listing of the program is included in Appendix C. The results of the analysis of two example applications, using SASHELL, are presented in this chapter.

The first example is the pinched cylinder. The exact analytical solution for a long cylinder pinched by a symmetrical circumferential line load (Fig. 4.1) is known [27, pp. 471; 10, pp. 280]. Finite element solutions, using (48 x 48) element stiffness matrices [11] and (24 x 24) element stiffness matrices [5,7], were obtained for the case of a cylindrical shell loaded by diametrically opposed concentrated loads (Fig. 4.2). This solution was compared [2] against an analytical solution based on the inextensional deformation theory (i.e. neglecting entirely the strain in the middle surface of the shell) [27, pp. 501-506].

The second example is the analysis of hyperboloid natural draft cooling tower under the action of wind load and

its own weight. Finite element analysis, using the computer program SORIII [14] and using conical shell elements to approximate the geometry [24] are known.

4.2 Logic Flow of SASHELL

In this section, the organization of the computer program SASHELL, which can serve as a summary for the solution technique of segmented shell structure as described in the preceding chapters, is outlined. Details of the required input are given in Appendix B.

- 1) The structure is divided into elements, each of which is a simple type of shell of revolution, and which are connected along nodal circles or "nodes". A concentrated load applied at a point along the meridional coordinate must be treated as a load acting on a node connecting two elements.
- 2) Nodal coordinates, system connectivity information and element types, properties and loading conditions are determined. The problem control parameters are established and input (Subroutine READIN and LOADIN).

The program now performs the following operations:

- 1) Each element is examined. If a coefficient which depends on the element geometric parameters (see the limitations in Sect. 5.3) exceeds a certain limit, the element is divided into subelements (segments) each of which satisfies this limit (subroutine SEGMENT).

- 2) The connectivity of the system is altered to include the new intermediate nodal points. Geometric parameters and loadings values at each segment boundary are calculated (subroutine SEGEOM).
- 3) The number of the structure's degrees of freedom are established.
- 4) If the external applied load on the structure is symmetric, the program discards step 5 and goes to step 6.
- 5) If the load is non-axisymmetric, the total number of points in the meridional and circumferential direction in the structure is determined and the "results" array is initialized.
- 6) The harmonic number, n, is set equal to zero.
- 7) The structure stiffness matrix and load vector are initialized. The nodal load coefficients, if any, which correspond to the harmonic n are added to the load vector.
- 8) The stiffness analysis starts by calculating the stiffness matrix and fixed end forces for each segment in the structure (subroutine STIFAN).
- 9) The geometric parameters and external applied loadings at the desired number of integration points in the segment under consideration are calculated. Dead weight of the segment, if required and if $n = 0$, is superimposed (subroutine PLSEG and DLSEG).

- 10) The initial conditions at the starting edge of the segment, as stated in Sect. 3.4 (Eqs. 3.12 and 3.15), are set. The governing equations (subroutine FLUGGE) are integrated, using a fourth order Runge-Kutta method, over the desired number of points to obtain the transfer matrix of the segment (subroutine RNGKT).
- 11) The segment stiffness matrix and fixed end forces are evaluated from the transfer matrix obtained in step 10, as described in Sect. 3.5 (subroutine STIFIX).
- 12) The results of step 11 are saved (subroutine STORE1).
- 13) The segment stiffness matrix and fixed end forces are modified to correspond to the stiffness matrix sign convention, as stated in Sect. 3.6.
- 14) The stiffness influence coefficients and fixed end forces are modified to account for nodal eccentricity, if any, as mentioned in Sect. 3.9. (subroutine ECCNTR).
- 15) If required, the segment stiffness influence coefficients and fixed end forces are transformed, due to discontinuity of the meridian at the node, to the structural global coordinates, as stated in Sect. 3.8 (subroutine GLTRAN).
- 16) The segment stiffness influence coefficients are assembled, with respect to the structure's degrees of freedom, into the master stiffness matrix. The segment fixed end forces are subtracted from the

corresponding values in the load vector (subroutine STORE).

- 17) Steps 9 to 16 are repeated for each segment in the structure.
- 18) The boundary conditions are imposed on the master stiffness equation (subroutine BOUNDC).
- 19) Segments edge displacements is obtained, using Gaussian elimination algorithm to solve the master stiffness equation (subroutine SOLVER).
- 20) The stiffness analysis, for harmonic number n, is completed. The displacements and stress resultants at the desired number of intermediate points in each segment are to be evaluated (subroutine SRADSP).
- 21) The segment edge displacements, obtained in step 19, are transformed, if necessary, to the segment local coordinates and to account for nodal eccentricity (subroutine GLTRAN and ECCNTR).
- 22) The known segment edge displacements are substituted in the corresponding segment stiffness equation, saved in step 12. The primary stress resultants at the segment boundaries are evaluated, as described in Sect. 3.7 (subroutine STORE1).
- 23) The shell equations are integrated, using the initial conditions calculated in step 22, in order to determine the displacements and primary and secondary stress resultants at the intermediate points within the segment, as described in Sect. 3.7 (subroutine RESULT).

- 24) If the load is symmetric (i.e., the required number of harmonics is zero), the results of step 23 are printed out and the program goes to step 26.
- 25) If the load is non-axisymmetric (i.e., the required number of harmonic is greater than zero), the displacements and stress resultants are calculated at the desired number of points in the circumferential direction. The results are superimposed in the "results" array (subroutine STORE2).
- 26) Steps 21 to 25 are repeated for each segment in the structure.
- 27) The harmonic number, n, is increased by one. Steps 7 to 26 are repeated until n is equal to the required number of harmonics.
- 28) The results saved in step 25 are printed out and the program stops.

4.3 Pinched Cylinder

The governing differential equation for a circular cylindrical element is

$$\frac{d^2W}{dx^2} (K \frac{d^2W}{dx^2}) + \frac{Et}{r^2} W = P_z \quad 4.1$$

where x measures the distance along the axis of the cylinder with the origin ($x = 0$) at midlength of the element. When the thickness of the shell is constant, this equation reduces to

$$\frac{d^4W}{dx^2} + 4\lambda^4 W = \frac{Pz}{K} \quad 4.2$$

in which the flexural rigidity, K, is

$$K = \frac{Et^3}{12(1 - \nu^2)} \quad 4.3$$

and the coefficient λ is defined as

$$\lambda = \sqrt[4]{\frac{3(1 - \nu^2)}{r^2 t^2}} \quad 4.4$$

For the special case of a long cylindrical shell pinched by a live load P uniformly distributed along a circular section (Fig. 4.1), the solution of Eq. 4.2 takes the form [27]

$$W = \frac{-P}{8\lambda^3} e^{-\lambda x} (\cos \lambda x + \sin \lambda x) \quad 4.5$$

The stress resultants may be expressed in terms of derivatives of the displacement W in the form

$$M_x = K \frac{d^2W}{dx^2} \quad 4.6.1$$

$$Q_x = K \frac{d^3W}{dx^3} \quad 4.6.2$$

$$M_\theta = \nu M_x \quad 4.6.3$$

$$N_\theta = \frac{Et}{r} W \quad 4.6.4$$

Numerical values of these expressions, at several points along a cylindrical element 20 feet long, 8 feet in diameter and with constant wall thickness equals to 1.24 inches, are shown in Table 4.1 for a live load $P = 1$ kip/ft. Output of the analysis of the same element using SASHELL is included in Appendix D. The results are presented graphically in Fig. 4.3. The results of the two solutions are identical up to the number of significant figures contained in the output.

For the case of a cylindrical shell pinched by two concentrated loads as shown in Fig. 4.2 the concentrated load is approximated as a live load (see Sect. 5.4) that has a value of 1.0 kip/ft at the loaded points and zero at a short distance from the load points (Fig. 4.4.1). The loading function is expanded in Fourier coefficients and the results of the analysis of each harmonic are superimposed.

The results of this loading case are affected by the number of harmonics considered in the analysis, which will be discussed in Sect. 5.4.

If the circumference of the cylinder shown in Fig. 4.4 is divided to 36 intervals and the load is approximated as shown, the equivalent concentrated load is

$$\bar{P} = \frac{2\pi r}{36} P \quad 4.7$$

$$= 0.698 \text{ kips}$$

$L = 20'.0$ $E = 30 \times 10^3$ ksi $K = 436$ K.ft
 $r = 4'$ $v = 0.3$ $\lambda = 2.0$
 $t = 1.24"$ $P = 1.0$ K/ft

X (ft)	λ_x	W (10^{-4} ft)	M_x	Q_x	M_θ	N_θ
0	0	-.3583	.1250	-.5000	+.0375	-3.997
0.25	0.5	-.2949	.0302	-.2661	+.0091	-3.290
0.5	1.0	-.1822	-.0138	-.0994	-.0041	-2.032
0.75	1.5	-.0854	-.0258	-.0079	-.0077	-0.953
1.0	2.0	-.0239	-.0224	+.0282	-.0067	-0.266
1.25	2.5	+.0059	-.0144	+.0329	-.0043	+0.066
1.5	3.0	+.0152	-.0070	+.0246	-.0021	+0.169
1.75	3.5	+.0139	-.0022	+.0142	-.0006	+0.155
2.0	4.0	+.0092	+.0002	+.0060	+.0001	+0.102
2.25	4.5	+.0047	+.0011	+.0012	+.0003	+0.052
2.5	5.0	+.0016	+.0011	-.0009	+.0003	+0.018
2.75	5.5	0	+.0007	-.0015	+.0002	0
3.0	6.0	-.0006	+.0004	-.0012	+.0001	-0.066

TABLE 4.1 Stresses and Radial Displacement in a Pinched Cylinder as per Eqs. 4.6

The analytical solution for a concentrated load, based on inextensional deformation theory [27, pg. 506], is of the form

$$w_{\phi} = \frac{Pr^3}{\pi KL} \sum_{n=2,4,6,\dots} \frac{1}{(n^2 - 1)^2} \cos n\theta \quad 4.8$$

where L is one-half the length of the cylinder. Eq. 4.8 yields

$$(w)_{\theta=0} = 0.382 \times 10^{-3} \text{ ft}$$

$$(w)_{\theta=\pi/2} = -0.351 \times 10^{-3} \text{ ft}$$

A comparison of these values with SASHELL values shown in Fig. 4.4.1 indicates good agreement for $\theta = \pi/2$ but considerable discrepancy for $\theta = 0$. The SASHELL solution predicts a displacement 17% larger than the inextensional solution at $\theta = 0$.

Now referring to Fig. 4.4.2, the cylindrical shell example as chosen by Cantin and Clough [7], is shown. For the same number of intervals (36), the equivalent concentrated load is

$$\bar{P} = 0.0721 \text{ kips}$$

The deflections for this case, from Eq. 4.8, are

$$(w)_{\theta=0} = 0.614 \times 10^{-2} \text{ ft}$$

$$(w)_{\theta=\pi/2} = -0.565 \times 10^{-2} \text{ ft}$$

The ratios of the SASHELL displacements are 1.10 and 1.14 to those of the inextensional theory for $\theta = \pi/2$ and $\theta = 0$, respectively.

4.4 Hyperboloid Natural Draft Cooling Tower

Large capacity power plants generate a substantial amount of operational heat that requires dissipation. One of the major structures in these power plants is the natural draft cooling tower in the form of the shell of revolution. The tower utilizes its height to create the necessary air flow in order to cool a large volume of water in a minimum land area. Hyperboloid cooling towers are the most preferable shape [14] when compared to conical or cylindrical shapes from the aerodynamic point of view.

4.4.1 Geometry of the Tower

The middle surface of a hyperboloid shell is shown in Fig. 1.7. The surface of a hyperboloid of revolution may be classified as a non-developable surface, which means that the surface will not tend to flatten out under load. This surface is generated by the rotation of a hyperbola about a vertical axis. The geometrical equation can be written as

$$\frac{r^2}{a^2} - \frac{x^2}{b^2} = 1$$

4.9

in which r is the horizontal radius, x is the vertical coordinate

measured from the origin at the throat of the shell, a is the throat radius at $x = 0$, and b is a constant in which the ratio b/a equals the slope of the asymptotes to the hyperbola.

The principal radii of curvature are given by

$$r_1 = - \frac{a^2 b^2}{(a^2 \sin^2 \phi - b^2 \cos^2 \phi)^{3/2}} \quad 4.10.1$$

$$r_2 = \frac{a^2}{(a^2 \sin^2 \phi - b^2 \cos^2 \phi)^{1/2}} \quad 4.10.2$$

where $\tan \phi = \frac{dx}{dr}$

$$= \frac{b}{a} \sqrt{\frac{r^2}{r^2 - a^2}} \quad 4.10.3$$

The expression for the derivative of r_1 with respect to the coordinate s (see Eq. 2.5.1) can be obtained by differentiating Eq. 4.10.1 to yield

$$r_{1s} = \frac{-3}{a^2 b^2} (b^4 r \cos \phi + a^4 x \sin \phi) \left(\frac{r^2}{a^4} + \frac{x^2}{b^4}\right)^{1/2} \quad 4.10.4$$

The middle surface of the hyperboloid tower considered in the following analysis is shown in Fig. 4.5. The shell is 355 ft high and is supported by columns evenly spaced on a circular base of 290 ft diameter. The throat of the tower is 165 ft in diameter and is located 60 ft below the top of the shell. The thickness varies from 30 inches at the bottom level

of the shell to 6 inches at 25 feet elevation from the bottom. In the top 10 feet of the shell, the thickness also varies from 6 inches to 24 inches. Other than the top and the bottom regions, the shell thickness remains constant at 6 inches. The increased thickness at the top provides a stiffening effect that reduces radial deformation under wind load [24]. The bottom ring at the base acts as an equivalent deep beam bridging between columns.

The constant b of Eqs. 4.10 can be calculated by substituting the values for $r = 145$ at $x = 295$ and $a = 82.5$ into Eq. 4.9, which yields $b = 204.1$ ft. For the purpose of comparing the results with References 14 and 24, the following concrete properties are used

$$\text{Young's Modulus} \quad E = 4 \times 10^6 \text{ psi}$$

$$\text{Poisson's Ratio} \quad \nu = 0.15$$

$$\text{Specific Weight} \quad \gamma = 150 \text{ lb/ft}^3$$

4.4.2 Load Description

The tower is analyzed for gravity load and wind pressure load.

The gravity load, which is symmetric with respect to the coordinate θ , is determined from the following equations

$$q = t \times \gamma \quad 4.11.1$$

$$P_z = -q \cos \phi \quad 4.11.2$$

$$P_s = q \sin \phi$$

4.11.3

where q is the intensity of weight per square area of the surface.

The wind load, which is the governing factor in the design of the cooling towers [14], is based on the ACI-ASCE Committee 334 recommendations [1]. The following equivalent static pressure distribution is used

$$q(H, \theta) = G C_\theta K_H q_{30} \quad 4.12$$

where the factors in this equation are described as follows:

- a) $q(H, \theta)$ is the equivalent static normal pressure on the surface of the tower at a location defined by coordinates H, θ . H is the vertical distance measured from the ground level, θ is the circumferential angle measured from the windward meridian.
- b) G is the dynamic gust factor which accounts for the overstress due to the tower response to various time variations in the wind pressure.
- c) C_θ is the coefficient of wind pressure distribution in the circumferential direction.
- d) K_H is the exposure factor which establishes the vertical profile of wind pressure, which in turn, depends on wind speed and roughness of terrain.
i.e., K_H can be evaluated from the equation

$$K_H = 2.64 \left(\frac{H}{Hg}\right)^{2\alpha}$$

4.13

where H is the height measured from the ground level; Hg is the gradient height above which the wind velocity is assumed constant and ranges from 900 ft for open country to 1500 ft for center of large cities; α is a constant, depending on the terrain roughness, and ranges from 1/7 for open country to 1/3 for center of large cities.

- e) q_{30} is the basic wind pressure (psf) and is equal to the dynamic pressure of the free stream of wind at 30 ft above the ground level at a given site. It may be computed from

$$q_{30} = 0.00256 V_{30}^2$$

4.14

where V_{30} = wind velocity (m.p.h.) at 30 ft above the ground level.

The ACI-ASCE Committee 334 has suggested the normalized wind pressure distribution in the circumferential direction as shown in Fig. 4.6.1. As in Reference 24, assuming $Hg = 900$ ft, $\alpha = 1/7$ and $V_{30} = 100$ m.p.h., the variation of the wind pressure with the height can be taken as shown in Fig. 4.6.2.

4.4.3 Analysis Conclusions

The results of the analysis of the hyperboloid tower, loaded as described above, are represented graphically for

dead load in Figs. 4.7.1 to 4.7.3, and for wind load in Figs. 4.8.1 to 4.8.10. Since the actual condition at the bottom of the shell is only partially fixed [24], the results of the analysis for two boundary conditions, fixed and hinged at the bottom, are shown in these figures. Excellent agreement is observed between the displacements and stress resultants shown and the results of References 14 and 24.

The approximation of the geometry with a series of cones [24] does not affect the results for this particular geometry of the tower. However, the meridian curvature R_1 varies only from -0.002 ft^{-1} at the throat to -0.0003 ft^{-1} at the bottom of the hyperboloid shell, and is equal to zero for a conical element. For shells with larger R_1 curvature the conical segment approximation may not be as accurate.

4.5 Comments on Results

The examples of this chapter have been selected to test the ability of SASHELL to analyze different types of shells. The pinched cylinder solutions are common test problems because of the difficulty of achieving solutions for concentrated loads. The hyperboloid cooling tower is an illustration of a shell with negative Gaussian curvature under complex loading conditions. It may be concluded that SASHELL is capable of yielding good results on a wide variety of shell problems.

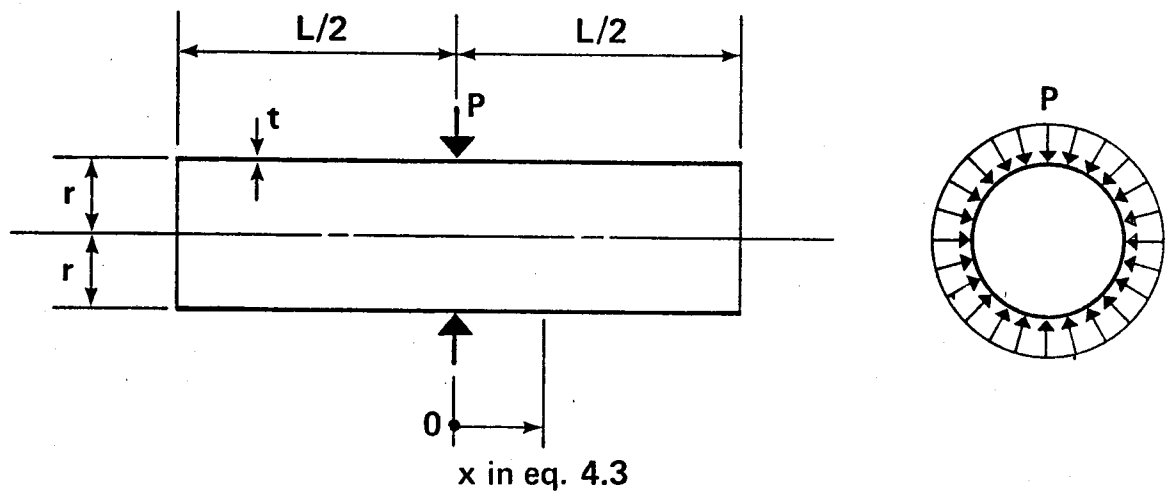


Fig. 4.1 "Pinched Cylinder" Circumferential Line Load

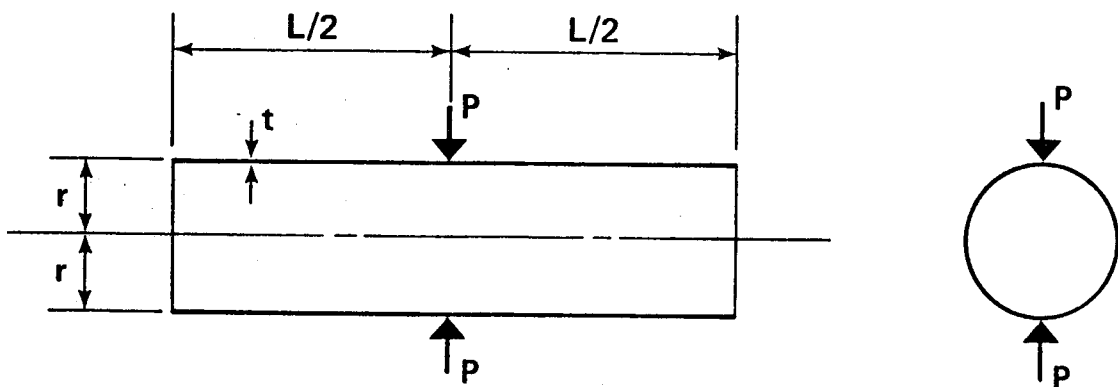


Fig. 4.2 "Pinched Cylinder" Two Concentrated Loads

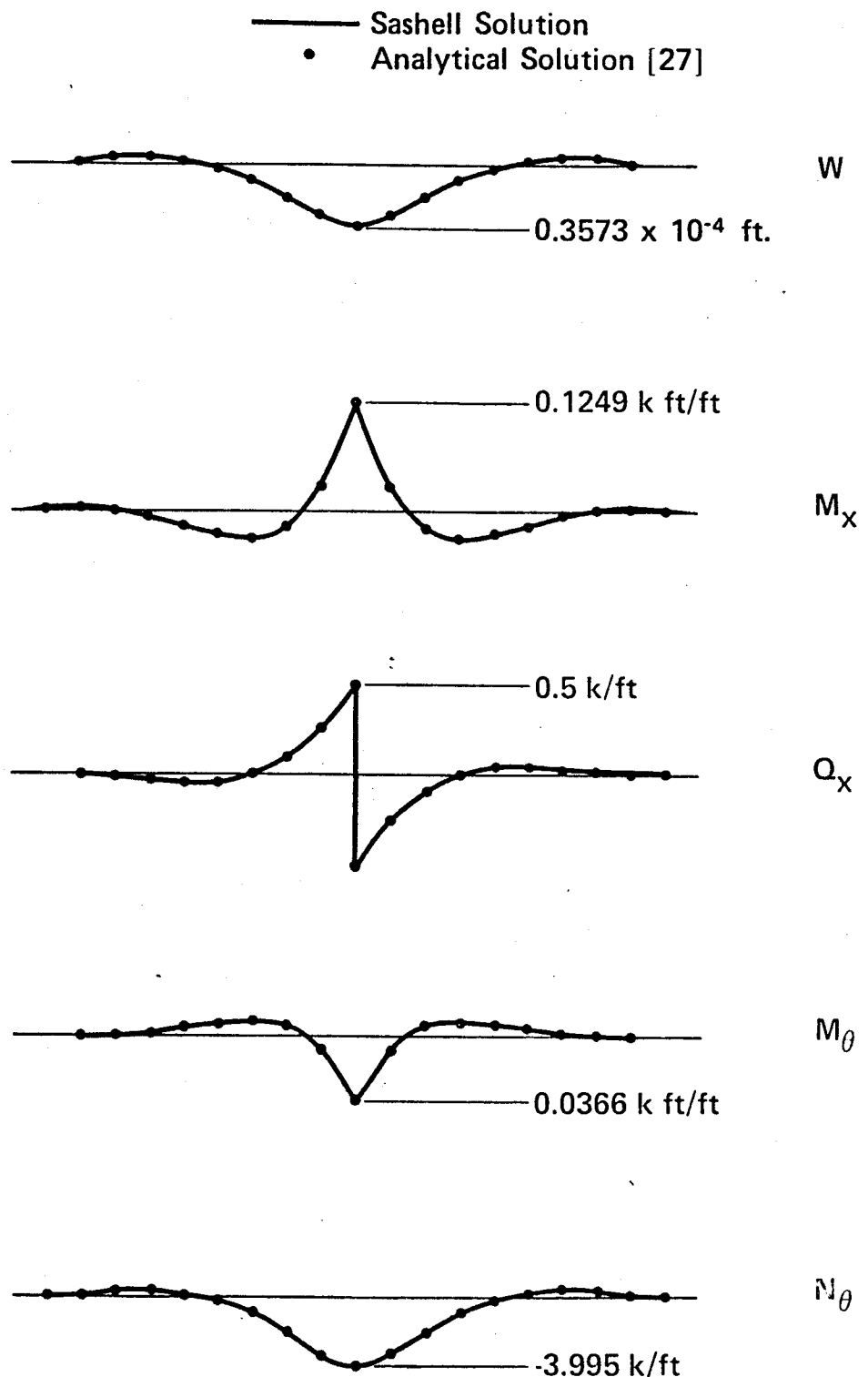


Fig. 4.3

"Pinched Cylinder" Circumferential Line Load Stress Resultants and Radial Displacement

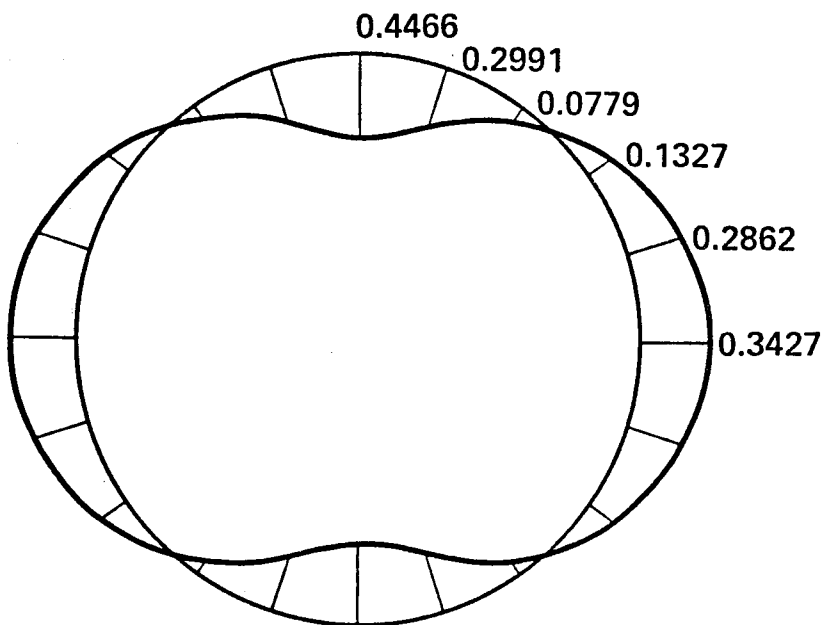
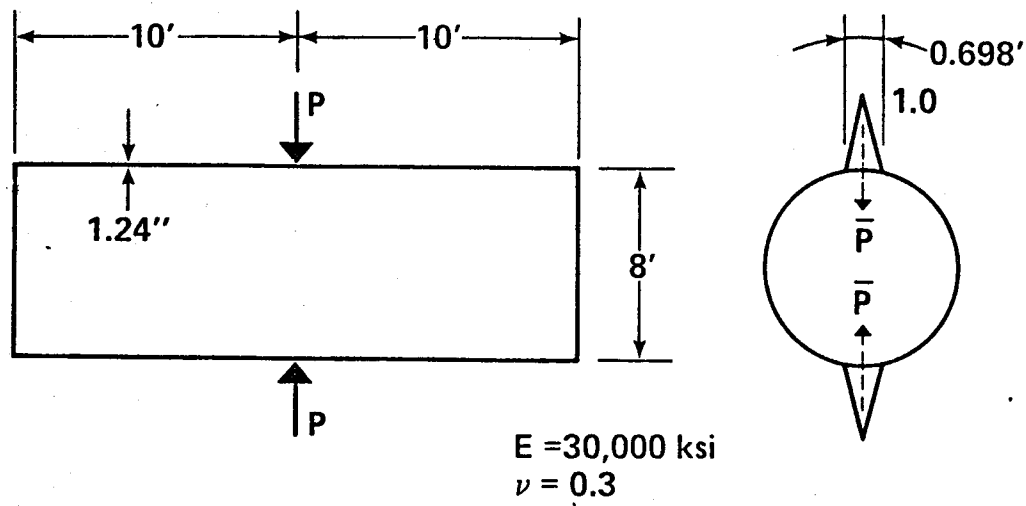


Fig. 4.4.1 "Pinched Cylinder" Two Concentrated Loads Radial Displacement ($r = 4.0 \text{ ft.}$)

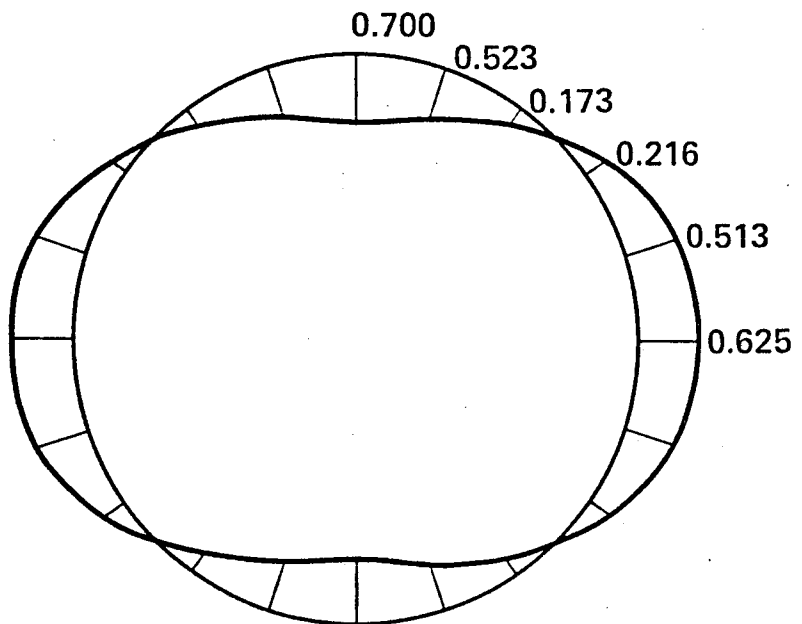
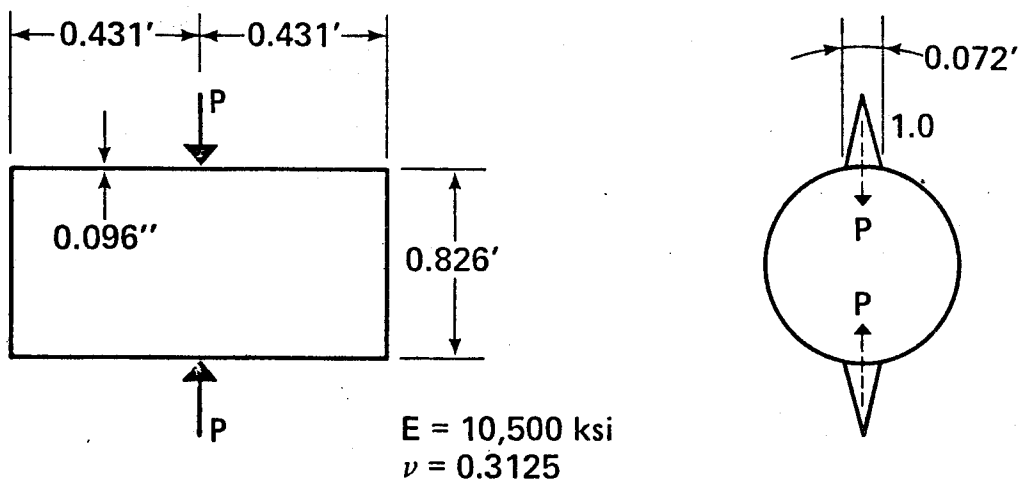


Fig. 4.4.2

"Pinched Cylinder" Two Concentrated Loads Radial Displacement ($r = 0.413 \text{ ft.}$)

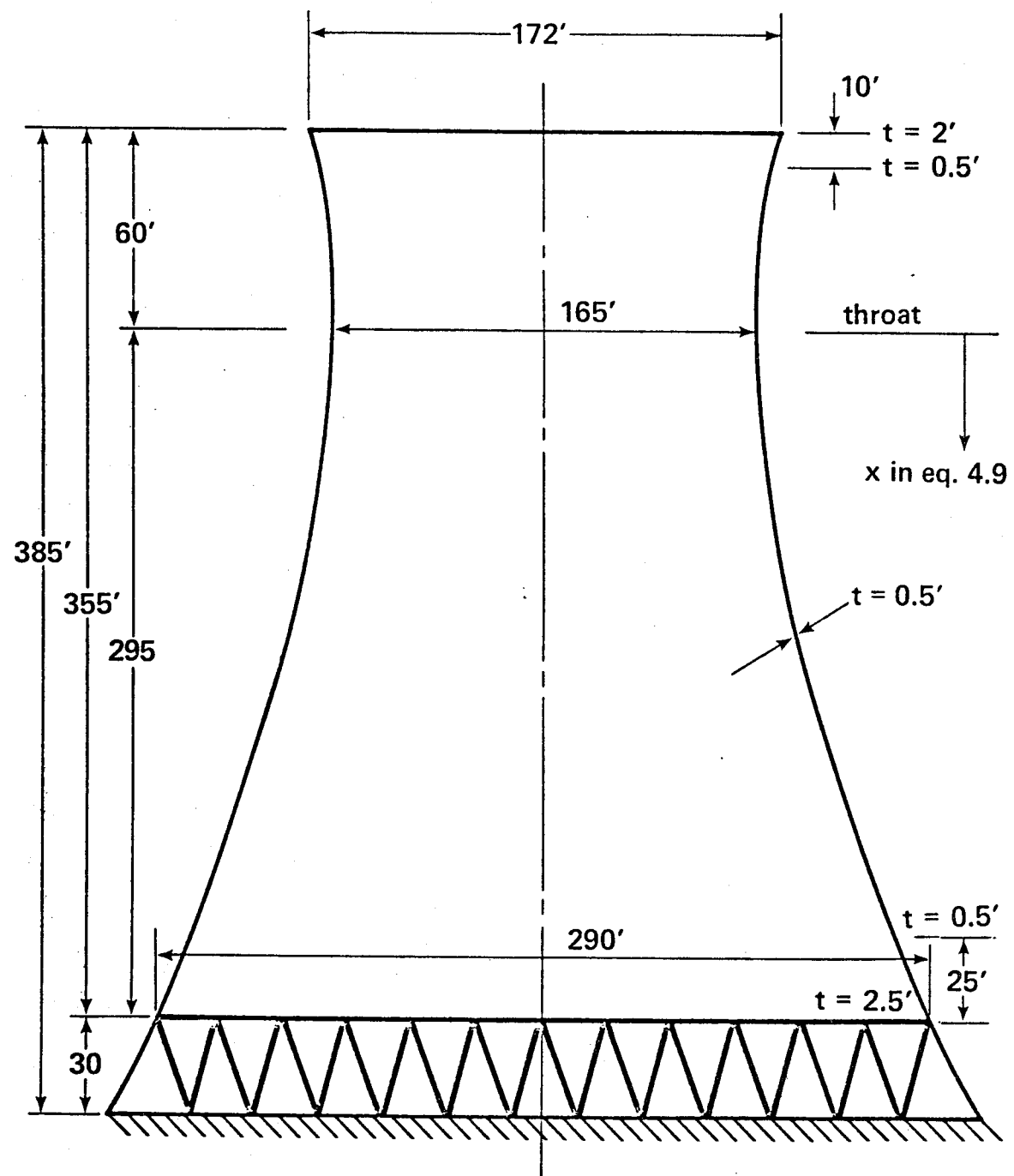


Fig. 4.5 Typical Hyperboloid Natural Draft Cooling Tower

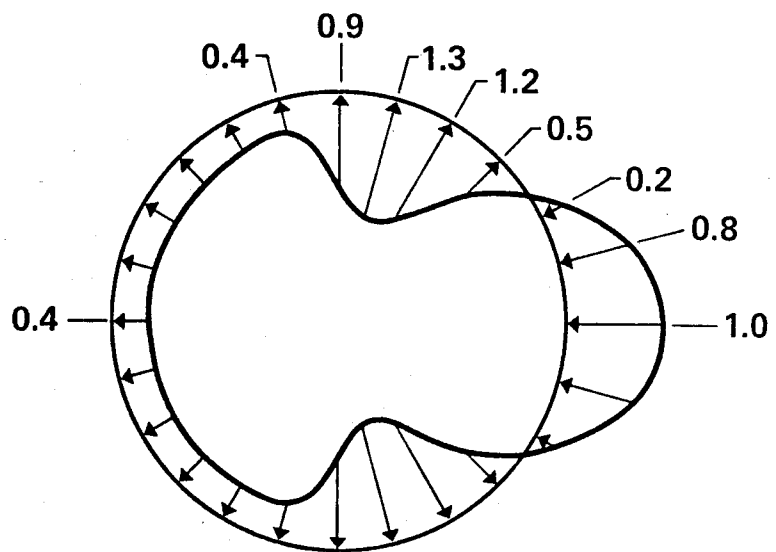


Fig. 4.6.1 Wind Pressure Coefficients C_θ

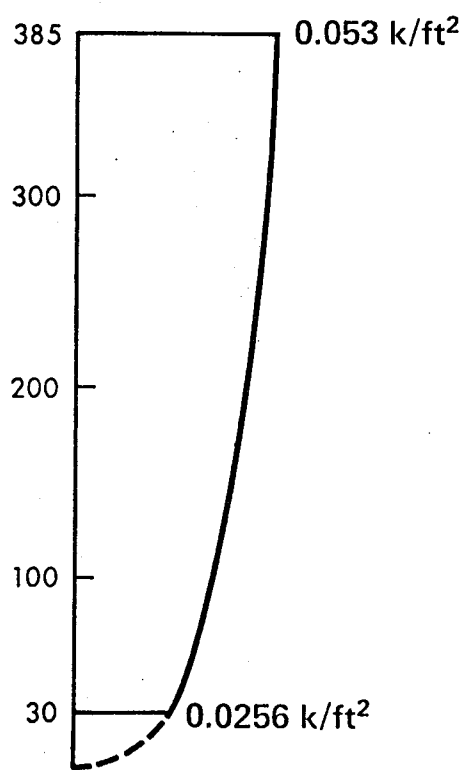


Fig. 4.6.2 Wind Pressure Profile ($\theta = 0$)

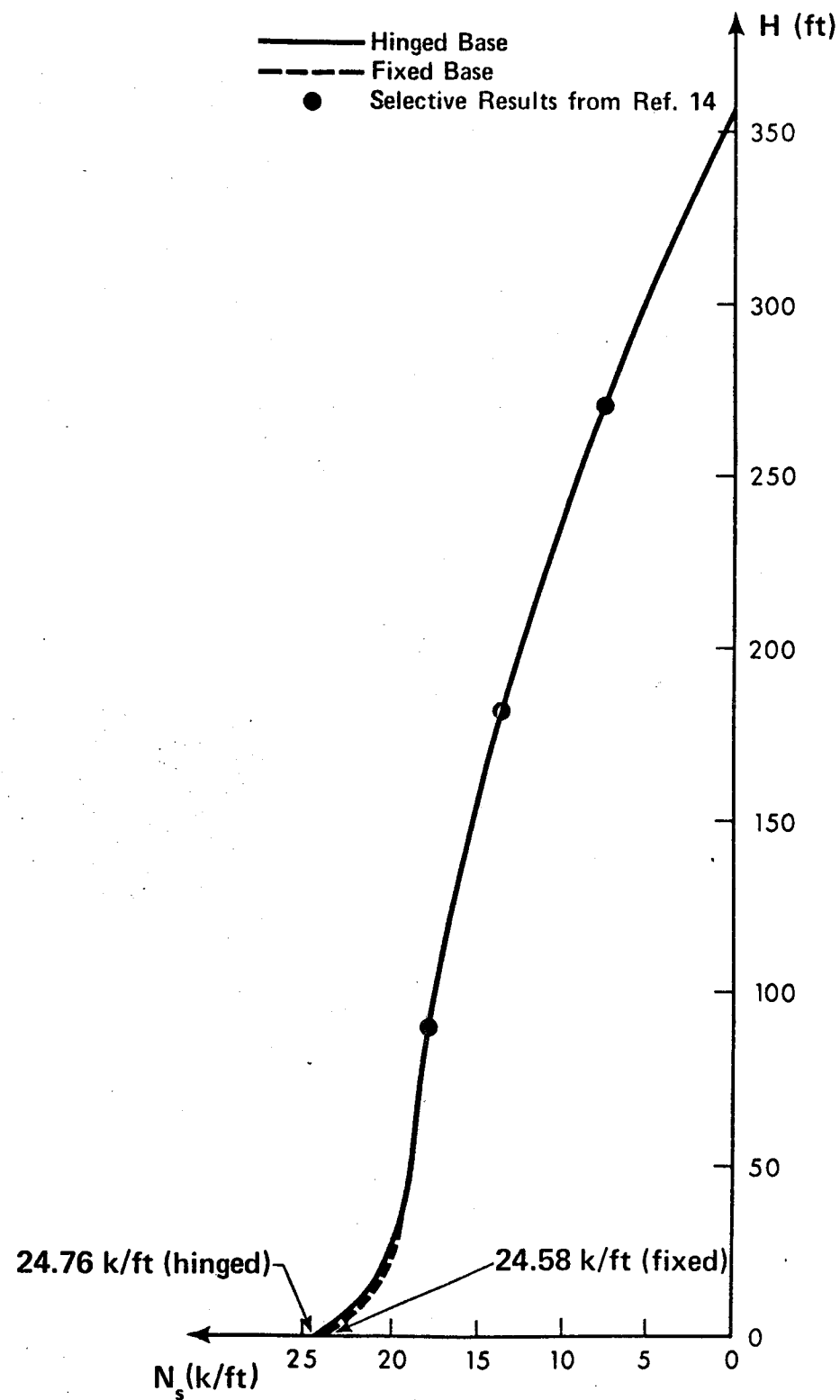


Fig. 4.7.1 Hyperboloid Tower Dead Load Membrane Force N_s

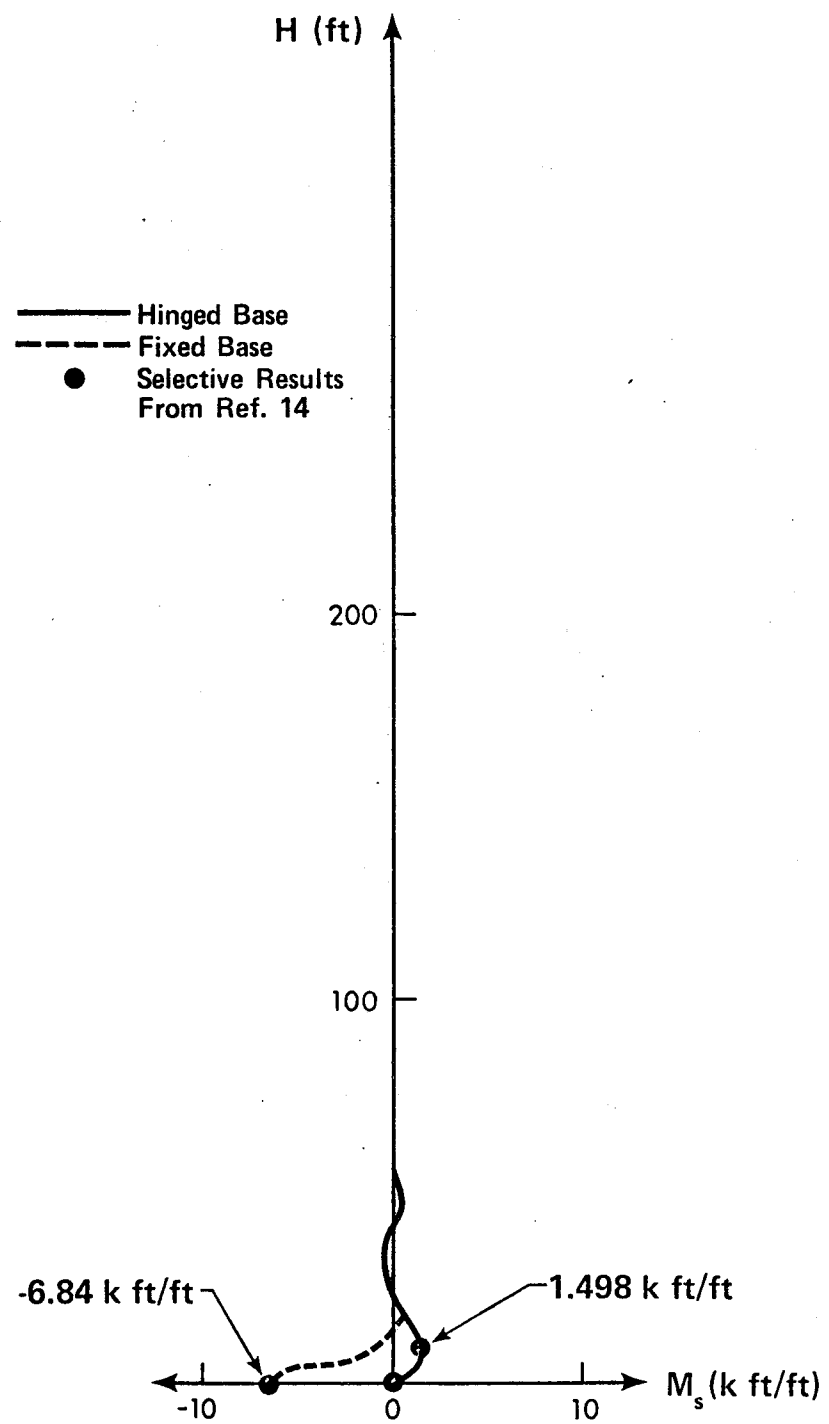


Fig. 4.7.2 Hyperboloid Tower Dead Load Meridional Moment M_s

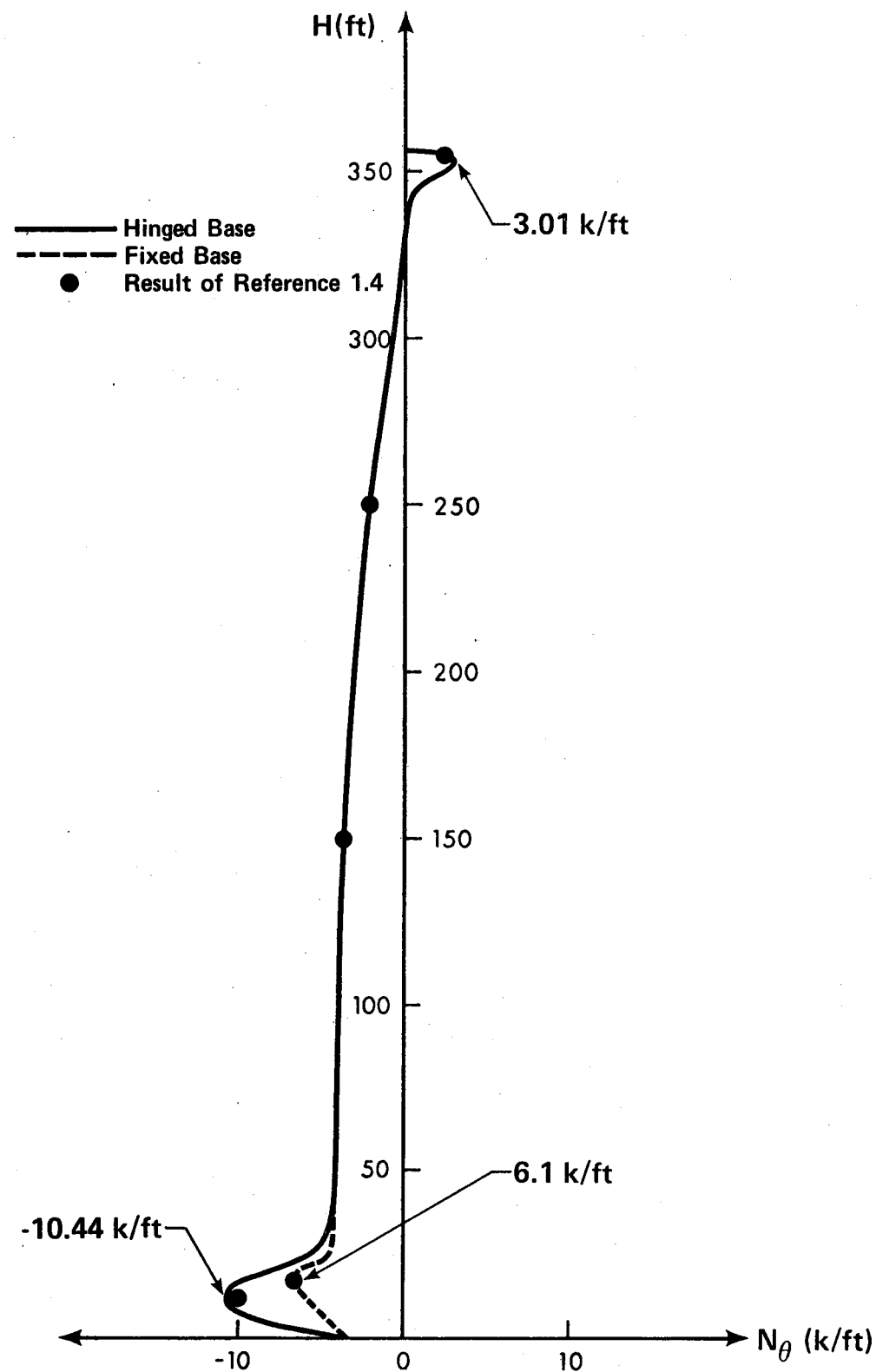


Fig. 4.7.3 Hyperboloid Tower Dead Load Membrane Force N_θ

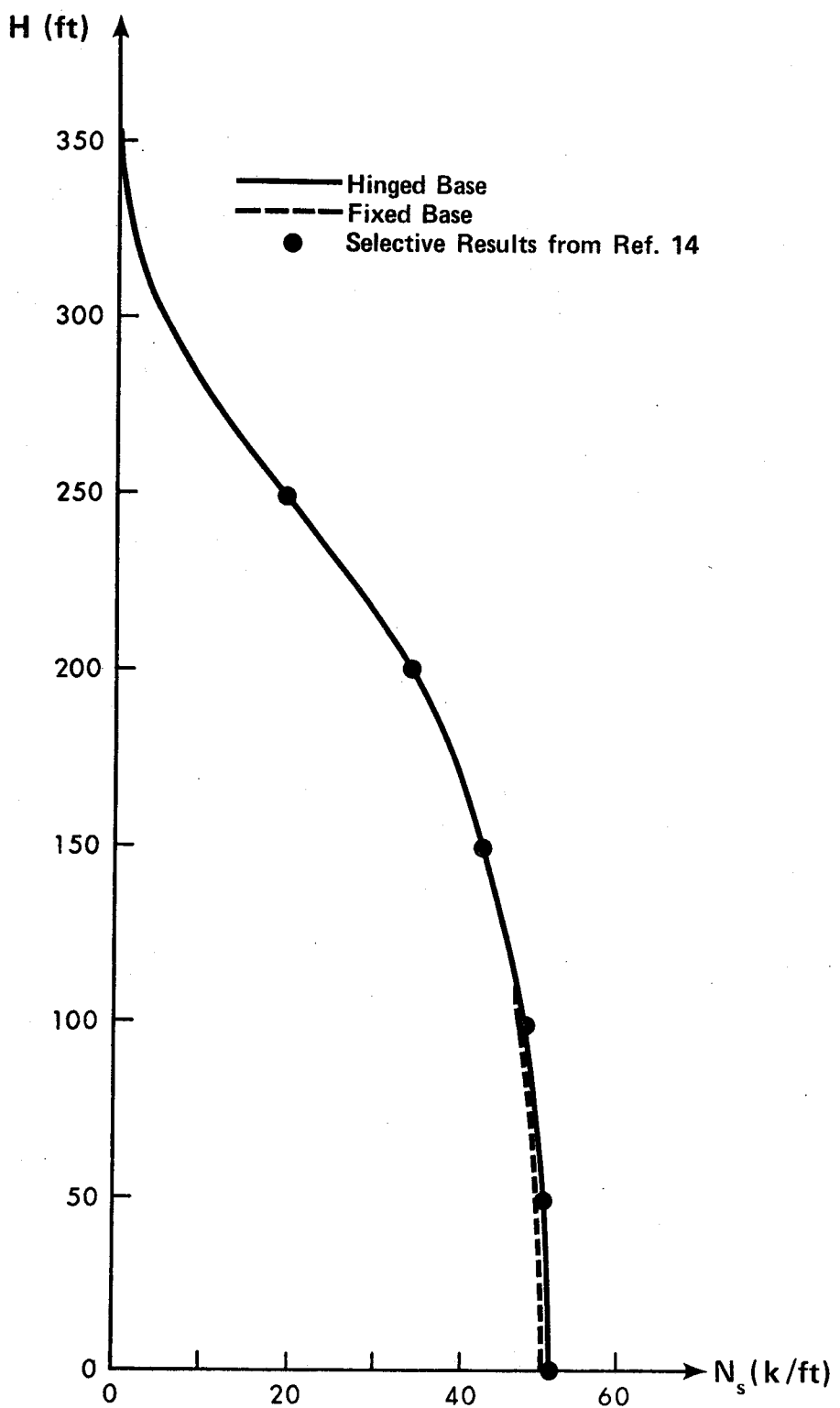


Fig. 4.8.1 Hyperboloid Tower Wind Load Membrane Force N_s ($\theta = 0$)

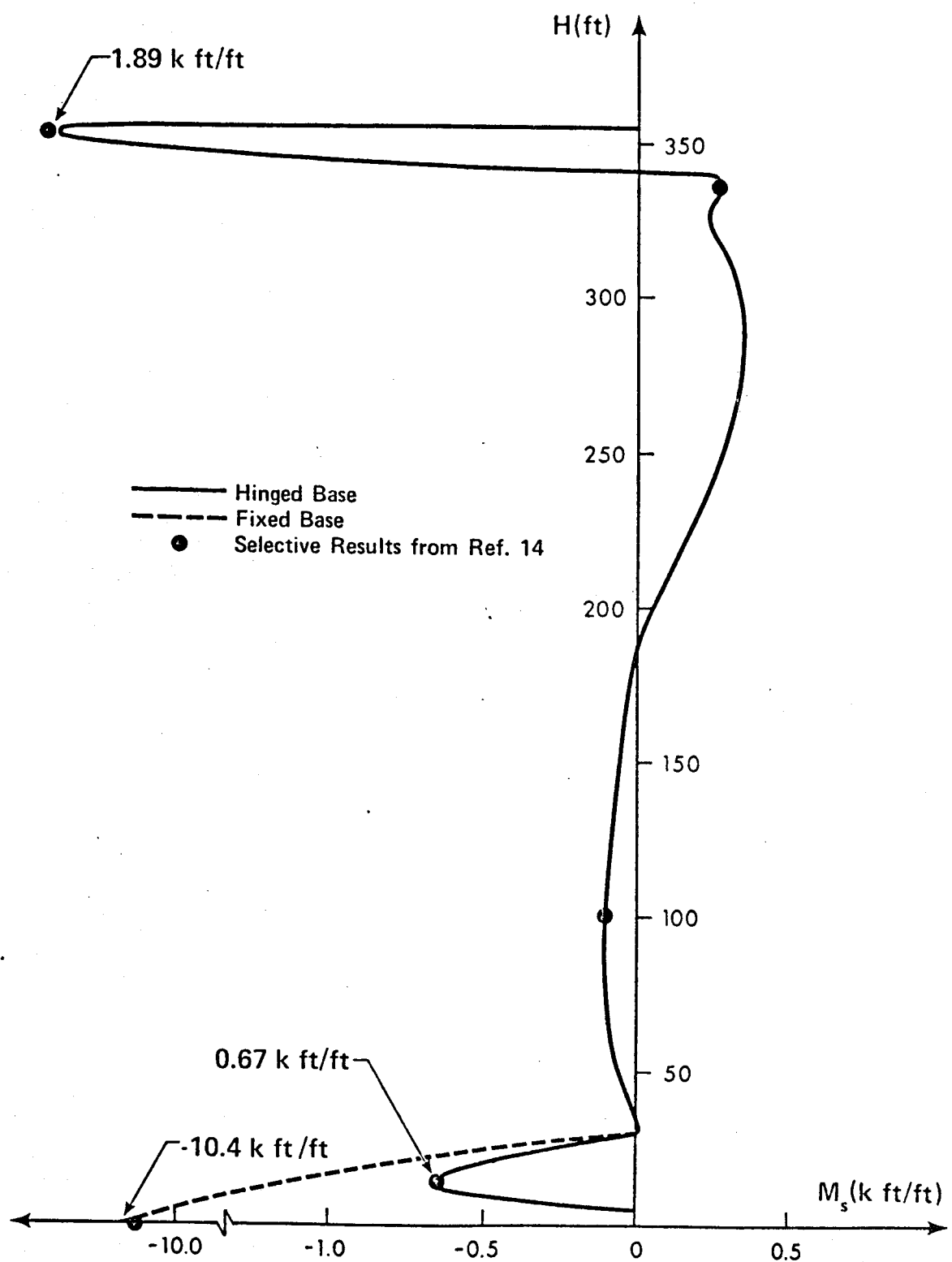


Fig. 4.8.2 Hyperboloid Tower Wind Load Meridional Moment M_s ($\theta = 0$)

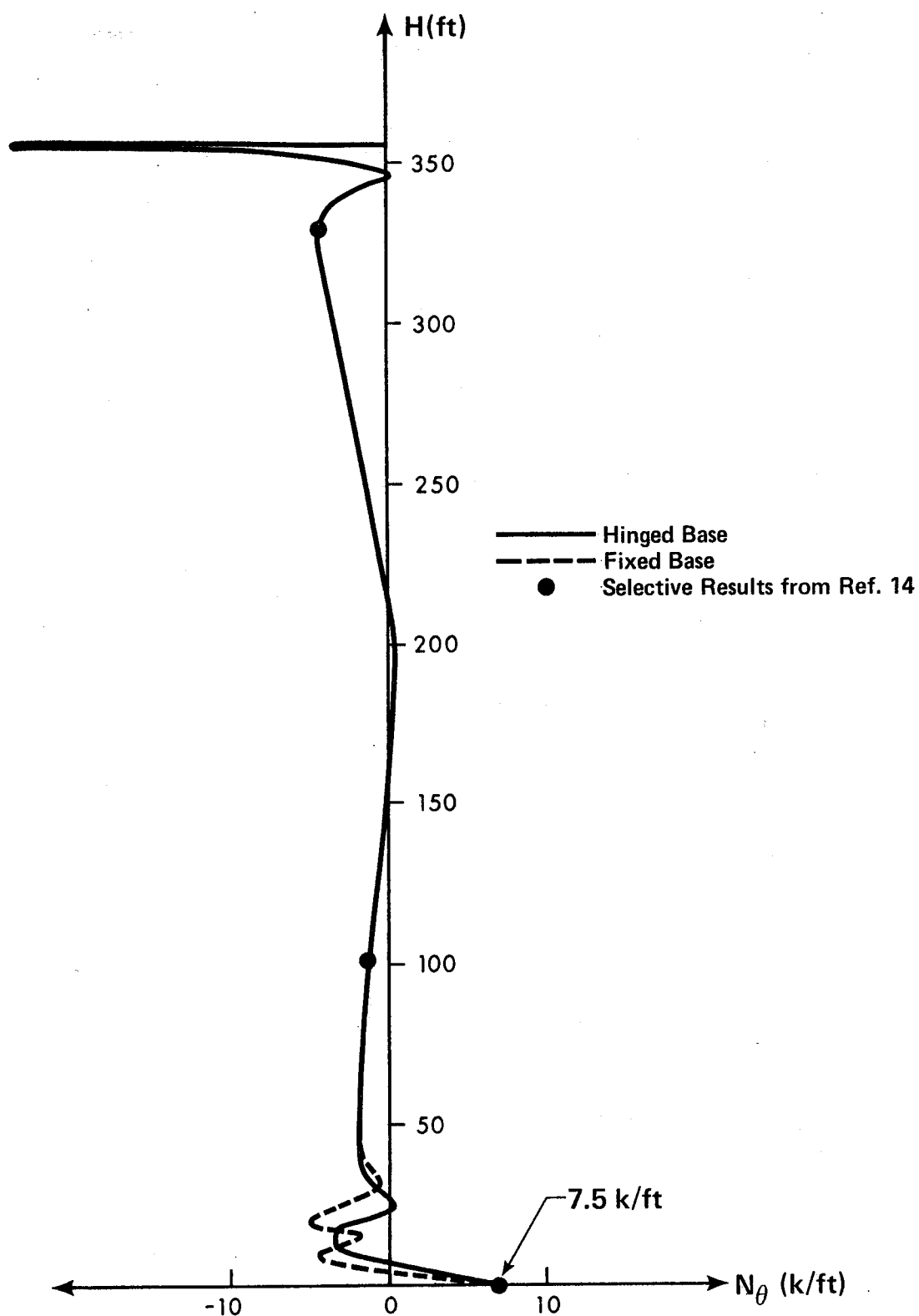


Fig. 4.8.3 Hyperboloid Tower Wind Load Membrane Force $N_\theta (\theta = 0)$

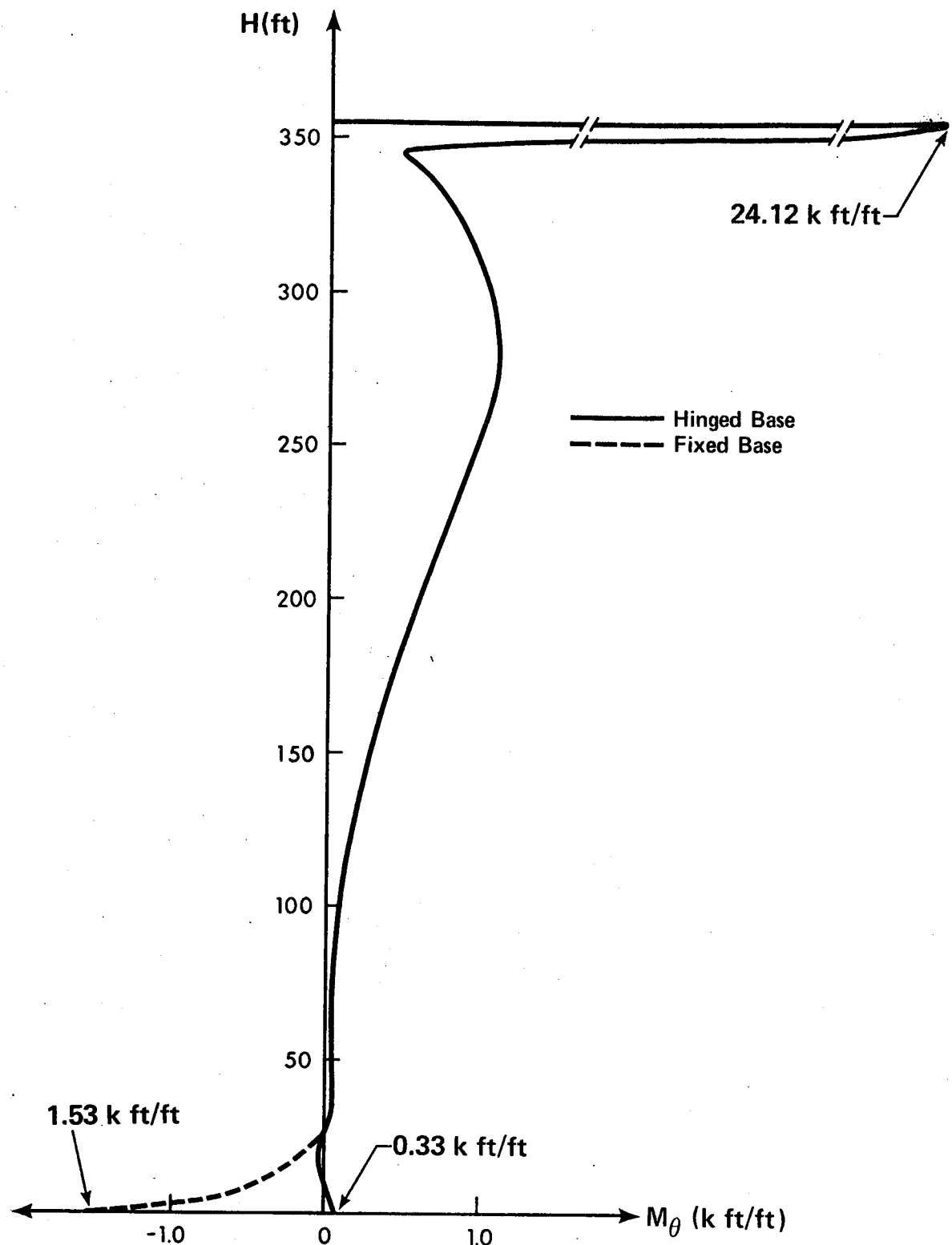


Fig. 4.8.4 Hyperboloid Tower Wind Load Circumferential Moment $M_\theta (\theta = 0)$

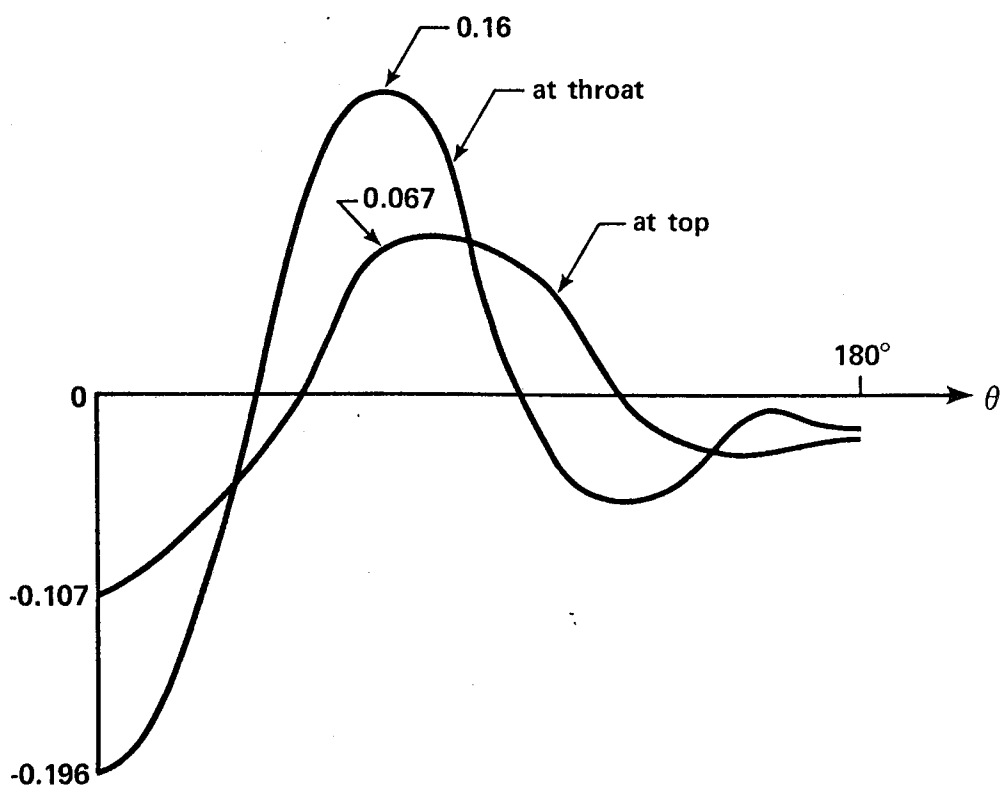


Fig. 4.8.9 Hyperboloid Tower Wind Load Circumferential Variation of W

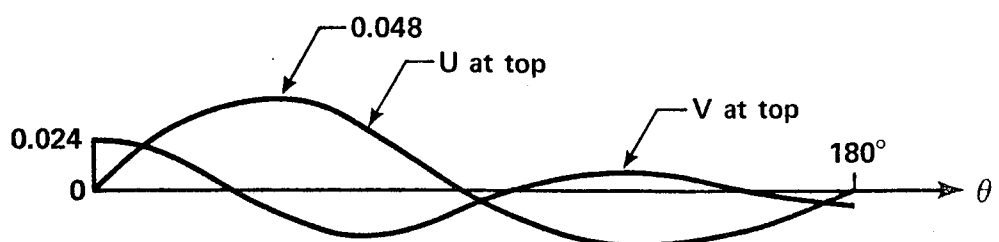


Fig. 4.8.10 Hyperboloid Tower Wind Load Circumferential Variation of V and U

CHAPTER 5
LIMITATIONS

5.1 Introduction

Three factors affect the solution technique presented in this thesis. These are summarized as follows.

- 1) Singularity of the governing equations at the apex.
- 2) Stability of the numerical integration process.
- 3) Convergence of Fourier expansions.

Each factor is discussed separately in the following sections.

5.2 Singularity of the Governing Equations at the Apex

If the shell has a pole (i.e., $r = 0$), coefficients in the governing sets of equations (Eqs. 2.14, 2.18 and 2.20) become singular. This is consistent with classical shell theory. A simple way to handle this situation is to choose the boundary, $s = 0$, not at the pole, but a very short distance away and then impose the boundary conditions at $s = 0$ as follows [6].

- 1) For harmonic number $n = 0$

$$\beta = V = U = S_s = 0$$

- 2) For harmonic number $n = 1$

$$W = M_s = N_s = T_s = 0$$

- 3) For harmonic number $n > 1$

$$W = V = U = M_s = 0$$

5.3 Stability of the Numerical Integration Process

Runge-Kutta fourth order integration method is used, in SASHELL, to integrate the basic set of equations (Eq. 2.24). This method is very well known and has the advantage of being self starting i.e., it needs only the information available at the preceding point. The method can be interpreted as follows:

- 1) The derivative is evaluated at the starting point of the interval.
- 2) The above derivative is used to obtain an approximate ordinate to determine an approximate derivative for the midpoint of the interval.
- 3) The above derivative is used to obtain a second approximation of the derivative at the midpoint of the interval.
- 4) The above derivative is used to obtain an approximate ordinate to determine an approximate derivative for the end point of the interval.
- 5) A weighted average of the above four derivatives is taken to determine a total increment in the function for the whole interval.

Analytically, this can be defined as follows:

$$\begin{aligned}
 Y_{i+1} = & Y_i + \frac{\Delta h}{6} \left\{ f(Y_i, h_i) + 2f\left(Y^*_{i+1/2}, h_{i+1/2}\right) \right. \\
 & \left. + 2f\left(Y^{**}_{i+1/2}, h_{i+1/2}\right) + f\left(Y^*_{i+1}, h_{i+1}\right) \right\} \quad 5.1
 \end{aligned}$$

where

$$Y_{i+1/2}^* = Y_i + \frac{\Delta h}{2} f(Y_f, h_i) \quad 5.2.1$$

$$Y_{i+1/2}^{**} = Y_i + \frac{\Delta h}{2} f\left(Y_{i+1/2}^*, h_{i+1/2}\right) \quad 5.2.2$$

$$Y_{i+1}^* = Y_i + \Delta h f\left(Y_{i+1/2}^*, h_{i+1/2}\right) \quad 5.2.3$$

$$h_{i+1/2} = h_i + \frac{\Delta h}{2} \quad 5.2.4$$

$$h_{i+1} = h_i \Delta h \quad 5.2.5$$

in which $f(Y_i, h_i)$ is the value of the function at point i , and Δh is the step size of the interval.

It has been found [25] that the direct integration methods, when applied to a shell problem, suffer a complete loss of accuracy when the generator of the shell exceeds a critical length. The reason for this phenomenon is explained clearly in Reference 18. The general solution of the governing equations, Eq. 3.18, is of the form

$$\{y_{(b)}\} = [H_{(b)}] \{y_{(a)}\} + \{Q_{(b)}\} \quad 5.3$$

Because of the exponentially decaying behavior of the stresses and displacements, it is observed that the coefficients of $[H]$ increase in magnitude in such a way that if the length of the shell element is increased by any factor n , then these coefficients

increase in magnitude, approximately, exponentially with n . For example, consider an element spans the region $a \leq s \leq b$. For some prescribed edge conditions at "a", we expect the corresponding solution at "b" to become smaller and smaller when the element ab is increased in length. (i.e., $y_{(b)}$ small, $H_{(b)}$ large and $y_{(a)}$ has a prescribed value). The longer the element, the larger $[H_{(b)}]$ and the smaller $\{y_{(b)}\}$. The only way to get a small value for $\{y_{(b)}\}$ is for the elements of $[H_{(b)}]$ to subtract out and that is the reason that at some critical length of the element all significant digits of $[H_{(b)}]$, in Eq. 5.3, are lost and so is the accuracy.

The loss of accuracy cannot be avoided by choosing a fine mesh for the integration. By taking more steps "partial instability" arises [8]. This means that the numerical solution deviates from the actual solution as we take more steps.

In Reference 18, the critical meridian length is limited with a length factor $\lambda L \leq 3 - 5$, where

$$\lambda L = L^4 \sqrt{\frac{3(1 - \gamma^2)}{r^2 h^2}} \quad 5.4$$

in which

L is the length of the meridian of the shell, R is the minimum radius of curvature, and h is the thickness of the shell.

In the author's opinion, this is very conservative limitation. The loss of accuracy, using the computer program SASHELL, does not arise until the length factor λL exceeds 25.

To demonstrate this, Table 5.1 shows some results of the analysis of clamped pressurized cylindrical shells, as obtained by the computer program SASHELL, with various lengths and different number of steps of integration. From the symmetry of the problem, the end moments and the absolute values of the end shears should be equal. It is obvious, from Table 5.1, that the solution is not affected much by the number of steps adopted for the integration and it begins to break when

- 1) λL exceeds 20 and the number of steps is less than 20.
- 2) λL approaches 29 for any number of steps.

As a conservative limitation, the upper bound of λL shall not exceed 25 and the number of points of integration (NP), needed for convergence, is limited as follows:

$$NP \leq 21 \quad \text{for} \quad \lambda L < 20$$

$$NP \leq 31 \quad \text{for} \quad 20 < \lambda L < 25$$

This limitation does not affect the efficiency of this technique. It can be observed from Table 5.1, that the computation time (CPU) required for the analysis is proportional to the number of steps adopted.

5.4 Convergence of Fourier Expansions

The load, when varying with the circumferential coordinates is expanded in a Fourier series. The analysis is

carried out to determine the stresses and displacements everywhere within the structure. When the load is represented "exactly", the solution converges.

Theoretically, the number of harmonics required for an arbitrary periodic function to be represented exactly, by means of Fourier series, is infinity, i.e.,

$$f(\theta) = \sum_{n=0}^{\infty} A_n \cos n\theta + \sum_{n=1}^{\infty} B_n \sin n\theta \quad 5.5$$

However, the load can always be described at a sufficient number of points to satisfy our engineering judgement of representing the actual loading conditions. Therefore, our concern is to examine the convergence of a function known only at a set of discrete points. If these points are equally spaced, say $2N$ points, taken over the interval $0 \leq \theta \leq 2\pi$, the spacing is,

$$\theta_i = \frac{2\pi i}{2N} \quad \text{for } i = 0, 1, 2, \dots, 2N-1 \quad 5.6$$

If now an approximation is assumed in the form

$$f(\theta) \approx \sum_{n=0}^M A_n \cos n\theta + \sum_{n=1}^M B_n \sin n\theta \quad 5.7$$

where the coefficients are to be determined in such a way that the integrated squared error over the interval of length 2π is least, then the requirement is

$$\int_0^{2\pi} \left[f(\theta) - \sum_{n=0}^M A_n \cos n\theta - \sum_{n=1}^M B_n \sin n\theta \right]^2 = \min \quad 5.8$$

Since the function $f(\theta)$ is described only at the points defined by θ_i (Eq. 5.6), we have $2N$ independent data points which are sufficient to determine the coefficients of $2N$ terms of an approximation in the form of Eq. 5.7. When $M \leq N$, Eq. 5.8 can be rewritten as follows

$$\sum_{n=0}^{2N-1} \left[f(\theta_i) - \sum_{n=0}^M A_n \cos n\theta_i - \sum_{n=1}^M B_n \sin n\theta_i \right]^2 = \min \quad 5.9$$

where $f(\theta_i)$ is the value of the function $f(\theta)$ at the point i . The solution is obtained when the partial derivatives of the left hand side of Eq. 5.9 with respect to A_n and B_n are equated to zero [15, pg. 446-457]. The coefficients are in the form

$$A_0 = \frac{1}{2N} \sum_{n=0}^{2N-1} f(\theta_i) \quad 5.10.1$$

$$A_n = \frac{1}{N} \sum_{n=0}^{2N-1} f(\theta_i) \cos n\theta_i \quad (n \neq 0, N) \quad 5.10.2$$

$$B_n = \frac{1}{N} \sum_{n=0}^{2N-1} f(\theta_i) \sin n\theta_i \quad 5.10.3$$

The calculation of each coefficient is independent of the calculation of the others and is independent of M as long as $M \leq N$. When $M = N$, the least-squares criterion (Eq. 5.9) becomes equivalent to the requirement that the "best" approximation of the function (Eq. 5.7) is obtained [15].

The loading cases of the examples discussed in Chapter 4 are shown in Fig. 5.1 and 5.2. The effect of the number of harmonics on the loading associated with these problems is considered in the following. Fourier coefficients of the wind pressure load on the hyperboloid tower are included in Table 5.2.1. Since the load is symmetric with respect to $\theta = 0$, the sine coefficients vanish. The results of superimposing the 12 coefficients, using Eq. 5.7, are shown in Table 5.2.2. It can be seen that these values approximate the load function to a very close agreement. Now examining the coefficients shown in Table 5.2.1. The 9th and the subsequent coefficients are small in comparison with the other coefficients. The magnitude of the 9th coefficient is in the same order of the 10th with opposite sign and so for the 11th and 12th. Therefore we expect that the approximation will be reasonably accurate if the series is terminated at the 8th harmonic. The results of an 8 harmonic approximation are shown in Table 5.2.2.

Fourier coefficients of the two concentrated loads of the pinched cylinder problem discussed in Sect. 4.3 are shown in Table 5.3.1. It can be seen that the odd cosine coefficients as well as the sine coefficients vanish for this case of symmetry

with respect to $\theta = 0$ and $\theta = \pi/2$. The approximation with 18 harmonics, for the loading function described at 36 points, represent the load more accurately when compared with the 12 harmonic approximation (Fig. 5.2 and Table 5.3.2). Therefore one can approximate this load by superimposing the results of $n = 0, 2, \dots, 16$.

As a general conclusion, one can consider N harmonics in the expansion of a load described at $2N$ points. A termination of the higher harmonics or exemption of a harmonic number in the series can be decided upon by examining the coefficient of each loading function as a special case.

$r = 10$ ft $E = 5000$ ksi $\nu = .15$ $h = 0.5$ ft $\lambda = 0.5852$

L (ft)	Number of Elements	Number of Points	CPU Time (sec)	λL	$M_s(0)$ (K.ft/ft)	$M_s(L)$ (K.ft/ft)	$Q_s(0)$ (K/ft)	$Q_s(L)$ (K/ft)
1	10	1	1.1	0.34	15.85	1.442	1.438	-1.676
2	10	1	1.15	0.44	5.85	1.442	1.442	-1.676
3	20	1	2.1	0.59	11.71	1.430	1.430	-1.675
4	40	1	2.1	0.59	23.41	1.451	4.5.05	-1.697
5	40	1	3.1	0.83	23.41	1.427	1.427	-1.672
6	50	1	2.1	0.59	29.26	-0.139	-2446.0	0.167
7	50	1	3.1	0.82	29.26	1.426	1.424	-2173.0
8	50	1	4.1	1.06	29.26	1.426	1.427	-1.671
9	50	1	5.1	1.32	29.26	1.426	1.427	-1.671
10	50	2	2.1	1.13	14.63	1.426	1.428	-1.671
11	60	1	3.1	0.84	35.11	1.388	121.8	-1.631
12	60	1	4.1	1.08	35.11	1.426	0.876	-62.74
13	60	1	5.1	1.31	35.11	1.426	2.367	-1.671
14	60	1	8.1	2.10	35.11	1.426	0.511	-1.671
15	60	2	2.1	1.12	17.55	1.426	1.426	-1.670
16	60	2	3.1	1.60	17.55	1.426	1.426	-1.670
17	100	1	10.1	2.50	58.52	-.075	-2.84x10 ⁸	-0.068
18	100	2	3.1	1.61	29.41	1.425	1.422	-1.670
19	100	3	2.1	1.68	19.50	1.425	1.425	-1.670

Table 5.1 Effect of Length and Number of Integration Points on the Accuracy of the Solution

Harmonic Number	Cosine Coefficient	θ	Load Value for 12 Harmonics	Load Value for 8 Harmonics
0	0.3833	0	-1.016	-1.010
1	-0.2792	7.5	-0.955	- .952
2	-0.6198	15	-0.783	-0.787
3	-0.5093	22.5	-0.528	-0.535
4	-0.0917	30	-0.216	-0.219
5	0.1179	37.5	0.136	0.141
6	0.0333	45	0.516	0.522
7	-0.0447	52.5	0.888	0.887
8	-0.0083	60	1.183	1.178
9	0.0093	67.5	1.335	1.335
10	-0.0136	75	1.316	1.319
11	0.0060	82.5	1.146	1.144
		90	0.883	0.878
		97.5	0.610	0.613
		105	0.416	0.429
		112.5	0.352	0.355
		120	0.383	0.366
		127.5	0.423	0.406
		135	0.416	0.427
		142.5	0.387	0.416
		150	0.383	0.391
		157.5	0.407	0.378
		165	0.416	0.388
		172.5	0.398	0.409
		180	0.383	0.420

TABLE 5.2.1
Fourier Coefficients
of Wind Pressure Load

TABLE 5.2.2 Effect of Number of
Harmonics on Representing
the Wind Pressure Load

Harmonic Number	Cosine Coefficient
0	0.0555
1	0
2	0.1111
3	0
4	0.1111
5	0
6	0.1111
7	0
8	0.1111
9	0
10	0.1111
11	0
12	0.1111
13	0
14	0.1111
15	0
16	0.1111
17	0

TABLE 5.3.1

Fourier Coefficients
of Two Diametrically
Opposed Concentrated
Loads

θ	Load Value for 18 Harmonics	Load Value for 12 Harmonics
0	0.994	0.611
5	0.635	0.522
10	0.055	0.301
15	-0.207	0.055
20	-0.055	-0.104
25	0.119	-0.131
30	0.055	-0.055
35	-0.079	0.041
40	-0.055	0.085
45	0.055	0.055
50	0.055	-0.012
55	-0.039	-0.061
60	-0.055	-0.055
65	0.026	-0.005
70	0.055	0.045
75	0.015	0.055
80	-0.055	0.019
85	0.005	-0.032
90	0.055	-0.055

TABLE 5.3.2 Effect of Number of
Harmonics on Representing
the Two Concentrated Loads

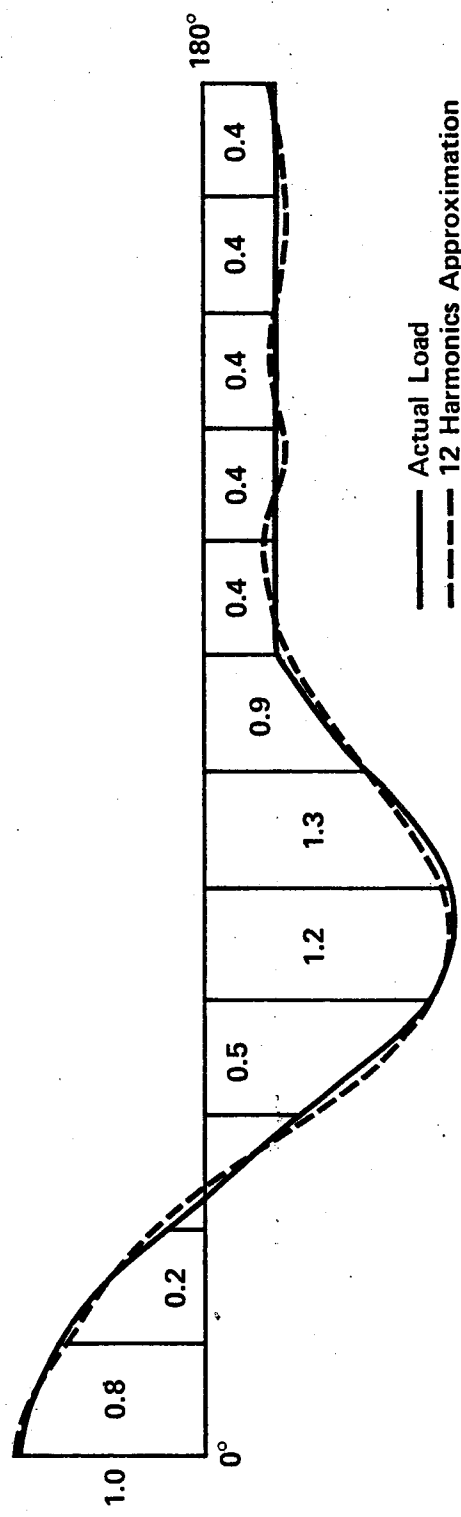


Fig. 5.1 Fourier Approximation for Wind Load

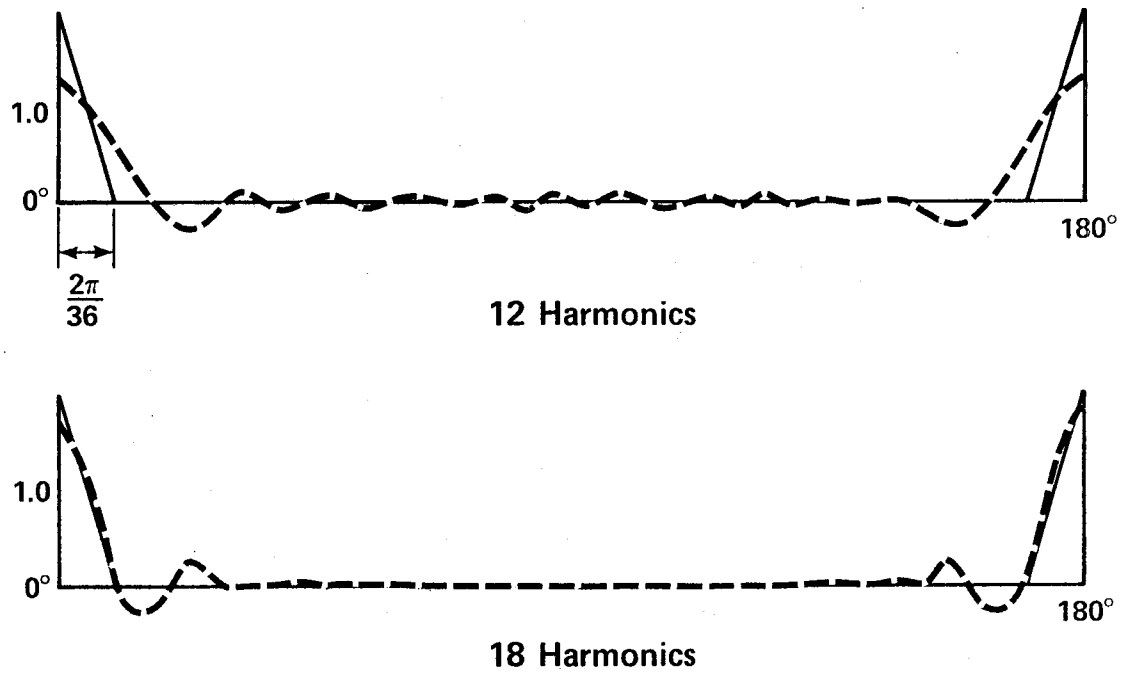


Fig. 5.2 Fourier Approximation for Two Diametrically Opposed Concentrated Loads

CHAPTER 6

SUMMARY AND CONCLUSIONS

In this study, a theory has been generalized. A computer program has been developed for the elastic analysis of axisymmetric segmented shell structure of general geometric configuration. General arbitrary loadings have been considered. Applications for a number of loading cases and elements have been presented.

The reduction of the governing partial differential equations of the classical shell theory to a set of eight first order ordinary differential equations involves only straight forward algebraic manipulations. The classical theory chosen as a foundation for the theory presented herein, Flügge's theory, is considered one of the most accurate theories available in the literature. The approximation in formulating the basic governing equations of this theory are such that the theory may be considered to be exact. The adaptation of the general form of these basic equations allows the geometry of any type of shell element to be considered, without any theoretical approximations which may be suitable for specific dimensions and not for others. Variation of the shell thickness along the meridian can be accounted for with accuracy comparable to that for constant thickness.

The loads, when approximated by means of Fourier series, may be represented with sufficient accuracy by including a number of harmonics, within practical limits. This approximation allows the consideration of general arbitrary types of loadings in a simple manner.

The excellent agreement between the results of the problems presented in this thesis and the results of other known solutions, analytical or numerical, demonstrate the accuracy of the solution technique and the reliability of the numerical integration process used.

It may be concluded that the solution technique presented in this study is simple and general for the elastic analysis of shells of revolution. The accuracy is consistent with a good shell theory. The geometric limitations are of no importance from the practical point of view.

Further development, by applying this method to the study of free vibration and elastic buckling criteria of shells of revolution is possible.

REFERENCES

1. ACI-ASCE Committee 334, *Concrete Shell Design and Construction, Design and Construction of Reinforced Concrete Cooling Tower Shells, Practice and Commentary Draft 1974.*
2. Ashwell, D.G., Gallagher, R.H., *Finite Elements for Thin Shells and Curved Members*, John Wiley & Sons, New York, 1976.
3. Baker, E.H., Kovalesky, L., Rish, F.L., *Structural Analysis of Shells*, McGraw-Hill Book Company Inc., New York, 1972.
4. Billington, D.P., *Thin Shell Concrete Structures*, McGraw-Hill Book Company Inc., New York, 1965.
5. Bogner, F.K., Fox, R.L. and Schmit, L.A., *A Cylindrical Shell Discrete Element*, A.I.A.A. Journal, Vol. 5, No. 4, April 1967, pp. 745-749.
6. Budiansky, B. and Radkowsky, P.P., *Numerical Analysis of Unsymmetrical Bending of Shells of Revolution*, A.I.A.A. Journal, Vol. 1, No. 8, August 1963, pp. 1833-1842.
7. Cantin, G.M. and Clough, R.W., *Curved Cylindrical Shell Finite Element*, A.I.A.A. Journal, Vol. 6, No. 6, June 1968, pp. 1057-1062.
8. Dorn, S.W., *Numerical Methods with Fortran IV Case Studies*, John Wiley & Sons, Inc., New York, 1972.
9. Dunham, R.S. and Nickell, R.E., *Finite Element Analysis of Axisymmetric Solids with Arbitrary Loadings*, Structural Engineering Report No. 67-6, University of California, Berkeley, June 1967.
10. Flügge, W., *Stresses in Shells*, 2nd Ed., Springer-Verlag, New York - Berlin, 1973.
11. Gallagher, R.H., *The Development and Evaluation of Matrix Methods for Thin Shell Structural Analysis*, Ph.D. Thesis, State University of New York, Buffalo, New York, 1966.

12. Goldberg, J.E., Bogdanoff, J.L. and Alspaugh, D.W., *Stresses in Spherical Domes Under Arbitrary Loading Including Thermal and Shrinkage Effects*, Non-Classical Shell Problems, Proceedings of Symposium, Warsaw, North Holland Publishing Co., Amsterdam, September 1963.
13. Grafton, P.E. and Strome, D.R., *Analysis of Axisymmetrical Shells by the Direct Stiffness Method*, A.I.A.A. Journal, Vol. 1, No. 10, October 1963, pp. 2342-2347.
14. Gurfinkel, G. and Wolser, A., *Analysis and Design of Hyperbolic Cooling Towers*, Journal of the Power Division, Vol. 98, No. P01, ASCE, June 1972, pp. 133-152.
15. Hildebrand, F.B., *Introduction to Numerical Analysis*, 2nd Ed., McGraw-Hill Inc., New York, 1974.
16. Iyer, S.H. and Simmonds, S.H., *Stiffness Influence Coefficients for Non-Axisymmetrical Loading on Closed Cylindrical Shells*, Structural Engineering Report, No. 31, The University of Alberta, Edmonton, October 1970.
17. Iyer, S.H. and Simmonds, S.H., *Wind Loading on Conical Shells*, Proceedings of the International Association of Shells Structure, I.A.S.S., Calgary, Canada, July 1972.
18. Kalnins, A., *Analysis of Shells of Revolution Subjected to Symmetrical and Non-Symmetrical Loads*, Journal of Applied Mechanics, Vol. 31, September 1964, pp. 467-476.
19. Kempner, J., *Remarks on Donnell's Equations*, Journal of Applied Mechanics, Vol. 22, No. 1, March 1955.
20. Meyer, R.R. and Harmon, M.B., *Conical Segment Method for Analyzing Open Crown Shells of Revolution for Edge Loading*, A.I.A.A. Journal, Vol. 1, No. 4, April 1963, pp. 886-891.
21. Murray, D.W., Rohardt, A.M. and Simmonds, S.H., *A Classical Flexibility Analysis for Gentilly Type Containment Structures*, Structural Engineering Report No. 63, The University of Alberta, Edmonton, June 1977.
22. Percy, J.H., Pian, T.H., Klein, S. and Norvaratna, D.R., *Application of the Matrix Displacement Method to Linear Elastic Analysis of Shells of Revolution*, A.I.A.A. Journal, Vol. 3, No. 11, November 1965, pp. 2138-2145.

23. Pestel, C.E., Leckie, F.A., *Matrix Methods in Elasto-Mechanics*, McGraw-Hill Book Company, New York, 1963.
24. Rizkalla, S.H., *An Investigation of Segmentally Constructed Hyperboloid Natural Draft Cooling Tower*, Ph.D. Thesis, North Carolina State University, Raleigh, 1976.
25. Sepetoski, W.K., Pearson, C.E., Dingwell, I.W. and Adkins, A.W., *A Digital Computer Program for a General Axially Symmetric Thin Shell Problem*, Journal of Applied Mechanics, Vol. 29, Transaction ASME, Vol. 84, Series E, 1962, pp. 655-661.
26. Soare, M., *Application of Finite Difference Equations to Shell Analysis*, Pergamon Press, New York, 1967.
27. Timoshenko, S. and Woinowsky-Krieger, S., *Theory of Plates and Shells*, 2nd Ed. McGraw-Hill Book Company, 1959.

APPENDIX A

SHELL THEORY

This appendix presents the analytical development of the basic equations, used in this study, as given by Flügge [10].

A.1 Geometry of Shells

The geometry of a shell is defined by specifying the form of the middle surface and the thickness of the shell at each point. The surface of a shell of revolution is generated by the rotation of a plane curve about an axis in its plane. This generating curve is called the "meridian". The intersection of the surface with planes perpendicular to the axis of revolution are "parallel circles". Two coordinates s, θ are required to describe any point on the middle surface of the shell:

- a) s measures the distance to the point along the meridian from the intersection of the middle surface with the axis of rotation, or from a datum parallel circle.
- b) θ is the angular "distance" of the point from a datum generator.

A third coordinate z is required to measure the distance along a normal to the middle surface.

The radii of curvature of a shell of revolution are:

- a) r is the radius of curvature of parallel circles
- b) r_1 is the radius of curvature of meridian

- c) r_2 is the length of the normal between any point on the middle surface and the axis of revolution.

The following fundamental geometrical relations can clearly be seen in Fig. A.1

$$r = r_2 \sin\phi \quad \text{A.1.1}$$

$$ds = r_1 d\phi \quad \text{A.1.2}$$

$$dr = ds \cos\phi \quad \text{A.1.3}$$

$$dx = ds \sin\phi \quad \text{A.1.4}$$

where ϕ represents the angular distance of the point under consideration from the axis of rotation.

From Eqs. A.1 one can write

$$\frac{dr}{ds} = \cos\phi \quad \text{A.2.1}$$

$$\frac{dr_2}{ds} = \frac{r_1 - r_2}{r_1} \cot\phi \quad \text{A.2.2}$$

For simplicity the derivatives with respect to s and θ will be indicated by dots and primes respectively, i.e.,

$$\frac{\partial}{\partial s} () \equiv ()^* \quad \text{A.3.1}$$

$$\frac{\partial}{\partial \theta} () \equiv ()' \quad \text{A.3.2}$$

A.2 Equations of Equilibrium

If a shell element is cut out by two meridians and two parallel circles, each pair infinitely close as seen in Fig. A.2, the element is stressed by ten stress resultant components which must be in equilibrium with the external applied load. These stress resultants are:

N_s, N_θ = normal in-plane forces per meridional and circumferential unit length, respectively.

$N_{s\theta}, N_{\theta s}$ = in-plane shear forces per meridional and circumferential unit length, respectively.

Q_s, Q_θ = transverse shear forces per meridional and circumferential unit lengths, respectively.

M_s, M_θ = meridional and circumferential moments per unit length, respectively.

$M_{s\theta}, M_{\theta s}$ = circumferential and meridional twisting moments per unit length, respectively.

The sign convention for the forces is shown in Fig. A.2

Referring to the three orthogonal axis s, θ, z , one can obtain six equations of equilibrium

$$\sum N_i = 0 \quad \text{A.4.1}$$

$$\sum M_i = 0 \quad \text{A.4.2}$$

where $\sum N_i$ is the sum of the forces in the i direction
 $(i = s, \theta, z)$.

ΣM_i is the sum of the moments about the i axis
 $(i = s, \theta, z)$

The six equilibrium equations in terms of the ten stress resultants are

$$r_1(rN_s)' + r_1N'_{\theta s} - r_1N_\theta \cos\phi - r_1Q_s + rr_1P_s = 0 \quad A.5.1$$

$$r_1(rN_{s\theta})' + r_1N'_{\theta} + r_1N_{\theta s} \cos\phi - r_1Q_\theta \sin\phi + rr_1P_\theta = 0 \quad A.5.2$$

$$r_1N_\theta \sin\phi + rN_s + r_1Q'_\theta + r_1(rQ_s)' - rr_1P_z = 0 \quad A.5.3$$

$$r_1(rM_s)' + r_1M'_{\theta s} - r_1M_\theta \cos\phi - rr_1Q_s = 0 \quad A.5.4$$

$$r_1(rM_{s\theta})' + r_1M'_{\theta} + r_1M_{\theta s} \cos\phi - rr_1Q_\theta = 0 \quad A.5.5$$

$$rr_1N_{\theta s} - rr_1N_{s\theta} - r_1M_{\theta s} \sin\phi + rM_{s\theta} = 0 \quad A.5.6$$

where P_s , P_θ , P_z are the resolved components of the external applied load in the s , θ , z , respectively. If the subscript s , in the above equations, is replaced by ϕ , and the relations

$$\frac{1}{r_1} \frac{\partial}{\partial\phi} () = ()' \quad A.6$$

is observed. The above set of equations (Eqs. A.5) can be reduced to the equilibrium equations in Reference 10, pg. 318. Six

equations of equilibrium are not enough to determine the ten stress resultants. The shell element is four times internally statically indeterminate and therefore, an analysis of the deformation of the shell is required in order to obtain the solution.

A.3 Strain-Displacement Relations

The displacement vector of a point lying on the middle surface of an element may be described by its three orthogonal components, defined as:

W = the displacement component in the radial direction, positive when it points away from the centre of curvature.

V = the displacement component in the meridional direction, positive in the direction of increasing the coordinate s .

U = the displacement component in the direction of the tangent to the parallel circle, positive in the direction of increasing the coordinate θ .

In addition, the auxiliary variable β , which represents the angle by which an element of the meridian rotates during deformation may be expressed in terms of the displacement components, Fig. A.3, as [10].

$$\beta = -W^* + \frac{V}{r_1}$$

A.7.1

By differentiation, the change in slope of the meridian due to deformation, is

$$\beta^* = -W^{**} + \frac{r_1 v^* - r_1^* v}{r_1^2}$$

A.7.2

Referring to Fig. A.4, one can obtain the relationship between the strains and the displacement components of a point on the middle surface.

The meridional strain is

$$\epsilon_s = \frac{\text{Elongation of the line element } ds}{ds}$$

$$= \frac{W}{r_1} + v^*$$

A.8.1

The hoop strain is

$$\epsilon_\theta = \frac{\text{Elongation of the line element } rd\theta}{rd\theta}$$

$$= \frac{U' + V \cos\phi + W \sin\phi}{r}$$

A.8.2

The shear strain, which is the change of the right angle between the two line elements ds and $rd\theta$ (Fig. A.4.3), is equivalent to

$$\gamma_{s\theta} = \gamma_1 + \gamma_2 =$$

$$= \frac{V'}{r} + U^* + \frac{U}{r} \cos\phi$$

A.8.3

Since the displacement is assumed to be very small in comparison with the principal radii of curvature, all products of two displacement components have been dropped in deriving the foregoing equations.

One may use the preceding equations to express the relationship between the strains and the displacement components of an arbitrary point at a distance z from the middle surface by simply replacing W , V , U with the displacement components of this point W_z , V_z , U_z , and replacing the radii r_1 , r_2 with $r_1 + z$ and $r_2 + z$, respectively.

Then

$$\epsilon_s = \frac{W_z}{r_1 + z} + V_z \quad A.9.1$$

$$\epsilon_\theta = U'_z + \frac{V_2 \cos\phi + W_z \sin\phi}{(r_2 + z) \sin\phi} \quad A.9.2$$

$$\gamma_{s\theta} = U_z - \frac{U_z \cos\phi - V'_z}{(r_2 + z) \sin\phi} \quad A.9.3$$

By introducing the assumption that lines normal to the middle surface before deformation remain normal after deformation, it can clearly be seen from Fig. A.5 that

$$W_z = W \quad A.10.1$$

$$V_z = V \frac{r_1 + z}{r_1} + W'z \quad A.10.2$$

$$U_z = U \frac{r_2 + z}{r_2} + W'\frac{z}{r} \quad A.10.3$$

Therefore, the strains at a distance z from the middle surface in terms of the displacements W , V , U at the middle surface can be obtained by substituting Eqs. A.10 into Eqs. A.9 to obtain

$$\epsilon_s = \frac{1}{r_1 + z} W + \frac{r^*_{1z}}{r_1 + z} W^* - \frac{r_{1z}}{r_1 + z} W^{**}$$

$$+ V^* - \frac{r^*_{1z}}{r_1(r_1 + z)} V \quad A.11.1$$

$$\epsilon_\theta = \frac{1}{r_2 + z} W - \frac{z \cot\phi}{r_2 + z} W^* - \frac{z}{r \sin\phi (r_2 + z)} W'''$$

$$+ \frac{\cot\phi (r_1 + z)}{r_1(r_2 + z)} V + \frac{1}{r} U' \quad A.11.2$$

$$\gamma_{s\theta} = \frac{r_1(r_2 + z)}{r_2(r_1 + z)} U^* - \frac{r_1(r_2 + z)}{r_2^2(r_1 + z)} \cot\phi U$$

$$+ \frac{(r_2 + z)}{r_1 \sin\phi(r_2 + z)} V' - \frac{z}{\sin\phi} \left(\frac{1}{r_2 + z} + \frac{r_1}{r_2(r_1 + z)} \right) W'' \quad A.11.3$$

$$+ \frac{\cot\phi}{r_2 \sin\phi} \left(\frac{z}{r_2 + z} + \frac{r_{1z}}{r_2(r_1 + z)} \right) W' \quad A.11.3$$

A.4 Stress-Strain Relations

Hooke's law relates the strains to the corresponding stresses in linearized form, as long as the stresses remain within the elastic limit. If T is the change in temperature measured from arbitrary level. Hooke's law may be written, in index notation, as

$$E\epsilon_i = \sigma_i - \nu(\sigma_j + \sigma_k) + E\alpha T \quad A.12.1$$

$$G\gamma_{ij} = \tau_{ij} \quad A.12.2$$

where

i, j, t take in turns the direction s, θ, z

σ_i is the normal stress in the i direction

τ_{ij} is the shearing stress in the i plane and
 j direction

$$G = \frac{E}{2(1 + \nu)} \quad A.13$$

The modulus of elasticity, E , Poisson's ratio, ν , the coefficient of thermal expansion, α , and thus the shear modulus, G , are the material constants.

As in the theory of plates, except in the immediate vicinity of concentrated forces, the stresses in z direction are small in comparison with the stresses in s, θ directions and their influence in Hooke's law may be neglected, i.e., it is assumed that

$$\sigma_z = \gamma_{sz} = \gamma_{\theta z} = 0 \quad A.14$$

Therefore, the stress-strain relations can be written as

$$\sigma_s = \frac{E}{1 - \nu^2} \left[\epsilon_s + \nu \epsilon_\theta - (1 + \nu) \alpha T \right] \quad A.15.1$$

$$\sigma_\theta = \frac{E}{1 - \nu^2} \left[\epsilon_\theta + \nu \epsilon_s - (1 + \nu) \alpha T \right] \quad A.15.2$$

$$\tau_{s\theta} = \frac{E}{2(1+\nu)} \gamma_{s\theta}$$

A.15.3

A.5 Elastic Law

The internal stress resultants can be determined by integrating the stresses through the shell thickness (Fig. A.6). They are defined as

$$N_s = \int_{-t/2}^{t/2} \sigma_s \frac{r_2 + z}{r_2} dz \quad A.16.1$$

$$N_\theta = \int_{-t/2}^{t/2} \sigma_\theta \frac{r_1 + z}{r_1} dz \quad A.16.2$$

$$N_{s\theta} = \int_{-t/2}^{t/2} \tau_{s\theta} \frac{r_1 + z}{r_2} dz \quad A.16.3$$

$$N_{\theta s} = \int_{-t/2}^{t/2} \tau_{\theta s} \frac{r_1 + z}{r_1} dz \quad A.16.4$$

$$M_s = \int_{-t/2}^{t/2} \sigma_s \frac{r_2 + z}{r_2} zdz \quad A.16.5$$

$$M_\theta = - \int_{-t/2}^{t/2} \sigma_\theta \frac{r_1 + z}{r_1} zdz \quad A.16.6$$

$$M_{s\theta} = \int_{-t/2}^{t/2} \tau_{s\theta} \frac{r_2 + z}{r_2} zdz \quad A.16.7$$

$$M_{\theta s} = \int_{-t/2}^{t/2} \tau_{\theta s} \frac{r_1 + z}{r_1} zdz \quad A.16.8$$

It should be noted that the expressions for Q_s , Q_θ have been omitted as they are equal to the integral of the shearing stresses in z direction. Also the minus sign in these expressions correspond to the positive directions assumed for the stress resultants as shown in Fig. A.6.

The expressions for σ_s , σ_θ , $\tau_{s\theta}$ (Eqs. A.15) can be entered into Eqs. A.16. Then Eqs. A.11 are substituted for the displacements and the integration with respect to z is performed. The results in the stress-resultant-displacement relationships.

$$\begin{aligned} N_s &= D \left[V^* + \frac{W}{r_1} + v \frac{U' + V \cos\phi + W \sin\phi}{r} \right] \\ &\quad + \frac{K}{r_1^2} \frac{r_2 - r_1}{r_2} \left[\left(\frac{V}{r_1} - W^* \right) r_1 + r_1 W^* + \frac{W}{r_1} \right] \\ &\quad - (1 + v) \alpha D T_{o2} \end{aligned} \quad A.17.1$$

$$\begin{aligned} N_\theta &= D \left[\frac{U' + V \cos\phi + W \sin\phi}{r} + v \left(V^* + \frac{W}{r_1} \right) \right] \\ &\quad - \frac{K}{rr_1} \frac{r_2 - r_1}{r_2} \left[\frac{V}{r_1} \left(\frac{r_1 - r_2}{r_2} \right) \cos\phi + \frac{W \sin\phi}{r_2} \right. \\ &\quad \left. + \frac{W''}{r} + W^* \cos\phi \right] - (1 + v) \alpha D T_{o1} \end{aligned} \quad A.17.2$$

$$\begin{aligned}
 N_{s\theta} &= D \left(\frac{1 - v}{2} \right) \left[U^* + \frac{V' - U \cos\phi}{r} \right] \\
 &\quad + \frac{K}{r_1^2} \left(\frac{1 - v}{2} \right) \frac{r_2 - r_1}{r_2} \left[U^* \left(\frac{r_2 - r_1}{r_2} \right) \right. \\
 &\quad \left. + U \frac{r_1 - r_2}{r_2} \frac{\cot\phi}{r_2} + W'^* \frac{r_1}{r} - W' \frac{r_1 \cos\phi}{r^2} \right] \quad A.17.3
 \end{aligned}$$

$$\begin{aligned}
 N_{\theta s} &= D \left(\frac{1 - v}{2} \right) \left[U^* + \frac{V' - U \cos\phi}{r} \right] \\
 &\quad + \frac{K}{rr_1} \left(\frac{1 - v}{2} \right) \frac{r_2 - r_1}{r_2} \left[V' \frac{r_2 - r_1}{r_1 r_2} - W'^* + \frac{W' \cos\phi}{r} \right] \quad A.17.4
 \end{aligned}$$

$$\begin{aligned}
 M_s &= K \left[W^{**} - W^* \frac{r^* 1}{r_1} - W \frac{r_1 - r_2}{r_2} \frac{1}{r_1^2} - \frac{V^*}{r_2} + V \frac{r^* 1}{r_1^2} \right. \\
 &\quad \left. + v \frac{W''}{r^2} + v \frac{W^* \cos\phi}{r} - v \frac{U'}{rr_2} - v \frac{V \cos\phi}{rr_1} \right] \\
 &\quad + (1 + v) \alpha K T_{12} \quad A.17.5
 \end{aligned}$$

$$\begin{aligned}
 M_\theta &= K \left[\frac{W''}{r^2} + \frac{W^* \cos\phi}{r} - \frac{W}{r_2^2} \frac{r_2 - r_1}{r_1} - \frac{U'}{rr_1} \right. \\
 &\quad \left. - \frac{V \cos\phi}{rr_1} \frac{2r_2 - r_1}{r_2} + v W^{**} - v W^* \frac{r_1^*}{r_1} \right. \\
 &\quad \left. - v \frac{V^*}{r_1} + v \frac{V r_1^*}{r_1^2} \right] + (1 + v) \alpha K T_{11} \quad A.17.6
 \end{aligned}$$

$$M_{s\theta} = K \frac{1 - \nu}{2} \left[\frac{2W'^*}{r} - \frac{2W'}{r^2} \cos\phi - \frac{U^*}{r_2} \frac{2r_1 - r_2}{r_2} + \frac{U}{r_2^2} \frac{2r_1 - r_2}{r_1} \cot\phi - \frac{V'}{rr_1} \right] \quad A.17.7$$

$$M_{\theta s} = K \frac{1 - \nu}{2} \left[\frac{2W'^*}{r} - \frac{2W'}{r^2} \cos\phi - \frac{U^*}{r_2} + \frac{U \cot\phi}{r_2^2} - \frac{V'}{rr_1} \frac{2r_2 - r_1}{r_2} \right] \quad A.17.8$$

Where the extensional rigidity, D, is defined as

$$D = \frac{Et}{1 - \nu^2} \quad A.18.1$$

and the flexural rigidity, K, is defined as

$$K = \frac{Et^3}{12(1 - \nu^2)} \quad A.18.2$$

The temperature terms T_{ok} and T_{1k} ($k = 1, 2$) are defined as follows:

$$T_{ok} = \frac{1}{t} \int_{-t/2}^{t/2} T dz + \frac{1}{tr_k} \int_{-t/2}^{t/2} T z dz \quad A.19.1$$

$$T_{1k} = \frac{12}{t^3} \int_{-t/2}^{t/2} T z dz + \frac{12}{t^3 r_k} \int_{-t/2}^{t/2} T z^2 dz \quad A.19.2$$

If a linear variation of the temperature T through the thickness is assumed, Eqs. A.19 can be integrated by parts to yield

$$T_{ok} = \left\{ \frac{T^o + T^i}{2} + (T^o - T^i) \frac{t}{12r_k} \right\} \quad A.20.1$$

$$T_{1k} = \left\{ \frac{T^o - T^i}{t} + \frac{T^o + T^i}{2r_k} \right\} \quad A.20.2$$

in which T^o and T^i are the temperature measured at the outer and inner face of the shell respectively. If the term t/r_k is neglected when compared with unity, the subscript k disappears from Eqs. A.20 and T_o , T_1 can be defined as the average temperature measured on the middle surface and the temperature gradient respectively.

By substituting Eq. A.6 into Eqs. A.17 and changing the subscript s to ϕ , Eqs. A.17 reduce to the elastic law in Reference 10, pg. 322.

Eqs. A.5 and A.17 are the governing equations for a shell of revolution. The sixth equation of equilibrium (Eq. A.5.6) is identically satisfied if $r_1 = r_2$. Therefore, the five remaining equations of equilibrium (Eqs. A.5) and the eight equations of the elastic law (Eqs. A.17) are 13 equations in 13 unknowns (the three displacement components and ten stress resultants). Theoretically, one can solve for the stresses and displacements at any point in the shell using these equations.

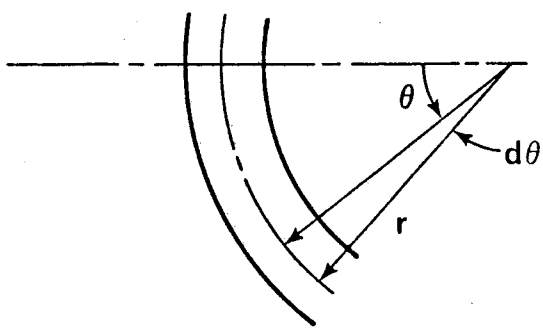
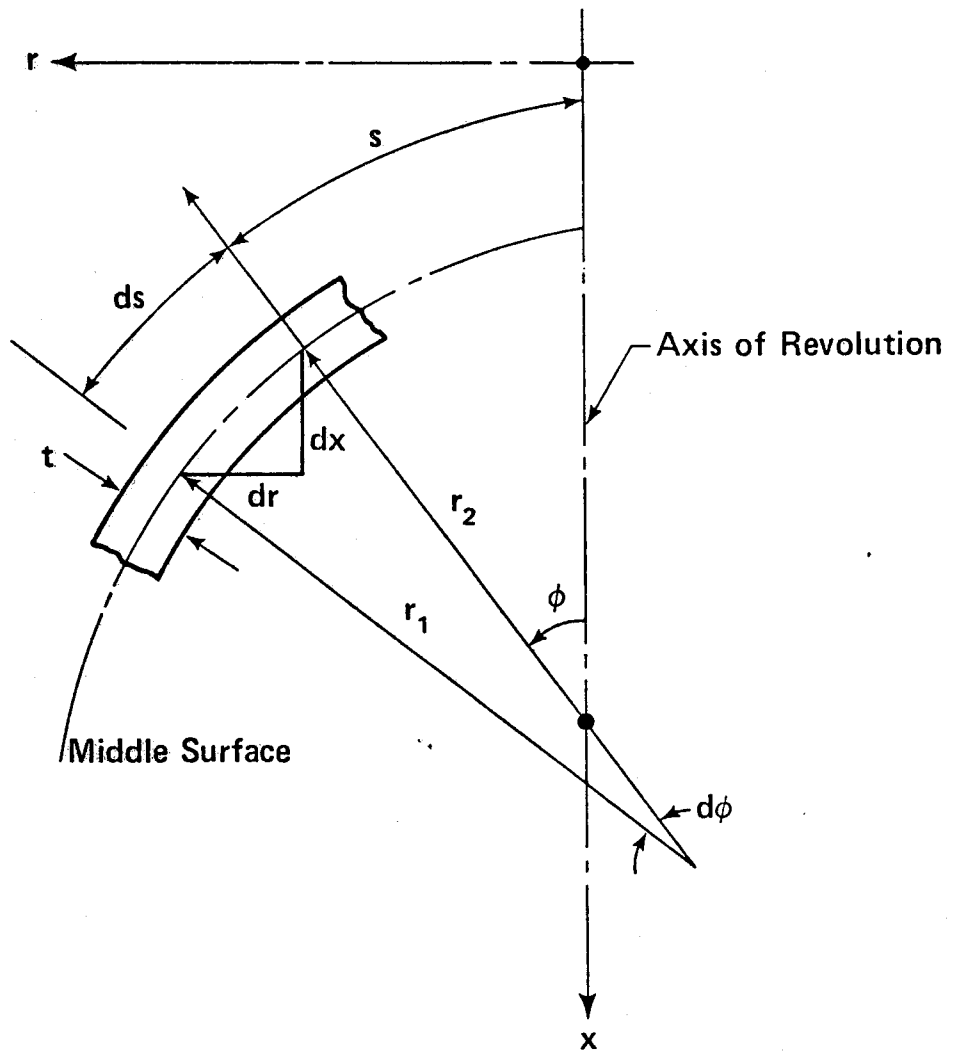


Fig. A.1 Meridian and Parallel Circle of a Shell of Revolution

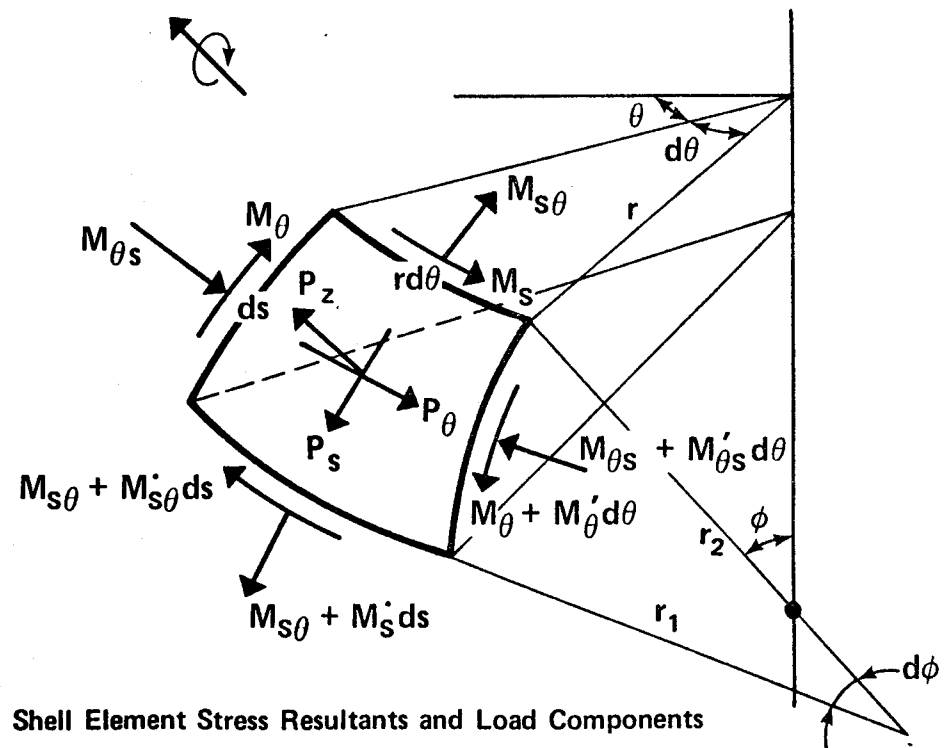
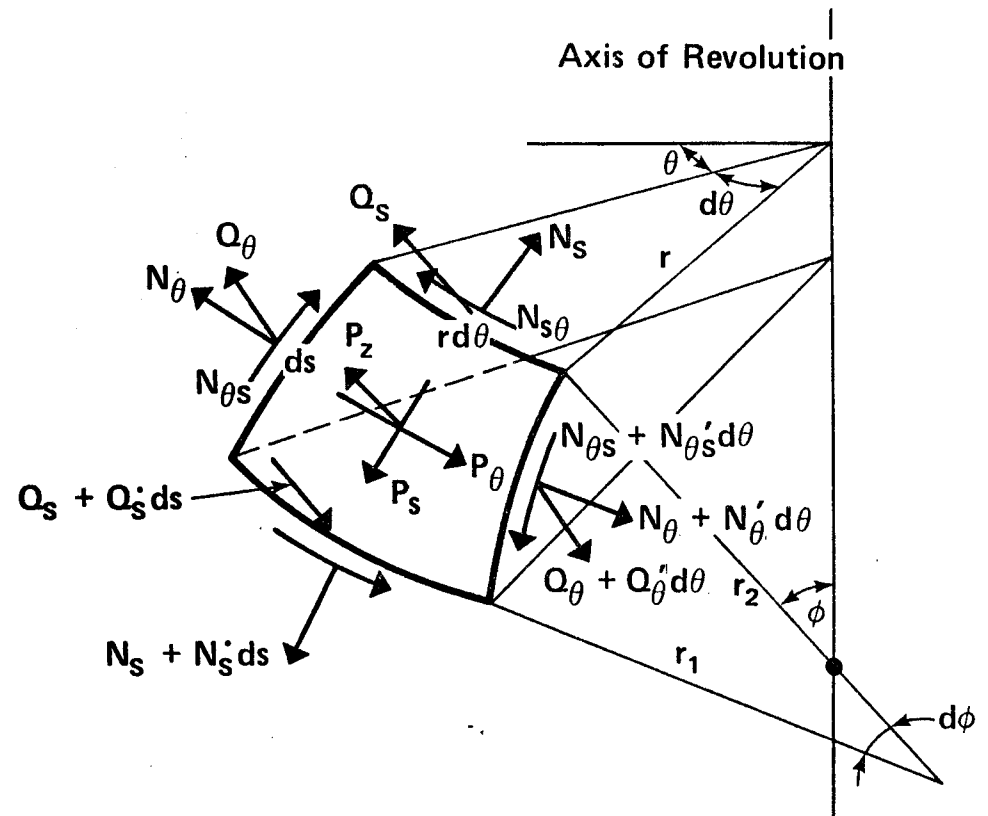


Fig. A.2 Shell Element Stress Resultants and Load Components

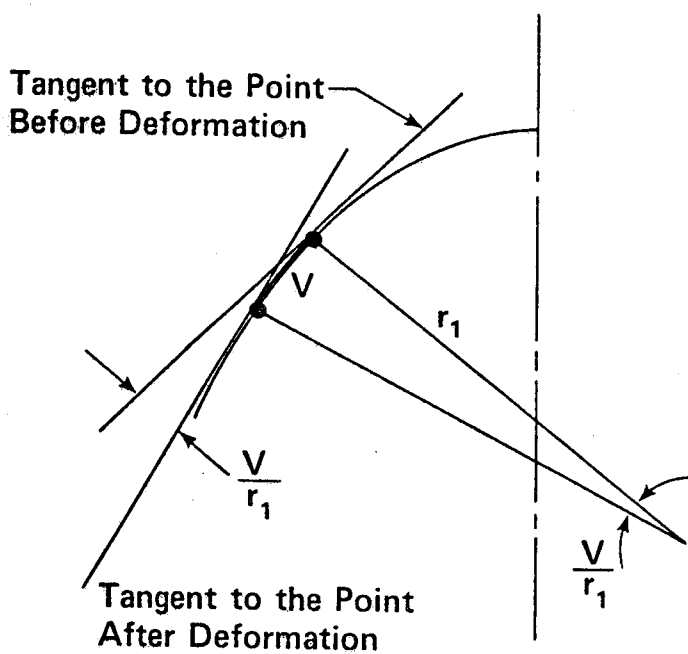


Fig. A.3.1 Meridional Rotation Due to Displacement V

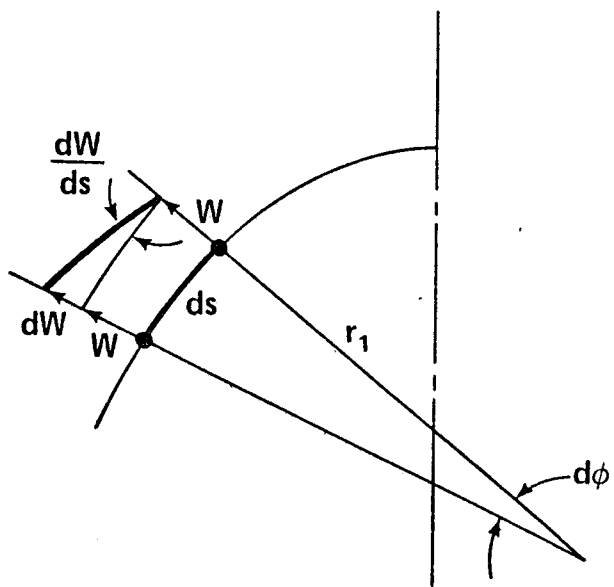


Fig. A.3.2 Meridional Rotation Due to Displacement W

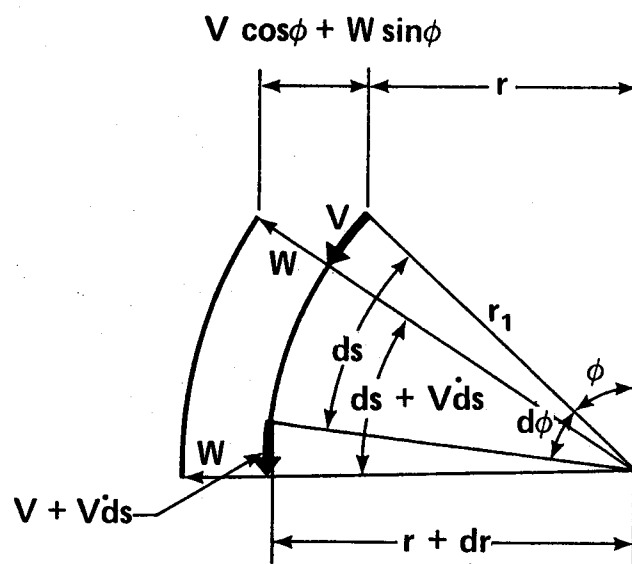


Fig. A.4.1 Meridian of a Shell Before and After Deformation

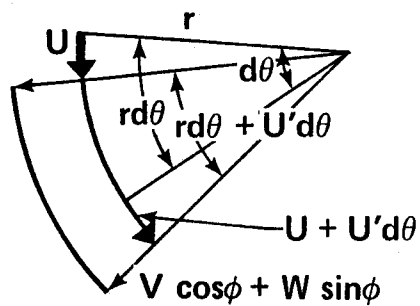


Fig. A.4.2 Parallel Circle Before and After Deformation

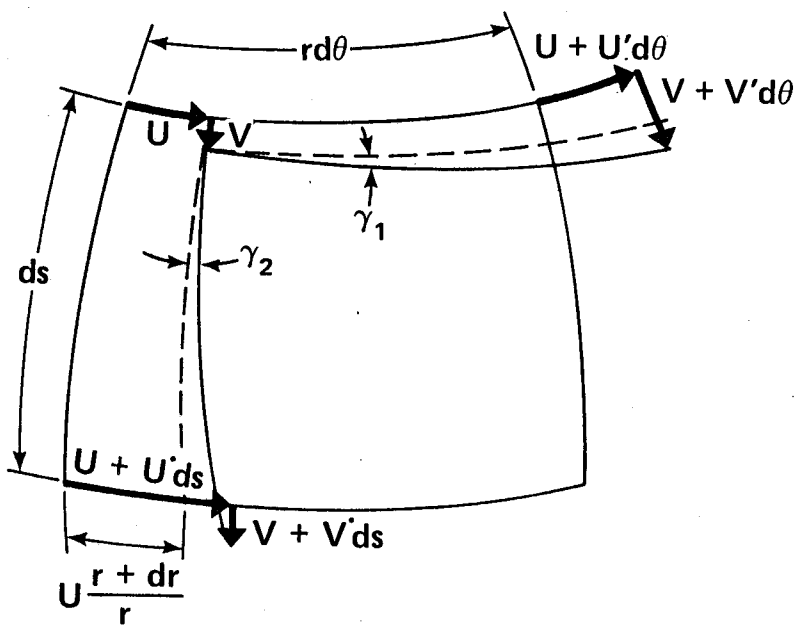
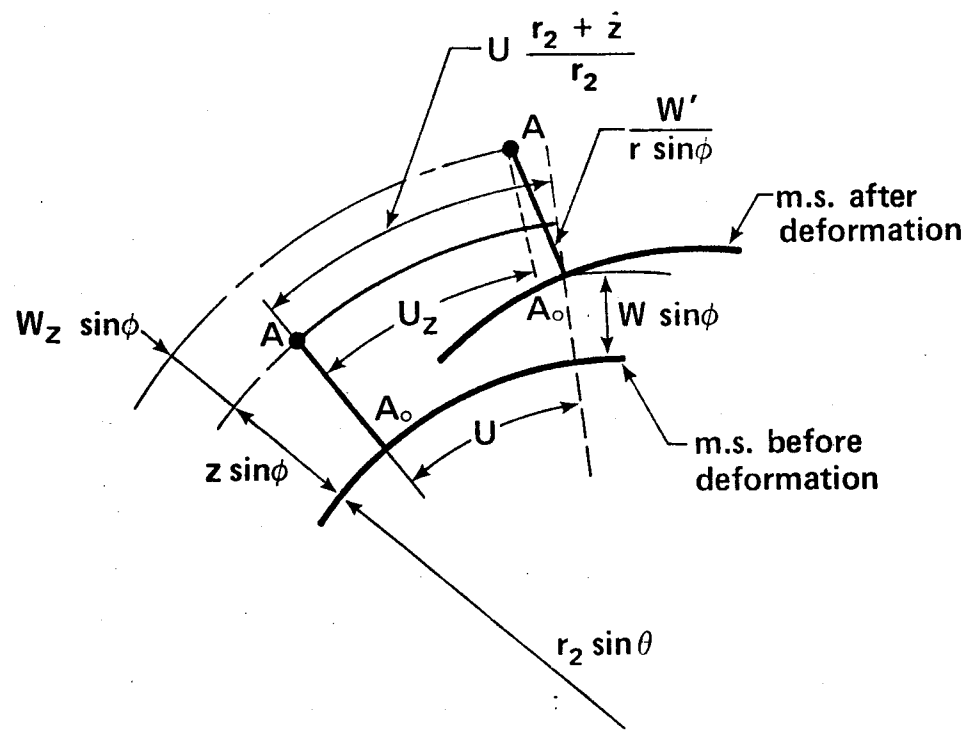
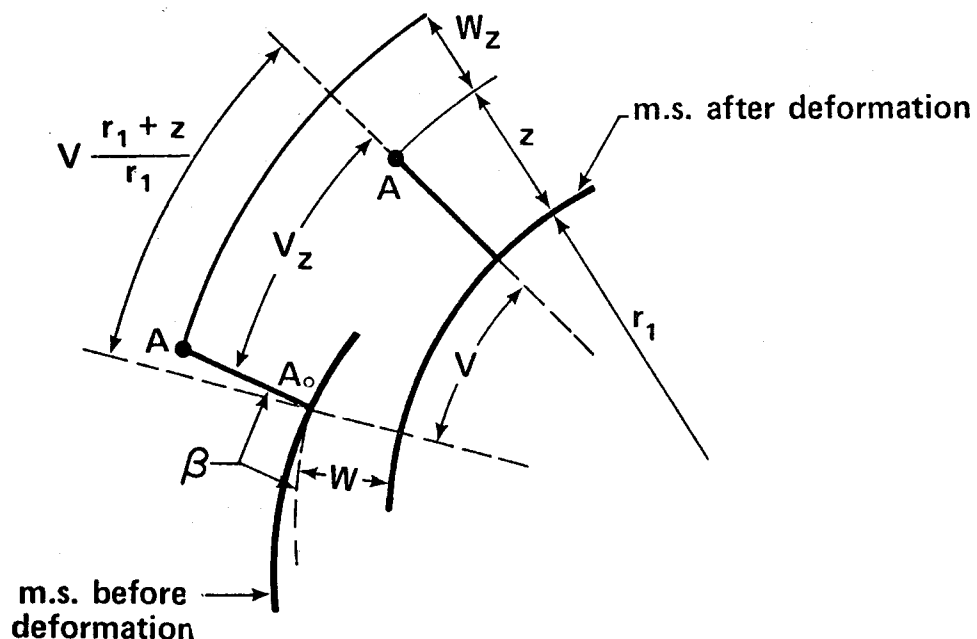


Fig. A.4.3 Change of the Right Angle Between Line Elements After Deformation



(a) Plane of Parallel Circle



(b) Meridian

Fig. A.5 Relation Between Displacement
of Two Points on Line Normal to the Middle Surface

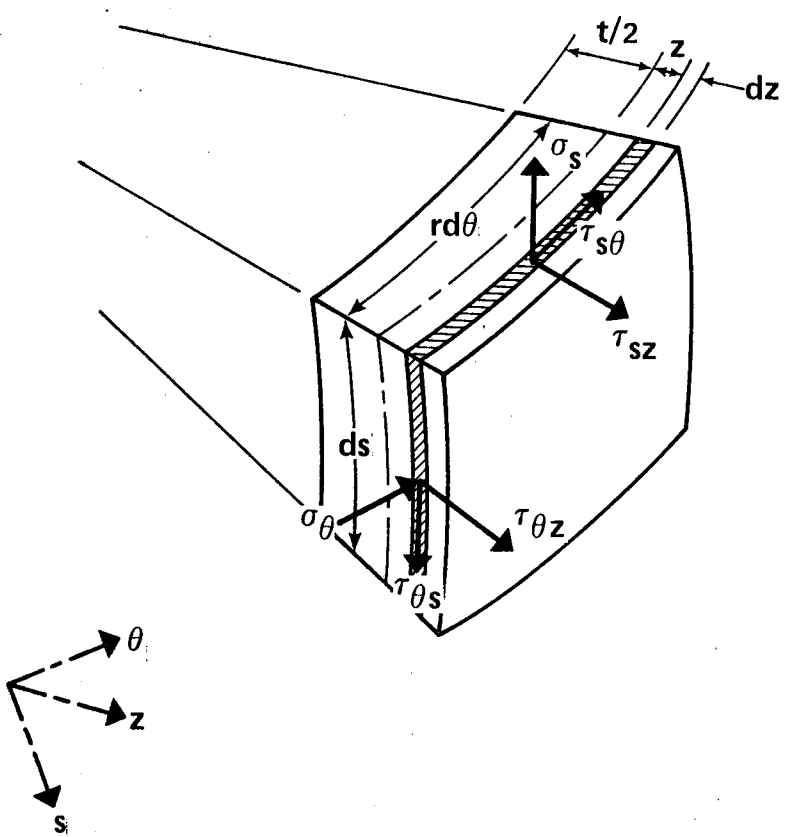


Fig. A.6 Stresses Acting on a Shell Element

APPENDIX B
USER'S MANUAL FOR PROGRAM SASHELL

Program SASHELL computes stress resultants and displacements for axisymmetric branched segmented shell structures due to their own weight, external applied loads and differential temperature variation (along the meridian or circumference).

In the present stage of development, the program is capable of analysing five types of shells of revolution of variable thickness. These are cylinders, circular plates, spheres, cones and hyperboloids of revolution. Loadings may be symmetric or non-axisymmetric with respect to the collatitude coordinate and may vary along the meridian.

The analysis procedure is based on the theory presented in this thesis and the program logic flow outlined in Sect. 4.2. A complete listing of the program is given in Appendix C. Input of the problems discussed in Chapter 4 and output of the pinched cylinder for a concentrated line load are given in Appendix D.

The input to SASHELL consists of several types of input cards. Certain card types may be repeated as required.

A typical explanation of a card type consists of the card type, a descriptive name indicating the nature of the data being entered and the format for the data on that card. This is followed by a symbolic line of input which, in turn, is followed by definitions of the input variables.

Limitations on SASHELL, due to the dimensions of the arrays in the program, are outlined following the explanation of the input cards.

TYPE 1: TITLE CARD

(Format 10A8)

80
AN IDENTIFIER STRING

One card which contains any title for the problem

TYPE 2: ANALYSIS CONTROL CARD

(Format 4I4,F7.0)

4	8	12	16	23
IPRINT	NP	NPCR	LDC	BETA

IPRINT : Print control parameter

If IPRINT = 0, the output will contain an echo check of the completed data. The loadings will be expanded in Fourier series, if required for the analysis, and the coefficients will be printed out.

If IPRINT = 1, the output will contain the echo check of the input data and the final results.

If IPRINT = 2, the output will contain the echo check of the input data, the results of the analysis for each harmonic and the superimposed final results.

If IPRINT = 3, full output including intermediate values will be printed out. (Used for checking purposes only.)

NP : Number of points along the element meridian for which the Runge-Kutta integration process is used. NP should not be specified less than 21 (see Limitations).

NPCR : Number of the circumferential points at which the final results are required.

If the loads are symmetric or antisymmetric with respect to the meridian passing through $\theta = 0$, NPCR is the number of points along half the circumference $(0, \pi)$. If the loads vary randomly in the circumferential direction, NPCR is the number of points along the full circumference of the element $(0, 2\pi)$.

If the loads are constants in the circumferential direction (symmetric), NPCR is equal to one.

LDC : Dead load control parameter.

If LDC = 0, dead load is excluded from the analysis.

If LDC = 1, dead load is evaluated and superimposed on the external applied loadings.

BETA : Maximum element length coefficient. BETA should not exceed 25 (see Limitations).

TYPE 3: STRUCTURE DATA CARD

(Format 2I3,4F12.0)

3	6	18	30	42	54
NE	NJ	EG	PUG	GAMG	TKG

NE : Number of elements

NJ : Number of junctions between elements (nodes).

EG : Global modulus of elasticity.
 PUG : Global Poisson's ratio.
 GAMG : Global specific weight.
 TKG : Global coefficient of thermal expansion

NOTE: If the structure consists of elements of different materials, the global properties are to be omitted and the structural data card specifies the number of elements and nodes only.

TYPE 4: NODAL DATA CARDS (format I4,2F10.0,4I4)

One card is required for each node.

	4	14	24	28	32	36	40
I	XCOOR(I)	RCOOR(I)	IDF(I,1)	IDF(I,2)	IDF(I,3)	IDF(I,4)	

I : Node number
 XCOOR(I) : Global X coordinate of node I along the axis of revolution directed downward from the top of the structure.
 RCOOR(I) : Radius of the parallel circle passing through node I. RCOOR(I) should not be specified as zero (see Limitations).
 IDF(I,J) : Identification of the jth degree of freedom at node I. J = 1,4 for the rotation of the meridian (β), the radial displacement component (W), the meridional displacement component (V) and the circumferential displacement component (U), respectively. When

$IDF(I,J) = 0$, the corresponding degree of freedom
is not restrained.

When $IDF(I,J) = 1$, the corresponding degree of
freedom is restrained.

TYPE 5: ELEMENT DATA CARDS

Two cards are required for each element.

First card Format (5I6,4F10.0)

6	12	18	24	30	40	50	60	70
I	IT(I)	NC(I,1)	NC(I,2)	NIP(I)	TH(I,1)	TH(I,2)	EC(I,1)	EC(I,2)

I : Element number

IT(I) : Element type

If $IT(I) = 1$, element I is a cylinder

If $IT(I) = 2$, element I is a cone or a
circular plate.

If $IT(I) = 3$, element I is a sphere of which $r_1 = r_2$.

If $IT(I) = 4$, element I is a sphere of which $r_1 \neq r_2$.

If $IT(I) = 5$, element I is a hyperboloid of revolution.

NC(I,1) : Node number at the top of element I.

NC(I,2) : Node number at the bottom of element I.

NIP(I) : Integer to indicate the number of intermediate points
in the element at which the final results are not
required. The number of equally spaced points at
which the final results will be printed out are

$\frac{NP-1}{NIP(I)} + 1$. A value of NP-1 will be assigned to NIP(I) when input is zero.

- TH(I,1) : Element thickness at the top.
 TH(I,2) : Element thickness at the bottom.
 EC(I,1) : Eccentricity of the top node from the middle surface of the element at the top.
 EC(I,2) : Eccentricity of the bottom node from the middle surface of the element at the bottom.

NOTE: The eccentricity is defined such that the radius of the parallel circle passes through the middle surface of the element is

$$r_{\text{midsurface}} = r_{\text{node}} - EC(I,J)$$

Thus, EC(I,J) is positive when directed inward from the node to the middle surface of the element.

Second card (Format 7F10.0)

10	20	30	40	50	60	70
HPCN(1,I)	HPCN(2,I)	HPCN(3,I)	GAMA(I)	E(I)	PU(I)	TCOEF(I)

HPCN(1,I) : Radius of curvature of the meridian for spherical element of type 4 (i.e., $r_1 \neq r_2$), or throat radius of a hyperboloid element (type 5). For elements other than of type 4 and type 5, HPCN(1,I) is 0.0.

HPCN(2,I) : Angle in degrees measured from the axis of revolution to the top edge of the spherical element of type 4, or hyperboloid constant in which the ratio $\frac{HPCN(2,I)}{HPCN(1,I)}$

equals to the slope of the asymptotes of the hyperbola. For elements other than of type 4 and 5, HPCN(2,I) is 0.0.

HPCH(3,I) : Angle in degrees measured from the axis of revolution to the top edge of the spherical element of type 4, or global X coordinate of the throat of the hyperboloid element. HPCH(3,I) is equal to 0.0 for elements other than of type 4 and 5.

GAMA(I) : Element specific weight. Specified if different from the global specific weight, otherwise GAMA(I) = 0.0 or blank.

E(I) : Element modulus of elasticity. Specified if different from the global modulus of elasticity, otherwise E(I) = 0.0 or blank.

PU(I) : Element Poisson's ratio. Specified if different from the global Poisson's ratio, otherwise PU(I) = 0.0 or blank.

TCOEF(I) : Element coefficient of thermal expansion. Specified if different from the global coefficient otherwise TCOEF(I) = 0.0 or blank.

NOTE: For a segmented structure which does not include spherical or hyperboloid elements and for which the other elements of which the structure consists have the same material properties, this card is a blank card.

TYPE 6: LOADING SPECIFICATION CARD (Format (6I5))

	5	10	15	20	25	30
NEL	NJL	NHL	NTL	NHPL	NHIN	

NEL : Number of externally loaded elements in the structure.

NJL : Number of loaded nodes in the structure.

NHL : Maximum number of harmonics required for the analysis including the zero harmonic (i.e., NHL = maximum harmonic number +1).

NTL : Loading type character.

If NTL = 0, loading is symmetric and the analysis is required for the zero harmonic only.

If NTL = 1, loading is non-axisymmetric in the circumferential direction, input is provided at a number of discrete points along the circumference of the shell, and the analysis is required for the cosine coefficients of Fourier series only (i.e., loading is symmetric with respect to a meridian passes through $\theta = \text{constant}$).

If NTL = 2, loading is non-axisymmetric in the circumferential direction, input is provided at a number of discrete points along the circumference of the shell, and the analysis is required for both are cosine and sine coefficients of Fourier series.

If NTL = 3, loading is nonaxisymmetric along the

along the circumferential direction and input directly as cosine coefficients of Fourier expansion only.

NHPL : Number of points along the circumference of the shell at which the loads values are described.

These points are defined such that the circumferential coordinate is $\frac{2\pi i}{NHPL}$ where $i = 0, 1, 2, \dots, NHPL - 1$.

NHIN : Integer which defines the increment in the harmonics, starting from the zero harmonic, to be specified when the analysis is required for a harmonic number $(0, NHIN, 2 NHIN, \dots, NHL - 1)$. The program sets $NHIN = 1$ when it is specified as zero or blank.

NOTE: If the load is described at NHPL points, NHL can be specified as $\frac{NHPL}{2}$ and NHIN can be set equal to one. When IPRINT = 0, the Fourier coefficients of the input load are obtained with the echo check of the input data. Then, the user may decide, upon examining these coefficients, on the final values of NHL and NHIN (see Chapter 5, Sect. 5.2.3).

TYPE 7: ELEMENT LOADING CONTROL INPUT CARDS (Format 6I5)

One card for each loaded element

	5	10	15	20	25	30
LL(I)	ILOAD (LL(I), K),	K = 1,5				

I : Integer takes the value of 1 to NEL

LL(I) : Number of the loaded element.

ILOAD(LL(I),K)

: Identifier for loading type on the element LL(I)

in the order:

ILOAD(*,1) for loading in the direction tangent
to the meridian (s).

ILOAD(*,2) for loading in the direction tangent
to the parallel circle (θ).

ILOAD(*,3) for loading in the direction perpendicular
to the tangent to the meridian (z).

ILOAD(*,4) for temperature at the shell exterior face.

ILOAD(*,5) for temperature at the shell interior face.

If ILOAD(*,K) = 0, no load of type K is applied.

If ILOAD(*,K) = 1, the applied load of type K is
constant along the meridian and to be specified at
one end of the element only.

If ILOAD(*,K) = 2, the applied load of type K varies
linearly along the meridian and is to be specified
at the two ends of the element.

If ILOAD(*,K) = 3, the applied load of type K
varies as a second degree function along the meridian
and is to be specified at the two ends of the element.

NOTE: Element loads are input in the element local coordinates.

TYPE 8: ELEMENT LOADING CARDS

This type of card depends upon NTL and is classified as TYPE 8-A, TYPE 8-B and TYPE 8-C for NTL equal to 0, 1 or 2, and 3 respectively.

TYPE 8-A: ELEMENT SYMMETRICAL LOADING CARDS (Format 2F10.0)

This type is required if NTL is equal to zero. Number of cards required, for each loaded element, is equal to, and input in the order consistent with, each non-zero term in the corresponding row in ILOAD array.

10	20
ACEL(K1)	ACEL(K2)

ACEL(K1) : Magnitude of the load at the element top.

ACEL(K2) : Magnitude of the load at the element bottom.

TYPE 8-B ELEMENT ASYMMETRIC TABULATED LOADING CARDS (Format 8F10.0)

This type is required if NTL is equal to 1 or 2.
Number of cards required, for each loaded element, is equal to
 $\frac{NHPL}{8}$ for, and input in the order consistent with, each non-zero
term in the corresponding row in ILOAD array.

$W(I)$: Magnitude of the load, at the points defined by $\frac{2\pi i}{NHPL}$ ($i = 0, 1, 2, \dots, NHPL-1$) along the circumference of the element, and for which Fourier expansion is required.

TYPE 8-C ELEMENT LOADING FOURIER COEFFICIENTS CARDS

(Format 8F10.0)

This type is required if NTL is equal to 4. Number of cards required, for each loaded element, is equal to $\frac{NHL}{8}$ for, and input in the order consistent with, each non-zero term in the corresponding row in ILOAD array.

10	20	30	40	50	60	70	80
AL(K) , K = 1, NHL							

AL(K) : Cosine coefficients of Fourier expansion for Harmonics 0, 1, 2, ..., NHL-1.

TYPE 9: NODAL LOADING CONTROL INPUT CARDS (Format I5)

One card for each loaded node (NJL cards)

5
J

J : Number of loaded node.

TYPE 10: NODAL LOADING CARDS

This type of card depends upon NTL and is classified as TYPE 10-A, TYPE 10-B and TYPE 10-C for NTL equal to 0, 1 or 2, and 3, respectively.

TYPE 10-A: NODAL SYMMETRICAL LOADING CARDS (Format (4F10.0))

This type is required if NTL is equal to zero. One card is required for each loaded node.

10	20	30	40
ANJL (II,1)	,	II = 1,4	

ANJL(II,1): Magnitude of the nodal load, in the global structure coordinates, in the following order.

II = 1, meridional couple, M_s , positive when rotating in the clockwise direction.

II = 2, force normal to the tangent to meridian at the corresponding node, S_s , positive in the outward direction from the axis of revolution.

II = 3, force in the direction tangent to the meridian, N_s , positive when directed downward parallel to the axis of revolution.

II = 4, force in the direction tangent to the parallel circle, T_s , positive when directed in the anticlockwise rotating direction around the structure.

NOTE: The sign convention of the nodal loads as defined above is equivalent to the stiffness matrix sign convention as described in Sect. 3.7.

TYPE 10-B: NODAL ASYMMETRICAL TABULATED LOADING CARDS

This type is required if NTL is equal to 1 or 2 and consists of the following cards, for each loaded node.

- (1) Asymmetric nodal load control input card. Required to identify which to the nodal loads, classified as in Type 10-A cards (M_s , S_s , N_s , T_s), is applied and to be input. One card (Format 4I4) is required

KLD(K), K = 1,4

K : Integer which takes a value of 1 to 4 and represents the nodal forces, as defined in TYPE 10-A cards, in the order M_s , S_s , N_s and T_s , respectively.

KLD(K) : If equal to zero, nodal force of the type K
is not applied.

If equal to 1, nodal force of the type K is applied.

- (2) Nodal loading magnitude card (Format 8F10.0)

Number of cards required is equal to $\frac{NHPL}{8}$ for, and

input in the order consistent with, each non-zero term in KLD.

W(I) : Magnitude of the nodal load, at the points defined by $\frac{2\pi i}{NHPL}$ ($i = 0, 1, 2, \dots, NHPL - 1$) along the circumference of the nodal circle, and for which Fourier expansion is required.

TYPE 10-C: NODAL LOADING FOURIER COEFFICIENTS CARDS

This type is required if NTL is equal to 3 and NJL is greater than 0. It consists of the following cards, for each loaded node:

- (1) Asymmetric nodal load control input card of the same type described in TYPE 10-B.

4	8	12	20
KLD(K), K = 1, 4			

- (2) Nodal loading magnitude card (Format 8F10.0)

Number of cards required is equal to $\frac{NHL}{8}$ for, and input in the order consistent with, each non-zero term in KLD.

10	20	30	40	50	60	70	80
AL(N), N = 1, NHL							

AL(N) : Cosine coefficients of FOURIER expansion for harmonics 0, 1, 2, ..., NHL - 1.

LIMITATIONS

Number of elements NE	> 20
Number of nodes NJ	> 21
Number of integration points NP	> 51
Number of circumferential points NPCR	> 11
Number of harmonics NHL	> 20
Number of circumferential points at which loadings is specified NHPL	> 40
Full band width NHB	> 80
Total number of Fourier coefficients in the problem for elements loading, associated with either cosine or sine factor and defined by NHL x NEL	> 200
Total number of Fourier coefficients in the problem for nodal loadings, associated with both cosine and sine factor and defined by 8 x NHL x NJL	> 200
Number of points in a non-axisymmetrically loaded structure at which the final results are required, and which can be calculated as	

$$\sum_{i=1}^{NE} NS_i \times \left\{ \frac{(NP-1)}{NIP_i} + 1 \right\} > 200$$

where NS_i = number of segments into which element i is subdivided and can be obtained by $\frac{L}{BETA} \sqrt[4]{3(1 - v^2)/r^2 t^2}$

In which, L , is the element length, r , is the element radius, t , is the element thickness and v is Poisson's ratio.

The above limitations are due to the dimension statements in the program SASHELL as listed in Appendix C. The dimension of the corresponding arrays may be modified to change these limitations.

Limitations on the theory employed in SASHELL are as follows (see Chapter 5).

- 1) RCOOR should not be specified as zero.
- 2) The length factor coefficient BETA should not be specified greater than 25.
- 3) The number of points of integration NP should not be less than 21 when BETA is specified less than 20, and not less than 31 when BETA is greater than 20 and less than 25.

APPENDIX C
PROGRAM LISTING

150.


```

      EX(2)=GEO(K1,2)
      EX(1)=GEO(K0,3)
      EX(3)=GEO(K1,3)
      PHX(1)=G2D(X1,3)
      PHX(2)=G2D(X0,4)
      PHX(3)=G2D(X1,4)
      PHX(4)=G2D(X0,5)
      SX(1)=GEO(K0,5)
      SX(2)=GEO(K1,5)
      SX(3)=GEO(X0,6)
      SX(4)=GEO(X1,6)
      ZP(1)=GEO(Z1,0)
      ZP(2)=GEO(Z2,0) GO TO 93
      LOC=LOC2+1
      LOC3=LOC1+4
      LOC3=LOC2+5
      KI=0
      DO 55 K=LOC1,LOC3
      K=K+1
      25 (L,N)=A24(L,N)
      55 CONTINUE
      IF (L,I.EQ.1) GO TO 93
      KI=0
      DO 96 L=LOC1,LOC3
      KI=KI+1
      96 PS(GL,2)=B24(L,N)
      COLUME
      CALL ASMT(L,TYPE,LT,LDC,NEL,NH,NP,GAMA(I),E(I),
     * PHC(I),ICOP(I),RK,THK,PHK,SKIDL,PS,YS)
      CALL STIFF(LPRINT,LT,NP,SM,ZE,DS,DSRI1)
      CALL STORE1(I,LMS1,LPRINT,LT,NP,SM,ZE,DS,DSRI1)
      IDENTIFICATION FOR STIFFNESS MATRIX SIGN CONVENTION
      L=NDOF+2
      DO 52 J=1,NF
      DO 52 J=1,NF
      52 CH(L,J)=-CH(L,J)
      DO 53 J=1,LT
      DO 53 L=1,LL
      53 T2(L,J)=T2(L,J)
      IDENTIFICATION FOR ECCENTRICITY
      DO 54 L=1,2
      DO 54 L=1,2
      54 T2(L,J)=1
      T2(L,J)=1
      T2(L,J)=1
      54 CONTINUE
      54 T2(L,J) GO TO 51
      Z=EC(E,L)
      IF (Z.EQ.0) GO TO 51
      E1=E(L)
      E2=E(L)
      CALL ECNTF(LPRINT,L,LT,NH,NP,Z,R1,R2,SM,ZE,DS)
      51 CONTINUE
      51 (Z,E2,E1) GO TO 58
      TRANSFORMATION OF STIFFNESS COEF TO GLOBAL COORDINATES
      DO 55 L=1,2
      IF (L.EQ.2) L=1
      55 (L,Z2,Z1) L=SEG

```

C SUBROUTINE BOUND (NE,NJ,NDOF,LT,NBB,NEQ,NCN,IDE,
 * DSP,SS,RHS)

C IMPLICIT REAL*8 (A-H,O-Z)

C DIMENSION NC(20,2),ACON(20,2),IDS(21,6),RHS(200,2),
 * SS(200,80),RHS(200,2)

C NB=NBB+1


```

505 FORMAT ('/ STRESS RESULTANTS DUE TO DISPL'/(8E14.6))
721
722 506 FORMAT ('/ FIXED END STRESSES DUE TO LOAD'/(8E14.6))
723 507 FORMAT ('/ STRESSES AT ENDS'/(6E14.6))
724 16 L1=L+1,N2
725      ELEM1
726      END
727      CCCCCCCCCCCCCCCCCCCCCCCCCCCCCCCCCCCCCCCCCCCCCCCCCCCCC
728      CCCCCCCCCCCCCCCCCCCCCCCCCCCCCCCCCCCCCCCCCCCCCCCCCCCCC
729      CCCCCCCCCCCCCCCCCCCCCCCCCCCCCCCCCCCCCCCCCCCCCCCCCCCCC
730      CCCCCCCCCCCCCCCCCCCCCCCCCCCCCCCCCCCCCCCCCCCCCCCCCCCCC
731      CCCCCCCCCCCCCCCCCCCCCCCCCCCCCCCCCCCCCCCCCCCCCCCCCCCCC
732      CCCCCCCCCCCCCCCCCCCCCCCCCCCCCCCCCCCCCCCCCCCCCCCCCCCCC
733      CCCCCCCCCCCCCCCCCCCCCCCCCCCCCCCCCCCCCCCCCCCCCCCCCCCCC
734      CCCCCCCCCCCCCCCCCCCCCCCCCCCCCCCCCCCCCCCCCCCCCCCCCCCCC
735      CCCCCCCCCCCCCCCCCCCCCCCCCCCCCCCCCCCCCCCCCCCCCCCCCCCCC
736      CCCCCCCCCCCCCCCCCCCCCCCCCCCCCCCCCCCCCCCCCCCCCCCCCCCCC
737      CCCCCCCCCCCCCCCCCCCCCCCCCCCCCCCCCCCCCCCCCCCCCCCCCCCCC
738      CCCCCCCCCCCCCCCCCCCCCCCCCCCCCCCCCCCCCCCCCCCCCCCCCCCCC
739      CCCCCCCCCCCCCCCCCCCCCCCCCCCCCCCCCCCCCCCCCCCCCCCCCCCCC
740      CCCCCCCCCCCCCCCCCCCCCCCCCCCCCCCCCCCCCCCCCCCCCCCCCCCCC
741      CCCCCCCCCCCCCCCCCCCCCCCCCCCCCCCCCCCCCCCCCCCCCCCCCCCCC
742      CCCCCCCCCCCCCCCCCCCCCCCCCCCCCCCCCCCCCCCCCCCCCCCCCCCCC
743      CCCCCCCCCCCCCCCCCCCCCCCCCCCCCCCCCCCCCCCCCCCCCCCCCCCCC
744      CCCCCCCCCCCCCCCCCCCCCCCCCCCCCCCCCCCCCCCCCCCCCCCCCCCCC
745      CCCCCCCCCCCCCCCCCCCCCCCCCCCCCCCCCCCCCCCCCCCCCCCCCCCCC
746      CCCCCCCCCCCCCCCCCCCCCCCCCCCCCCCCCCCCCCCCCCCCCCCCCCCCC
747      CCCCCCCCCCCCCCCCCCCCCCCCCCCCCCCCCCCCCCCCCCCCCCCCCCCCC
748      CCCCCCCCCCCCCCCCCCCCCCCCCCCCCCCCCCCCCCCCCCCCCCCCCCCCC
749      CCCCCCCCCCCCCCCCCCCCCCCCCCCCCCCCCCCCCCCCCCCCCCCCCCCCC
750      CCCCCCCCCCCCCCCCCCCCCCCCCCCCCCCCCCCCCCCCCCCCCCCCCCCCC
751      CCCCCCCCCCCCCCCCCCCCCCCCCCCCCCCCCCCCCCCCCCCCCCCCCCCCC
752      CCCCCCCCCCCCCCCCCCCCCCCCCCCCCCCCCCCCCCCCCCCCCCCCCCCCC
753      CCCCCCCCCCCCCCCCCCCCCCCCCCCCCCCCCCCCCCCCCCCCCCCCCCCCC
754      CCCCCCCCCCCCCCCCCCCCCCCCCCCCCCCCCCCCCCCCCCCCCCCCCCCCC
755      CCCCCCCCCCCCCCCCCCCCCCCCCCCCCCCCCCCCCCCCCCCCCCCCCCCCC
756      CCCCCCCCCCCCCCCCCCCCCCCCCCCCCCCCCCCCCCCCCCCCCCCCCCCCC
757      CCCCCCCCCCCCCCCCCCCCCCCCCCCCCCCCCCCCCCCCCCCCCCCCCCCCC
758      CCCCCCCCCCCCCCCCCCCCCCCCCCCCCCCCCCCCCCCCCCCCCCCCCCCCC
759      CCCCCCCCCCCCCCCCCCCCCCCCCCCCCCCCCCCCCCCCCCCCCCCCCCCCC
760      CCCCCCCCCCCCCCCCCCCCCCCCCCCCCCCCCCCCCCCCCCCCCCCCCCCCC
761      CCCCCCCCCCCCCCCCCCCCCCCCCCCCCCCCCCCCCCCCCCCCCCCCCCCCC
762      CCCCCCCCCCCCCCCCCCCCCCCCCCCCCCCCCCCCCCCCCCCCCCCCCCCCC
763      CCCCCCCCCCCCCCCCCCCCCCCCCCCCCCCCCCCCCCCCCCCCCCCCCCCCC
764      CCCCCCCCCCCCCCCCCCCCCCCCCCCCCCCCCCCCCCCCCCCCCCCCCCCCC
765      CCCCCCCCCCCCCCCCCCCCCCCCCCCCCCCCCCCCCCCCCCCCCCCCCCCCC
766      CCCCCCCCCCCCCCCCCCCCCCCCCCCCCCCCCCCCCCCCCCCCCCCCCCCCC
767      CCCCCCCCCCCCCCCCCCCCCCCCCCCCCCCCCCCCCCCCCCCCCCCCCCCCC
768      CCCCCCCCCCCCCCCCCCCCCCCCCCCCCCCCCCCCCCCCCCCCCCCCCCCCC
769      CCCCCCCCCCCCCCCCCCCCCCCCCCCCCCCCCCCCCCCCCCCCCCCCCCCCC
770      CCCCCCCCCCCCCCCCCCCCCCCCCCCCCCCCCCCCCCCCCCCCCCCCCCCCC
771      CCCCCCCCCCCCCCCCCCCCCCCCCCCCCCCCCCCCCCCCCCCCCCCCCCCCC
772      CCCCCCCCCCCCCCCCCCCCCCCCCCCCCCCCCCCCCCCCCCCCCCCCCCCCC
773      CCCCCCCCCCCCCCCCCCCCCCCCCCCCCCCCCCCCCCCCCCCCCCCCCCCCC
774      CCCCCCCCCCCCCCCCCCCCCCCCCCCCCCCCCCCCCCCCCCCCCCCCCCCCC
775      CCCCCCCCCCCCCCCCCCCCCCCCCCCCCCCCCCCCCCCCCCCCCCCCCCCCC
776      CCCCCCCCCCCCCCCCCCCCCCCCCCCCCCCCCCCCCCCCCCCCCCCCCCCCC
777      CCCCCCCCCCCCCCCCCCCCCCCCCCCCCCCCCCCCCCCCCCCCCCCCCCCCC
778      CCCCCCCCCCCCCCCCCCCCCCCCCCCCCCCCCCCCCCCCCCCCCCCCCCCCC
779      CCCCCCCCCCCCCCCCCCCCCCCCCCCCCCCCCCCCCCCCCCCCCCCCCCCCC
780      CCCCCCCCCCCCCCCCCCCCCCCCCCCCCCCCCCCCCCCCCCCCCCCCCCCCC
781      END
782      CCCCCCCCCCCCCCCCCCCCCCCCCCCCCCCCCCCCCCCCCCCCCCCCCCCCC
783      C
784      SUBROUTINE SOLVER (A,B,LT,NEQ,NFS)
785      CCCCCCCCCCCCCCCCCCCCCCCCCCCCCCCCCCCCCCCCCCCCCCCCCCCCCCCCC
786      CCCCCCCCCCCCCCCCCCCCCCCCCCCCCCCCCCCCCCCCCCCCCCCCCCCCCCCCC
787      IMPLICIT REAL *8 (A-H,O-Z)
788      DIMENSION A(200,60),B(200,2)
789      C
790      NHB=(NFB+1)/2
791      NL=N_EQ+1
792      NB=N_HB+1
793      NEQ=N_HB+1
794      NFB=NFB
795      C
796      DO 250 N=1,NL
797      IP(A(N,NH3)-LE,0+) GO TO 700
798      N1=N+1
799      N2=N+NHB-1
800      IP(A(N,LE,NM) GO TO 10
801      RE=N_EQ*NHB-N
802      N2=NEQ+
803      10 CONTINUE
804      C
805      DO 100 K=N,B,N
806      A(N,K)=A(N,K)/A(N,NH3)
807      DO 110 L=1,LT
808      B(N,L)=B(N,L)/A(N,NH3)
809      C
810      NN=NHB
811      DO 250 I=N,1,N2
812      IP(A(I,N) .EQ. 0.) GO TO 250
813      NN=NN-1
814      C=A(I,N)
815      J=NN
816      DO 200 J=N,B,NR
817      JJ=JJ+1
818      A(I,J,J)=A(I,J,J)-C*A(N,J)
819      DO 210 L=1,LT
820      B(I,L)=B(I,L)-C*B(N,L)
821      250 CONTINUE
822      C BACK SUBSTITUTION
823      C
824      I=NEQ
825      DO 300 I=1,LT
826      B(NEQ,L)=B(NEQ,L)/A(NEQ,NB)
827      C
828      DO 400 N=1,NL
829      I=I-1
830      IP(N-1,NH3) NE=N_HB+N
831      DO 400 L=1,LT
832      DO 400 J=N_B,NR
833      K=I+J-NH3
834      400 B(I,L)=B(I,L)-A(I,J)*B(J,L)
835      C
836      SSFT(I,J,K)=SSRT(I,J,KK)+D1*SSR(I,K)
837      CONTINUE
838      WRITE(c,3000) N,A(N,NH3)
839      STOP
840      3000 FORMAT ('NEGATIVE OR ZERO ELEMENT ON MATRIX DIAGONAL',5,

```



```

361      K2=K1+1
962      READ(5,1100) (ACEL(K),KK=K1,K2)
J=0
963
964      WRITE(6,2101)L,K,KL
965      DO 15 KK=K1,K2
966      J=J+1
967      WRITE(6,2101)L,K,KL
968      WRITE(6,2102)J,ACEL(K)
969
970      CONTINUE
15
971      CONTINUE
20
C      GO TO 20C
972      GO TO 20C
16      CONTINUE
973      NL=NPL/2
974      K=NHL-1
975      DO 20 I=1,NHL
976      L=I*(L)
977
978      DO 50 K=1,5
979      K=L*ODG(L,K)
980      IZ=(L-EQ.0) GO TO 30
981      DO 40 J=1,NSPL
982      IZ=(L-EQ.0).AND.J.GT.1) GO TO 28
983      IZ=(L-EQ.3) GO TO 23
984      READ(5,1400)(H(JJ),JJ=1,NHL)
985      CALL PORT(*,NML,AL,BL)
986      CALL TL-EQ.3) READ(6,1400)(AL(JJ),JJ=1,NHL)
23
28      CONTINUE
26      K=Z+2
27      Z=K+2
28      K=K+1+NHL-1
989
990      Z=0
991      IZ=EQ.2) GO TO 24
992      DO 35 KKK=1,K2
993      K=Z+1
994      ACEL(K)=AL(K)
995      IZ=(L-EQ.1) GO TO 27
996      K=0
997      DO 36 KK=K1,K2
998      K=K+1
999      BCAL(K)=BL(K)
1000     GO TO 27
1001     DO 25 KK=K1,K2
1002     K3=K3+1
1003     BCAL(K)=AL(K3)
1004     IZ=(L-EQ.1) GO TO 27
1005     K=0
1006     DO 26 KK=K1,K2
1007     K3=K3+1
1008     ACEL(K)=BL(K3)
1009     CONTINUE
1010     WRITE(6,2202)J,(ACEL(KK),KK=K1,K2)
1011     WRITE(L,C-1) GO TO 40
1012     WAIT(6,2202)J,(BCAL(KK),KK=K1,K2)
1013     CONTINUE
1014     CONTINUE
1015     CONTINUE
1016
C      IF (NL-EQ.0) RETURN
1017     WRITE(6,2710)
1018
1019     DO 150 I=1,BJ
1020
150     INCL(I)=0
DO 155 I=1,NHL
1022     READ(5,2700)J
1023     INCL(J)=1
1024     CONTINUE
1025     IF (NL-N.E.Q) GO TO 171
1026     NJ4=NJ**4
1027     DO 151 J=1,NJ4
1028     ANJL(G,J)=0.0
1029     DO 170 I=1,NJ
1030     IF (ANJL(I),EQ.0) GO TO 170
1031     IN4=NJ**4
1032     IN=IN4-J
1033     N=1
1034     NH=0
1035     READ(5,1600)(ANJL(II,N),II=IN,IN4)
1036     WRITE(6,2700)I
1037     WRITE(6,2720)NH,(ANJL(II,N),II=IN,IN4)
1038     CONTINUE
1039
1040     NL=NPL/2
1041     NL=NHL-1
1042     NJ8=NJ**8
1043     DO 210 K=1,NJ8
1044     DC 210 J=1,NJ8
1045     ANJL(J,N)=0.0
210     ANJL(J,N)=0.0
DO 250 I=1,NJ
250     IF (ANJL(I),EQ.0) GO TO 250
READ(5,1650),(KLD(K),K=1,4)
1048
1049     IN=I*8
1050     IN=IN6-7
1051     DC 180 K=1,4
1052     IF (KLD(K),EQ.0) GO TO 180
1053     IF (NPL-EQ.3) GO TO 160
1054     READ(5,1400)(W(KK),K=1,NHL)
1055     CALL FORTN(N,NL,NL,AL,BL)
1056     IF (NL-EQ.3) READ(5,1400)(AL(KK),KK=1,NHL)
1057     DO 180 N=1,NHL
1058     IF (K,EQ.4) GO TO 181
1059     K1=K-N-1
1060     K2=K+4
1061     GO TO 132
1062     K2=K+K-1
1063     K=K+2
1064     ANAL(K1,N)=AL(N)
1065     IF (NPL-EQ.3) GO TO 180
1066     ANAL(K2,N)=BL(N)
1067     CONTINUE
1068     WRITE(6,2700)I
1069     DO 190 N=1,NHL
1070     NH=N-1
1071     WRITE(6,2720)NH,(ANJL(K,N),K=IN,IN8)
1072     CONTINUE
1073     250 CONTINUE
1074     251 RETURN
C
1075
1076     C
1077
1078
1079
1080
1001 FORMAT(6I5)
1100 FORMAT(2F10.0)
1400 FORMAT(1E10.0)
C      FORMAT STATEMENTS

```


162.

```

1621      IP(J1,K)=P(J1,K)+B*Z(J3,K)
1622      P(J3,K)=P(J3,K)*C
1623      CONTINUE
1624      RETURN
1625      C   30  CONTINUE
1626      DO 16 K=1,LT
1627      D(3,K)=D(1,K)*A+D(3,K)
1628      IF(NP.EQ.6) GO TO 16
1629      D(4,K)=D(2,K)*B+D(4,K)*C
1630      C   16  CONTINUE
1631      RETURN
1632      C   40  CONTINUE
1633      DO 17 K=1,LT
1634      D(7,K)=D(5,K)*A+D(7,K)
1635      IF(NP.EQ.6) GO TO 17
1636      D(6,K)=D(6,K)*B+D(8,K)*C
1637      C   17  CONTINUE
1638      RETURN
1639      C
1640      COMMON/HYP/AH,BH,XH,XW
1641      DIMENSION PSR(8,1),SSR(12,1),YI(10,2),ZI(10,2),
1642      IMPLICIT REAL*8(A-H,O-Z)
1643      EXTERNAL F,P1,P2,P3,P4,P5,P6,P7,P8,P9,P10,P11,P12,P13,P14,P15,P16,P17,P18,P19,P20
1644      C
1645      C   EVALUATE THE DISPLACEMENTS AND THE STRESSES AT
1646      C   INTERMEDIATE POINTS BY RUNGE-KUTTA PROCESS USING THE
1647      C   INITIAL CONDITIONS VI AT THE BOUNDARY.
1648      C
1649      CCCCCCCCCCCCCCCCCCCCCCCCCCCCCCCCCCCCCCCCCCCCCCCCCCCCC
1650      CCCCCCCCCCCCCCCCCCCCCCCCCCCCCCCCCCCCCCCCCCCCCCCCCCCCC
1651      CCCCCCCCCCCCCCCCCCCCCCCCCCCCCCCCCCCCCCCCCCCCCCCCCCCCC
1652      CCCCCCCCCCCCCCCCCCCCCCCCCCCCCCCCCCCCCCCCCCCCCCCCCCCCC
1653      CCCCCCCCCCCCCCCCCCCCCCCCCCCCCCCCCCCCCCCCCCCCCCCCCCCCC
1654      CCCCCCCCCCCCCCCCCCCCCCCCCCCCCCCCCCCCCCCCCCCCCCCCCCCCC
1655      CCCCCCCCCCCCCCCCCCCCCCCCCCCCCCCCCCCCCCCCCCCCCCCCCCCCC
1656      CCCCCCCCCCCCCCCCCCCCCCCCCCCCCCCCCCCCCCCCCCCCCCCCCCCCC
1657      CCCCCCCCCCCCCCCCCCCCCCCCCCCCCCCCCCCCCCCCCCCCCCCCCCCCC
1658      CCCCCCCCCCCCCCCCCCCCCCCCCCCCCCCCCCCCCCCCCCCCCCCCCCCCC
1659      CCCCCCCCCCCCCCCCCCCCCCCCCCCCCCCCCCCCCCCCCCCCCCCCCCCCC
1660      CCCCCCCCCCCCCCCCCCCCCCCCCCCCCCCCCCCCCCCCCCCCCCCCCCCCC
1661      CCCCCCCCCCCCCCCCCCCCCCCCCCCCCCCCCCCCCCCCCCCCCCCCCCCCC
1662      NM=NRP
1663      NM1=NRP-1
1664      IF(IT.EQ.5) GO TO 26
1665      RJ=(RK(2)-RK(1))/NM1
1666      TJ=(TJK(2)-TJK(1))/NM1
1667      PJ=(PK(2)-PK(1))/NM1
1668      SJ=(SK(2)-SK(1))/NM1
1669      DO 20 I=1,NRK
1670      I=I-1
1671      TX(I)=THK(I)*I*I*TJ
1672      FY(I)=PHK(I)*I*I*TJ
1673      CONTINUE
1674      GO TO (21,22,23,23), IT
1675      DO 15 I=1,NRK
1676      RX(I)=RK(I)
1677      GO TO 24
1678      DO 16 I=1,NRK
1679      I=I-1
1680      BX(I)=RK(I)*I*I*RJ

```

```

1631      GO TO 24
1632      23      24H=PI(K,1)
1633      DSP=DSIN(PHI)
1634      Z=ZK(I)/DSN
1635      ZY(I)=EK(1)
1636      A=AH*ZN-RK(I)
1637      DC 17 Z=2, DRK
1638      ZA=Z(I)
1639      DSN=DCIN(PHI)
1640      IF(I>I-3) RX(I)=R2/DSN
1641      IF(I>I-4) RX(I)=AR/DSN-XR
1642      CONTINUE
1643      GO TO 24
1644      CALL RPPB(LA,WRK,RK,THK,SK,RX,XZ,TJ)
1645      CONTINUE
1646      I=5*LI
1647      DO 25 K=1,NP
1648      DC 25 I=1,II
1649      25      PDC(I,K)=0.0
1650      DC 255 I=1,II
1651      PIX(I)=6.0
1652      IF((DC,ZI-1.0,NEL,P0,0)) GO TO 55
1653      CALL PSES(IPT,LT,NP,IDL,PS,PLD,PIX)
1654      CONTINUE
1655      IF(DC>0.0, NH, GT,0) GO TO 56
1656      CALL DISGS(I,IITA,N2,DW,FX,TX,PLD)
1657      CONTINUE
1658      I=12PZ+12,3) GO TO 60
1659      K=ITZ(I,12,10) NP
1660      DO 59 K=1,NP
1661      KZ=Z(I,K,(PLDI,KI,I=1,II)
1662      KZ=Z(I,K,(PLDI,KI,I=1,II)
1663      FORWARD ///* LOADS ON SEGMENT AT 'I5' POINTS */
1664      * POINT NUMBER 'I4X' PX.'I2X', PY.'I2X', PZ.'I0X',
1665      * TEMP.'I2X', T.GRAD.'I/ /
1666      59      FORWARD(5,6,10E10,3)
1667      CONTINUE
1668      60      CONTINUE
1669      DO 11 K=1,LT
1670      11      DO 11 I=1,NP
1671      11      IZP(I,K)=VI(I,1)
1672      DO 12 K=1,LT
1673      12      KZ=N2*K
1674      12      TDP(KK,K)=1.0
1675      C      START INTEGRATION BY RUNGE KUTTA
1676      DO 160 J=1,NRK
1677      DO 1 I=1,NDOP
1678      DSPI(I,J)=VI(I,1)
1679      KZ=I+NDOP
1680      DO 71 KZ=Z(I,J)
1681      CONTINUE
1682      DO 2 I=1,NDOP
1683      KK=I+NDOP
1684      2      25K(I,J)=VI(KK,1)
1685      IZP(I,K)=VI(I,K)+AK(I,K)/2.
1686      DO 73 I=1,NDOP
1687      KK=I+NDOP
1688      73      PSR(KK,J)=VI(KK,2)
1689      CONTINUE
1690      IF(I>I-2,SKR) GO TO 200
1691      DO 4 K=1,LT
1692      DO 8 I=1,NP
1693      AK(I,K)=SU*TDFP(I,K)
1694      DO 5 K=1,LT
1695      DO 5 I=1,NP
1696      TDP(I,K)=VI(I,K)+AK(I,K)/2.
1697      X25=IX(I,J)+TJ/2.
1698      X22=IX(I,J)+TJ/2.
1699      X35=IX(I,J)+TJ/2.
1700
1741      74      CONTINUE
1742      ZF(I-EQ,WRK) GO TO 30
1743      J=I+1
1744      IF(I>NE-5) GO TO 27
1745      XJ2=I2*XJ
1746      RJ=RX(I,J)-RX(J)
1747      AK2=S*SRJ
1748      SJ=(I2+RJ2)**.5
1749      PJ=FX(G1)-FX(J)
1750      CONTINUE
1751      DO 3 K=1,LT
1752      DO 4 I=1,NP
1753      3      ZP(I,J,K)=VI(I,K)
1754      IZP(I,J,K)=VI(I,K)
1755      X1=ZI(J)
1756      X2=ZI(J)
1757      X3=FX(J)
1758      40      I=1,II
1759      40      PX(I)=PLD(I,J)
1760      CALL PLUGS(ZI,WH,WV,X1,X2,X3,PX,0,TJ,TZ,SA)
1761      CALL SPROU(SA,TFP,TDFP,S,10,NE,KP1,LT)
1762      30      CONTINUE
1763      DO 31 K=1,LT
1764      DO 32 I=1,NDOP
1765      30      DSD(I,K)=TDP(I,K)
1766      30      DO 33 I=1,NDOP
1767      30      DO 34 K=1,NDOP
1768      30      DS(I,J)=DSD(I,K)
1769      30      DS(I,J)=DSD(KK,J)
1770      30      CALL YPROD(E1,DDS,ES1,5,4,5,NDOP,LT)
1771      30      DS(I,J)=DSD(I,J)
1772      30      CALL YPROD(E2,DDS,ES2,5,4,5,NDOP,LT)
1773      30      DC 62 I=1,5
1774      30      SSR(I,J)=ES1(I,1)+ES2(I,1)+23(I,1)
1775      30      IF(NP,NE-8) GO TO 84
1776      30      SSA(6,J)=PSR(4,J)+R2*SSR(3,J)
1777      30      GO TO 86
1778      34      CONTINUE
1779      34      SSR(6,J)=R2*SSR(3,J)
1780      34      IF(ILT,EO,1) GO TO 87
1781      34      DO 85 I=1,5
1782      34      KK=6*I
1783      34      SSR(KK,J)=ES1(I,2)+ES2(I,2)+E3(I,2)
1784      34      IF(I>NE-8) GO TO 88
1785      34      SSR(12,J)=PSR(8,J)+R2*SSR(9,J)
1786      34      GO TO 87
1787      38      CONTINUE
1788      38      SSR(12,J)=R2*SSR(9,J)
1789      38      CONTINUE
1790      38      IF(I>EQ,SKR) GO TO 200
1791      38      DO 4 K=1,LT
1792      38      DO 8 I=1,NP
1793      38      AK(I,K)=SU*TDFP(I,K)
1794      38      DO 5 K=1,LT
1795      38      DO 5 I=1,NP
1796      38      TDP(I,K)=VI(I,K)+AK(I,K)/2.
1797      38      X25=IX(I,J)+TJ/2.
1798      38      X22=IX(I,J)+TJ/2.
1799      38      X35=IX(I,J)+TJ/2.
1800

```



```

2251      16  CONTINUE
2252      DO 32 K=1,NP
2253      KM1=K-1
2254      KM2=K+1*KD1
2255      PLJ(I,J,K)=PLJ(I,J)+KM2*PLNC(1)
2256      IF(I>L, EQ. 1) GO TO 32
2257      PLJ(I-5,K)=25*(I5,2)+KM2*PLNC(2)
2258      32  CONTINUE
2259      130  CONTINUE
2260      269  CONTINUE
2261      285 1    RETURN
2262      END
2263
2264      C   SUBROUTINE DLSEG (IT, ITA, NP, UNW, YX, PLD)
2265      C   IMPLICIT REAL*8 (A-H,O-Z)
2266      C   DIMENSION A(N,N),B(N,N),C(N,N)
2267      DO 10 I=1,N
2268      DO 10 J=1,N
2269      C(I,J)=A(I,J)+B(I,J)
2270      10  RETURN
2271      END
2272      END OF FILE
2273
2274
2275      CCCCCCCCCCCCCCCCCCCCCCCCCCCCCCCCCCCCCCCCCCCCCCCCC
2276
2277      CCCCCCCCCCCCCCCCCCCCCCCCCCCCCCCCCCCCCCCCCCCCCCCCC
2278
2279      CCCCCCCCCCCCCCCCCCCCCCCCCCCCCCCCCCCCCCCCCCCCCCCCC
2280
2281      CCCCCCCCCCCCCCCCCCCCCCCCCCCCCCCCCCCCCCCCCCCCCCCCC
2282
2283      CCCCCCCCCCCCCCCCCCCCCCCCCCCCCCCCCCCCCCCCCCCCCCCCC
2284
2285      CCCCCCCCCCCCCCCCCCCCCCCCCCCCCCCCCCCCCCCCCCCCCCCCC
2286
2287      CCCCCCCCCCCCCCCCCCCCCCCCCCCCCCCCCCCCCCCCCCCCCCCCC
2288
2289      CCCCCCCCCCCCCCCCCCCCCCCCCCCCCCCCCCCCCCCCCCCCCCCCC
2290
2291      CCCCCCCCCCCCCCCCCCCCCCCCCCCCCCCCCCCCCCCCCCCCCCCCC
2292
2293      CCCCCCCCCCCCCCCCCCCCCCCCCCCCCCCCCCCCCCCCCCCCCCCCC
2294
2295      CCCCCCCCCCCCCCCCCCCCCCCCCCCCCCCCCCCCCCCCCCCCCCCCC
2296
2297      CCCCCCCCCCCCCCCCCCCCCCCCCCCCCCCCCCCCCCCCCCCCCCCCC
2298
2299      CCCCCCCCCCCCCCCCCCCCCCCCCCCCCCCCCCCCCCCCCCCCCCCCC
2299
2300      CCCCCCCCCCCCCCCCCCCCCCCCCCCCCCCCCCCCCCCCCCCCCCCCC
2301
2302      CCCCCCCCCCCCCCCCCCCCCCCCCCCCCCCCCCCCCCCCCCCCCCCCC
2303
2304      CCCCCCCCCCCCCCCCCCCCCCCCCCCCCCCCCCCCCCCCCCCCCCCCC
2305
2306      CCCCCCCCCCCCCCCCCCCCCCCCCCCCCCCCCCCCCCCCCCCCCCCCC
2307
2308      CCCCCCCCCCCCCCCCCCCCCCCCCCCCCCCCCCCCCCCCCCCCCCCCC
2309
2310      CCCCCCCCCCCCCCCCCCCCCCCCCCCCCCCCCCCCCCCCCCCCCCCCC
2311
2312      CCCCCCCCCCCCCCCCCCCCCCCCCCCCCCCCCCCCCCCCCCCCCCCCC
2313
2314      CCCCCCCCCCCCCCCCCCCCCCCCCCCCCCCCCCCCCCCCCCCCCCCCC
2315
2316      CCCCCCCCCCCCCCCCCCCCCCCCCCCCCCCCCCCCCCCCCCCCCCCCC
2317
2318      CCCCCCCCCCCCCCCCCCCCCCCCCCCCCCCCCCCCCCCCCCCCCCCCC
2319
2320      CCCCCCCCCCCCCCCCCCCCCCCCCCCCCCCCCCCCCCCCCCCCCCCCC
2321
2322      CCCCCCCCCCCCCCCCCCCCCCCCCCCCCCCCCCCCCCCCCCCCCCCCC
2323
2324      CCCCCCCCCCCCCCCCCCCCCCCCCCCCCCCCCCCCCCCCCCCCCCCCC
2325
2326      CCCCCCCCCCCCCCCCCCCCCCCCCCCCCCCCCCCCCCCCCCCCCCCCC
2327
2328      CCCCCCCCCCCCCCCCCCCCCCCCCCCCCCCCCCCCCCCCCCCCCCCCC
2329
2330      CCCCCCCCCCCCCCCCCCCCCCCCCCCCCCCCCCCCCCCCCCCCCCCCC
2331
2332      CCCCCCCCCCCCCCCCCCCCCCCCCCCCCCCCCCCCCCCCCCCCCCCCC
2333
2334      CCCCCCCCCCCCCCCCCCCCCCCCCCCCCCCCCCCCCCCCCCCCCCCCC
2335
2336      CCCCCCCCCCCCCCCCCCCCCCCCCCCCCCCCCCCCCCCCCCCCCCCCC
2337
2338      C   SUBROUTINE LGADD (N,B,C,N,M)
2339
2340      CCCCCCCCCCCCCCCCCCCCCCCCCCCCCCCCCCCCCCCCCCCCCCCCC
2341      IMPLICIT REAL*8 (A-H,O-Z)
2342      DIMENSION A(N,N),B(N,N),C(N,N)
2343      DO 10 I=1,N
2344      DO 10 J=1,N
2345      C(I,J)=A(I,J)+B(I,J)
2346      10  RETURN
2347      END
2348
2349
```

APPENDIX D
DATA FILES AND SAMPLE OUTPUT
OF EXAMPLE APPLICATIONS

45 NATURAL DRAFT HYPERBOLOID COOLING TOWER: WIND LOAD
 46 1,21,8,0,25.0,
 47 5,6,4000.0,.15,.15,0.0,
 48 1,0.0,85.99,
 49 2,10.0,84.94,
 50 3,116.67,85.62,
 51 4,223.33,105.7,
 52 5,330.0,136.8,
 53 6,355.0,145.0,0,1,1,1,
 54 1,5,1,2,2,2.0,0.5,
 55 82.5,204.1,60.0,0.0,
 56 2,5,2,3,2,0.5,0.5,
 57 82.5,204.1,60.0,0.0,
 58 3,5,3,4,2,0.5,0.5,
 59 82.5,204.1,60.0,0.0,
 60 4,5,4,5,2,0.5,0.5,
 61 82.5,204.1,60.0,0.0,
 62 5,5,5,6,2,0.5,2.5,
 63 82.5,204.1,60.0,0.0,
 64 5,0,8,2,24,1,
 65 1,0,0,2,0,0,
 66 2,0,0,2,0,0,
 67 3,0,0,2,0,0,
 68 4,0,0,2,0,0,
 69 5,0,0,2,0,0,
 70 -.0530,-.0424,-.0106,.0265,.0636,.0689,.0477,.0212,
 71 .0212,.0212,.0212,.0212,.0212,.0212,.0212,
 72 .0212,.0212,.0477,.0689,.0636,.0265,-.0106,-.0424,
 73 -.0526,-.0421,-.0105,.0263,.0632,.0684,.0474,.0210,
 74 .0210,.0210,.0210,.0210,.0210,.0210,.0210,
 75 .0210,.0210,.0474,.0684,.0632,.0263,-.0105,-.0421,
 76 -.0526,-.0421,-.0105,.0263,.0632,.0684,.0474,.0210,
 77 .0210,.0210,.0210,.0210,.0210,.0210,.0210,
 78 .0210,.0210,.0474,.0684,.0632,.0263,-.0105,-.0421,
 79 -.0478,-.0383,-.0096,.0239,.0574,.0622,.0430,.0191,
 80 .0191,.0191,.0191,.0191,.0191,.0191,.0191,
 81 .0191,.0191,.0430,.0622,.0574,.0239,-.0096,-.0383,
 82 -.0478,-.0383,-.0096,.0239,.0574,.0622,.0430,.0191,
 83 .0191,.0191,.0191,.0191,.0191,.0191,.0191,
 84 .0191,.0191,.0430,.0622,.0574,.0239,-.0096,-.0383,
 85 -.0414,-.0331,-.0083,.0207,.0497,.0538,.0372,.0165,
 86 .0165,.0165,.0165,.0165,.0165,.0165,.0165,
 87 .0165,.0165,.0372,.0538,.0497,.0207,-.0883,-.0331,
 88 -.0414,-.0331,-.0083,.0207,.0497,.0538,.0372,.0165,
 89 .0165,.0165,.0165,.0165,.0165,.0165,.0165,
 90 .0165,.0165,.0372,.0538,.0497,.0207,-.0883,-.0331,
 91 -.0304,-.0243,-.0061,.0152,.0365,.0395,.0273,.0122,
 92 .0122,.0122,.0122,.0122,.0122,.0122,.0122,
 93 .0122,.0122,.0273,.0395,.0365,.0152,-.0061,-.0243,
 94 -.0304,-.0243,-.0061,.0152,.0365,.0395,.0273,.0122,
 95 .0122,.0122,.0122,.0122,.0122,.0122,.0122,
 96 .0122,.0122,.0273,.0395,.0365,.0152,-.0061,-.0243,
 97 -.0256,-.0205,-.0051,.0127,.0301,.0332,.023,.0102,
 98 .0102,.0102,.0102,.0102,.0102,.0102,.0102,
 99 .0102,.0102,.0230,.0332,.0307,.0127,-.0051,-.0205,

1 NATURAL DRAFT HYPERBOLOID COOLING TOWER; DEAD LOAD
2 2,21,1,1,25.0,
3 3,4,576000.0,.15,.15,0,0,
4 1,0,0,86.0,
5 2,10.0,84.94,
6 3,330.0,136.81,
7 4,355.0,145.0,0,1,1,1,
8 1,5,1,2,1,2.0,0.5,
9 82.5,204.1,60.0,0.0,
10 2,5,2,3,1,0.5,0.5,
11 82.5,204.1,60.0,0.0,
12 3,5,3,4,1,0.5,2.5,
13 82.5,204.1,60.0,0.0,
14 0,0,0,0,
15 PINCHED CYLINDER "LINE CIRCUMFERENTIAL LOAD"
16 2,41,1,0,25.0,
17 2,3,4320000.,.3,.15,
18 1,0,0,4,0,1,1,1,1,
19 2,10.0,4.,0,0,0,0,
20 3,20.0,4.,1,1,1,1,
21 1,1,1,2,1,0.1033,
22 0.0,
23 2,1,2,3,1,0.1033,
24 0.0,
25 0,1,0,0,0,0,
26 2,
27 0.0,-1.0,0.0,0.0,
28 PINCHED CYLINDER "2 CONCENTRATED LOADS"
29 2,41,1,0,25.0,
30 2,3,4320000.,.3,.15,
31 1,0,0,4,0,1,1,1,1,
32 2,10.0,4.,0,0,0,0,
33 3,20.0,4.,1,1,1,1,
34 1,1,1,2,1,0.1033,
35 0.0,
36 2,1,2,3,1,0.1033,
37 0.0,
38 0,1,18,2,36,2,
39 2,
40 0,1,0,0,
41 -1.0,0.0,0.0,0.0,0.0,0.0,0.0,0.0,0.0,
42 0.0,0.0,0.0,0.0,0.0,0.0,0.0,0.0,0.0,
43 0.0,0.0,-1.0,0.0,0.0,0.0,0.0,0.0,0.0,
44 0.0,0.0,0.0,0.0,0.0,0.0,0.0,0.0,0.0,

1 PINCHED CYLINDER "LINE CIRCUMFERENTIAL LOAD"

*** ANALYSIS DATA ***

15	15	15	15	15	15	15
16	16	16	16	16	16	16
17	17	17	17	17	17	17
18	18	18	18	18	18	18
19	19	19	19	19	19	19
20	20	20	20	20	20	20

*** STRUCTURAL DATA ***

15	NUMBER OF ELEMENTS	=	2
16	NUMBER OF NODES	=	3
17	CYCLICAL YOUNG'S MODULUS	=	0.4320E+07
18	CYCLICAL POISSON'S RATIO	=	0.3000E+00
19	CYCLICAL UNIT WEIGHT	=	0.1500E+00
20	CYCLICAL THERMAL COEFFICIENT	=	0.0

*** NODAL DATA ***

15	NODE	XCOORD	RCOOR	R	W	V	U
16	1	0.0	4.0000	1	1	1	1
17	2	10.0000	4.0000	0	0	0	0
18	3	20.0000	4.0000	1	1	1	1

*** ELEMENT DATA ***

15	EL	IT	TH	SN	NPI	TH1	TH2	EC1	EC2	HF1	HF2	HF3	UNW	FR	E	TCDEF
16	1	1	2	1	0.1033	0.1033	0.0	0.0	0.0	0.0	0.0	0.0	0.15000	3000	0.4320E+07	
17	2	1	3	1	0.1033	0.1033	0.0	0.0	0.0	0.0	0.0	0.0	0.15000	3000	0.4320E+07	

*** LOADING SPECIFICATIONS ***

15	41	NUMBER OF LOADED ELEMENTS	=	0
16	42	NUMBER OF LOADED NODES	=	1
17	43	NUMBER OF HARMONICS TO FIT	=	1
18	44	LOADING TYPE CODE	=	0
19	45	NUMBER OF CIRCUMFR. POINTS	=	0
20	46	HARMONIC INCREMENTAL	=	1

DISPLACEMENT	R	U	V	W
1129				-0.0
1130	-0.0	-0.0	-0.0	-0.0
1131	-0.0	-0.0	-0.0	-0.0
1132	-0.0	-0.0	-0.0	-0.0
1133	-0.0	-0.0	-0.0	-0.0
1134	-0.1891E-06	0.2870E-07	-0.3087E-07	0.0
1135	-0.2005E-06	0.8047E-06	-0.6259E-07	0.0
1136	-0.1423E-06	0.1247E-06	-0.9525E-07	0.0
1137	-0.7697E-07	0.1523E-06	-0.1238E-06	0.0
1138	-0.2935E-07	0.1654E-06	-0.1623E-06	0.0
1139	-0.2970E-03	0.1911E-06	-0.1926E-06	0.0
1140	0.7568E-03	0.1682E-06	-0.2301E-06	0.0
1141	0.9008E-03	0.1630E-06	-0.2640E-06	0.0
1142	0.6731E-03	0.1640E-06	-0.2978E-06	0.0
1143	0.3631E-03	0.1626E-06	-0.3131E-06	0.0
1144	0.1627E-03	0.1620E-06	-0.3651E-06	0.0
1145	0.3815E-09	0.1617E-06	-0.3991E-06	0.0
1146	-0.1243E-09	0.1617E-06	-0.4329E-06	0.0
1147	-0.2467E-09	0.1618E-06	-0.4666E-06	0.0
1148	-0.3244E-09	0.1618E-06	-0.5000E-06	0.0
1149	-0.6310E-09	0.1619E-06	-0.5341E-06	0.0
1150	-0.1341E-08	0.1622E-06	-0.5679E-06	0.0
1151	-0.2451E-08	0.1626E-06	-0.6017E-06	0.0
1152	-0.5596E-08	0.1634E-06	-0.6394E-06	0.0
1153	-0.3798E-08	0.1644E-06	-0.6692E-06	0.0
1154	-0.1212E-08	0.1651E-06	-0.7030E-06	0.0
1155	-0.2298E-07	0.1610E-06	-0.7350E-06	0.0
1156	-0.4792E-07	0.1522E-06	-0.7700E-06	0.0
1157	-0.7604E-07	0.1367E-06	-0.8043E-06	0.0
1158	-0.8950E-07	0.1191E-06	-0.8378E-06	0.0
1159	-0.5235E-07	0.9608E-07	-0.8709E-06	0.0
1160	-0.9190E-07	0.9821E-07	-0.9356E-06	0.0
1161	-0.4073E-06	0.1567E-06	-0.9689E-06	0.0
1162	-0.9275E-06	0.3202E-06	-0.1010E-05	0.0
1163	-0.1577E-05	0.1092E-05	-0.1043E-05	0.0
1164	-0.2027E-05	0.1573E-05	-0.1146E-05	0.0
1165	-0.1584E-05	0.1711E-05	-0.1200E-05	0.0
1166	-0.9264E-05	0.8070E-05	-0.1297E-05	0.0
1167	-0.1763E-04	0.2178E-05	-0.1212E-05	0.0
1168	-0.3200E-04	-0.8348E-05	-0.1222E-05	0.0
1169	-0.4456E-04	-0.1307E-04	-0.1022E-05	0.0
1170	-0.4183E-04	-0.2937E-04	-0.6055E-06	0.0
1171	-0.1391E-11	-0.3573E-04	-0.2855E-11	0.0

1/4 DE FILE

PRIMARY STRESS RESULTANTS		MS	SS	NS	TS
17.6	17.7			0.5736E-03	-0.2253E-02
17.8	17.9			0.1493E-03	-0.1200E-02
18.0	18.1			-0.5068E-04	-0.4388E-03
18.2	18.3			-0.1032E-03	-0.2554E-04
18.4	18.5			-0.8552E-04	0.1324E-03
18.6	18.7			-0.4792E-04	0.1484E-03
18.8	18.9			-0.1478E-04	0.1080E-03
19.0	19.1			0.6421E-05	0.5971E-04
19.2	19.3			0.1668E-04	0.2353E-04
19.4	19.5			0.1977E-04	0.3970E-05
19.6	19.7			-0.1929E-04	-0.5344E-05
19.8	19.9			0.1766E-04	-0.6745E-05
20.0	20.1			0.1612E-04	-0.5053E-05
20.2	20.3			0.1515E-04	-0.2555E-05
20.4	20.5			0.1480E-04	-0.2266E-05
20.6	20.7			0.1499E-04	-0.1655E-05
20.8	20.9			0.1550E-04	0.2914E-05
21.0	21.1			0.1635E-04	0.2991E-05
21.2	21.3			0.1667E-04	0.6502E-06
21.4	21.5			0.1631E-04	0.5786E-05
21.6	21.7			0.1335E-04	-0.1876E-04
21.8	21.9			0.6384E-05	-0.3772E-04
22.0	22.1			-0.1566E-05	-0.5751E-04
22.2	22.3			-0.2152E-04	-0.6403E-04
22.4	22.5			-0.1542E-04	-0.3010E-04
22.6	22.7			-0.2543E-04	-0.8902E-04
22.8	22.9			0.2113E-04	0.3338E-03
23.0	23.1			0.1531E-03	0.7370E-03
23.2	23.3			0.3969E-03	0.1209E-02
23.4	23.5			0.7432E-03	0.1492E-02
23.6	23.7			0.1081E-02	0.1028E-02
23.8	23.9			0.1119E-02	-0.1088E-02
24.0	24.1			0.3033E-03	-0.5910E-02
24.2	24.3			-0.2134E-02	-0.1414E-01
24.4	24.5			-0.6987E-02	-0.2450E-01
24.6	24.7			-0.1538E-01	-0.3325E-01
24.8	24.9			-0.2556E-01	-0.2874E-01
25.0	25.1			-0.2111E-01	0.7236E-02
25.2	25.3			-0.1419E-01	0.9891E-01
25.4	25.5			0.2990E-01	-0.2661E+00
25.6	25.7			0.1249E+00	-0.5000E+00
25.8	25.9			0.0	0.0

SECONDARY STRESS RESULTANTS		MST	NTS	NST
HT	HTS			
1	1.696E-03	0.0	0.0	-0.1804E-01
2	0.4328E-04	0.0	0.0	-0.1477E-01
3	-0.1893E-04	0.0	0.0	-0.9037E-02
4	-0.3475E-04	0.0	0.0	-0.4148E-02
5	-0.2333E-04	0.0	0.0	-0.1084E-02
6	0.1561E-04	0.0	0.0	0.3640E-03
7	-0.4970E-05	0.0	0.0	0.7758E-03
8	0.1663E-05	0.0	0.0	0.6837E-03
9	0.5153E-05	0.0	0.0	0.4376E-03
10	0.6104E-05	0.0	0.0	0.2123E-03
11	0.5914E-05	0.0	0.0	0.6431E-04
12	0.5368E-05	0.0	0.0	-0.1043E-04
13	0.4865E-05	0.0	0.0	-0.3676E-04
14	0.4549E-05	0.0	0.0	-0.3914E-04
15	0.4354E-05	0.0	0.0	-0.3345E-04
16	0.4466E-05	0.0	0.0	-0.2563E-04
17	0.4667E-05	0.0	0.0	-0.1297E-04
18	0.4704E-05	0.0	0.0	0.1363E-04
19	0.5038E-05	0.0	0.0	0.6593E-04
20	0.4929E-05	0.0	0.0	0.1511E-03
21	0.4931E-05	0.0	0.0	0.2580E-03
22	0.4747E-05	0.0	0.0	0.3367E-03
23	0.4476E-05	0.0	0.0	0.2737E-03
24	0.4051E-04	0.0	0.0	-0.1224E-03
25	-0.2141E-05	0.0	0.0	-0.1096E-02
26	0.5819E-05	0.0	0.0	-0.2835E-02
27	0.4521E-04	0.0	0.0	-0.5209E-02
28	0.1184E-03	0.0	0.0	-0.7355E-02
29	0.2231E-03	0.0	0.0	-0.7108E-02
30	0.3265E-03	0.0	0.0	-0.5682E-03
31	0.3742E-03	0.0	0.0	0.1765E-01
32	0.1031E-03	0.0	0.0	0.5253E-01
33	0.1038E-03	0.0	0.0	0.1038E+00
34	-0.6248E-03	0.0	0.0	0.1573E+00
35	-0.2089E-02	0.0	0.0	0.1725E+00
36	-0.4310E-02	0.0	0.0	0.7145E+01
37	-0.6795E-02	0.0	0.0	0.2619E+00
38	-0.7933E-02	0.0	0.0	-0.9503E+00
39	-0.4473E-02	0.0	0.0	-0.2034E+01
40	0.3644E-02	0.0	0.0	-0.3296E+01
41	0.3709E-01	0.0	0.0	-0.3999E+01

END OF FILE

		DISPLACEMENT			
	R	U	V	W	
30.0					
30.1	1	-0.1425E-11	-0.3573E-04	0.2855E-11	-0.0
30.2	2	-0.4168E-04	-0.2937E-04	0.6064E-06	0.0
30.3	3	-0.4450E-04	-0.1790E-04	0.1026E-05	0.0
30.4	4	-0.3152E-04	-0.8117E-05	0.1236E-05	0.0
30.5	5	-0.1705E-04	-0.1291E-05	0.1292E-05	0.0
30.6	6	-0.6489E-05	0.9008E-06	0.1266E-05	0.0
30.7	7	-0.6414E-06	0.1719E-05	0.1206E-05	0.0
30.8	8	0.1678E-05	0.1531E-05	0.1143E-05	0.0
30.9	9	0.1996E-05	0.1036E-05	0.1088E-05	0.0
31.0	10	0.1490E-05	0.5848E-06	0.1042E-05	0.0
31.1	11	0.8424E-06	0.2395E-06	0.1003E-05	0.0
31.2	12	0.3454E-06	0.1427E-06	0.9690E-06	0.0
31.3	13	0.5763E-07	0.7558E-07	0.9362E-06	0.0
31.4	14	-0.3662E-07	0.9918E-07	0.9038E-06	0.0
31.5	15	-0.8381E-07	0.1210E-06	0.8710E-06	0.0
31.6	16	-0.6926E-07	0.1407E-06	0.8379E-06	0.0
31.7	17	-0.4130E-07	0.1548E-06	0.8044E-06	0.0
31.8	18	-0.1801E-07	0.1622E-06	0.7707E-06	0.0
31.9	19	-0.4022E-08	0.1648E-06	0.7369E-06	0.0
32.0	20	0.2311E-08	0.1449E-06	0.7030E-06	0.0
32.1	21	0.3885E-08	0.1641E-06	0.6692E-06	0.0
32.2	22	0.3252E-03	0.1631E-06	0.6354E-06	0.0
32.3	23	0.2040E-03	0.1625E-06	0.6017E-06	0.0
32.4	24	0.1035E-03	0.1621E-06	0.5679E-06	0.0
32.5	25	0.4666E-09	0.1617E-06	0.5341E-06	0.0
32.6	26	0.2670E-09	0.1618E-06	0.5004E-06	0.0
32.7	27	0.2351E-09	0.1617E-06	0.4666E-06	0.0
32.8	28	0.8581E-10	0.1617E-06	0.4329E-06	0.0
32.9	29	-0.5129E-09	0.1611E-06	0.3991E-06	0.0
33.0	30	-0.1888E-08	0.1620E-06	0.3653E-06	0.0
33.1	31	-0.4204E-08	0.1628E-06	0.3316E-06	0.0
33.2	32	-0.7103E-08	0.1642E-06	0.2978E-06	0.0
33.3	33	-0.9148E-08	0.1633E-06	0.2440E-06	0.0
33.4	34	-0.7146E-08	0.1684E-06	0.2301E-06	0.0
33.5	35	0.4167E-03	0.1690E-06	0.1962E-06	0.0
33.6	36	0.3150E-07	0.1650E-06	0.1623E-06	0.0
33.7	37	0.7964E-07	0.1515E-06	0.1186E-06	0.0
33.8	38	0.1445E-06	0.1236E-06	0.9537E-07	0.0
33.9	39	0.2012E-06	0.7974E-07	0.6263E-07	0.0
34.0	40	0.1891E-06	0.2860E-07	0.3086E-07	0.0
34.1	41	0.1285E-10	-0.2959E-11	-0.1048E-12	0.0
34.2	42				

END OF FILE

343

			PRIMARY STRESS RESULTANTS	NS	TS
			MS	SS	
344	345	1	0.1249E+00	-0.5000E+00	-0.6027E-01
346	346	2	0.2481E-01	-0.2657E+00	-0.6027E-01
347	347	3	-0.1447E-01	-0.9719E-01	-0.6027E-01
348	348	4	-0.2609E-01	-0.5456E-02	-0.6027E-01
349	349	5	-0.2197E-01	0.2932E-01	-0.6027E-01
350	350	6	-0.1386E-01	0.3237E-01	-0.6027E-01
351	351	7	-0.6514E-02	0.2392E-01	-0.6027E-01
352	352	8	-0.1324E-02	0.1323E-01	-0.6027E-01
353	353	9	0.4505E-03	0.5233E-02	-0.6027E-01
354	354	10	0.1159E-02	0.7052E-03	-0.6027E-01
355	355	11	0.1037E-02	-0.1156E-02	-0.6027E-01
356	356	12	0.6855E-03	-0.1471E-02	-0.6027E-01
357	357	13	0.3494E-03	-0.1127E-02	-0.6027E-01
358	358	14	0.1209E-03	-0.6111E-03	-0.6027E-01
359	359	15	0.6121E-05	-0.2760E-03	-0.6027E-01
360	360	16	-0.3262E-04	-0.5405E-04	-0.6027E-01
361	361	17	-0.3212E-04	0.4324E-04	-0.6027E-01
362	362	18	-0.1723E-04	0.5004E-04	-0.6027E-01
363	363	19	-0.1930E-05	0.5268E-04	-0.6027E-01
364	364	20	0.8820E-05	0.3177E-04	-0.6027E-01
365	365	21	0.1454E-04	0.1424E-04	-0.6027E-01
366	366	22	0.1365E-04	0.362E-05	-0.6027E-01
367	367	23	0.1672E-04	-0.1742E-05	-0.6027E-01
368	368	24	0.1603E-04	-0.5130E-05	-0.6027E-01
369	369	25	0.1533E-04	-0.2581E-05	-0.6027E-01
370	370	26	0.1484E-04	-0.1140E-05	-0.6027E-01
371	371	27	0.1479E-04	0.7958E-06	-0.6027E-01
372	372	28	0.1572E-04	0.315E-05	-0.6027E-01
373	373	29	0.1635E-04	0.5502E-05	-0.6027E-01
374	374	30	0.1734E-04	0.6855E-05	-0.6027E-01
375	375	31	0.1950E-04	0.4755E-05	-0.6027E-01
376	376	32	0.1969E-04	-0.4852E-05	-0.6027E-01
377	377	33	0.1605E-04	-0.7465E-04	-0.6027E-01
378	378	34	0.5023E-05	-0.3333E-04	-0.6027E-01
379	379	35	-0.1683E-04	-0.1120E-03	-0.6027E-01
380	380	36	-0.5027E-04	-0.1502E-03	-0.6027E-01
381	381	37	-0.3719E-04	-0.1298E-03	-0.6027E-01
382	382	38	-0.1032E-03	0.3237E-04	-0.6027E-01
383	383	39	-0.4941E-04	0.4466E-03	-0.6027E-01
384	384	40	0.1497E-03	0.1201E-02	-0.6027E-01
385	385	41	0.5788E-03	0.2255E-02	-0.6027E-01

END OF FILE

335

590	391	SECONDARY STRESS RESULTANTS	MTS	HST	NTS	NST	NT	NTS	NST
392	393								
394	1	0.3658E-01	0.0	0.0	-0.3995E+01	0.0	0.0	0.0	0.0
395	2	0.8622E-02	0.0	0.0	-0.3272E+01	0.0	0.0	0.0	0.0
396	3	-0.5131E-02	0.0	0.0	-0.2001E+01	0.0	0.0	0.0	0.0
397	4	-0.8611E-02	0.0	0.0	-0.9186E+01	0.0	0.0	0.0	0.0
398	5	-0.7219E-02	0.0	0.0	-0.2401E+01	0.0	0.0	0.0	0.0
399	6	-0.4425E-02	0.0	0.0	0.8061E-01	0.0	0.0	0.0	0.0
400	7	-0.2055E-02	0.0	0.0	0.1718E+00	0.0	0.0	0.0	0.0
401	8	-0.5571E-03	0.0	0.0	0.1513E+00	0.0	0.0	0.0	0.0
402	9	0.1677E-03	0.0	0.0	0.9679E-01	0.0	0.0	0.0	0.0
403	10	0.3798E-03	0.0	0.0	0.4688E-01	0.0	0.0	0.0	0.0
404	11	0.3372E-03	0.0	0.0	0.1419E-01	0.0	0.0	0.0	0.0
405	12	0.2298E-03	0.0	0.0	-0.2680E-02	0.0	0.0	0.0	0.0
406	13	0.1103E-03	0.0	0.0	-0.7330E-02	0.0	0.0	0.0	0.0
407	14	0.3226E-04	0.0	0.0	-0.6950E-02	0.0	0.0	0.0	0.0
408	15	0.5599E-06	0.0	0.0	-0.4648E-02	0.0	0.0	0.0	0.0
409	16	-0.1154E-04	0.0	0.0	-0.2366E-02	0.0	0.0	0.0	0.0
410	17	-0.1096E-04	0.0	0.0	-0.8022E-03	0.0	0.0	0.0	0.0
411	18	-0.5957E-05	0.0	0.0	0.1469E-04	0.0	0.0	0.0	0.0
412	19	-0.9127E-06	0.0	0.0	0.3064E-03	0.0	0.0	0.0	0.0
413	20	0.2575E-05	0.0	0.0	0.3172E-03	0.0	0.0	0.0	0.0
414	21	0.441CE-05	0.0	0.0	0.2228E-03	0.0	0.0	0.0	0.0
415	22	0.5069E-05	0.0	0.0	0.1153E-03	0.0	0.0	0.0	0.0
416	23	0.5038E-05	0.0	0.0	0.4519E-04	0.0	0.0	0.0	0.0
417	24	0.4862E-05	0.0	0.0	0.2779E-05	0.0	0.0	0.0	0.0
418	25	0.4615E-05	0.0	0.0	-0.1738E-04	0.0	0.0	0.0	0.0
419	26	0.4456E-05	0.0	0.0	-0.2707E-04	0.0	0.0	0.0	0.0
420	27	0.4432E-05	0.0	0.0	-0.3402E-04	0.0	0.0	0.0	0.0
421	28	0.4574E-05	0.0	0.0	-0.3907E-04	0.0	0.0	0.0	0.0
422	29	0.4900E-05	0.0	0.0	-0.3445E-04	0.0	0.0	0.0	0.0
423	30	0.5381E-05	0.0	0.0	-0.2917E-05	0.0	0.0	0.0	0.0
424	31	0.5858E-05	0.0	0.0	0.8019E-04	0.0	0.0	0.0	0.0
425	32	0.5932E-05	0.0	0.0	0.2378E-03	0.0	0.0	0.0	0.0
426	33	0.4862E-05	0.0	0.0	0.4692E-03	0.0	0.0	0.0	0.0
427	34	0.1577E-05	0.0	0.0	0.7105E-03	0.0	0.0	0.0	0.0
428	35	-0.4976E-05	0.0	0.0	0.7792E-03	0.0	0.0	0.0	0.0
429	36	-0.1506E-04	0.0	0.0	0.3227E-03	0.0	0.0	0.0	0.0
430	37	-0.2630E-04	0.0	0.0	-0.1182E-02	0.0	0.0	0.0	0.0
431	38	-0.3144E-04	0.0	0.0	-0.4291E-02	0.0	0.0	0.0	0.0
432	39	-0.1577E-04	0.0	0.0	-0.9185E-02	0.0	0.0	0.0	0.0
433	40	0.4342E-04	0.0	0.0	-0.1468E-01	0.0	0.0	0.0	0.0
434	41	0.1719E-03	0.0	0.0	-0.1806E-01	0.0	0.0	0.0	0.0

END OF FILE